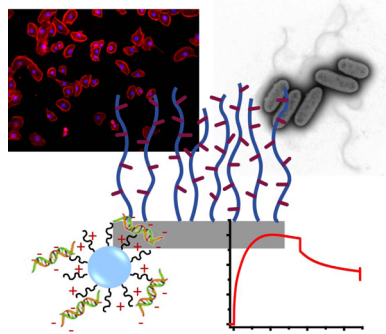


Surface-Initiated Polymer Brushes in the Biomedical Field: Applications in Membrane Science, Biosensing, Cell Culture, Regenerative Medicine and Antibacterial Coatings

Mahenthra Krishnamoorthy,^{†,‡} Shoghik Hakobyan,[§] Madeleine Ramstedt,^{*,§} and Julien E. Gautrot^{*,†,‡}

[†]Institute of Bioengineering and [‡]School of Engineering and Materials Science, Queen Mary University of London, Mile End Road, London E1 4NS, United Kingdom

[§]Department of Chemistry, Umeå University, SE-90187 Umeå, Sweden



CONTENTS

1. Introduction	10977
2. Protein Interaction with Polymer Brushes and Biofunctionalization	10977
2.1. Brush Architecture and Responsiveness	10977
2.2. Infiltration of Nanoparticles and Molecules	10979
2.3. Interaction with Proteins	10980
2.4. Protein Resistance	10982
2.5. Biofunctionalization of Polymer Brushes	10984
2.5.1. Protein Adsorption	10984
2.5.2. Brush Functionalization with Small Molecules and Peptides	10984
2.5.3. Protein Coupling and Binding	10986
3. Applications to Membrane Science and Sample Purification	10989
3.1. Surface Coating for Membrane Applications and Sample Purification	10989
3.1.1. Polymer Brushes Grown from a Variety of Membranes	10989
3.1.2. Performance and Application of Brush-Functionalized Membranes for Sample Purification, Separation, and Filtration	10989
3.2. Protein Capture with Binding Elements	10990
4. Polymer Brush-Based Biosensing Platforms	10991
4.1. Types of Polymer-Brush-Based Sensing Platforms	10991
4.1.1. Label-Free Biosensing	10991
4.1.2. Biosensing Based on Immunoassays and Fluorescent Tag Labeling	10991
4.2. Impact of Protein Resistance on Sensing Specificity	10993
4.2.1. Low-Fouling Brushes for Biosensing	10993
4.2.2. Development of Brush-Based Label-Free Sensors for Detection in Serum and Plasma	10994
4.3. Impact of the Coupling Chemistry and Brush Architecture	10994
4.3.1. Impact of the Brush Architecture	10994
4.3.2. Choice of Biofunctionalization Strategy	10995
5. Polymer Brush-Based Platforms for Cell Culture and Regenerative Medicine	10996
5.1. Biofunctional Brushes for Controlling Cell-Materials Interfaces	10996
5.1.1. Importance of Brush-Based Low-Fouling Coatings for Cell Culture and Implant Design	10996
5.1.2. Impact of the Brush Chemistry	10996
5.1.3. Peptide-Functionalized Brushes for Promoting Cell Adhesion and Culture	10996
5.1.4. Brush Coatings Functionalized with Protein Fragments, Proteins, and Growth Factors for Cell Culture and Regenerative Medicine	10997
5.2. Polymer Brushes for Drug and Gene Delivery	10998
5.3. Responsive Brushes for Controlled Cell Adhesion and Detachment	10999
5.3.1. General Considerations for the Design of Brush-Based Responsive Substrates for Cell and Cell-Sheet Harvesting	10999
5.3.2. Mechanism of Cell Detachment and Parameters Affecting the Performance of the Coatings	11000
5.3.3. PNIPAM- and PDEGMA-Based Brushes for Cell and Cell-Sheet Harvesting	11000
5.3.4. Impact of the Underlying Substrate	11001
5.3.5. Brush Functionalization	11001
5.4. Patterned Brushes for Controlling the Cell Microenvironment	11001
5.4.1. Strategies Developed for the Micro-patternning of Polymer Brushes for Cell Patterning and Culture	11001
5.4.2. Impact of the Brush Chemistry on Cell Patterning	11003

Received: May 10, 2014

Published: October 29, 2014

5.4.3. Cell-Based Assays Developed Using Polymer-Brush-Based Platforms	11004
6. Antibacterial Coatings Based on Polymer Brushes	11005
6.1. Examples of the Experimental Setup for Determining the Antibacterial Properties of Polymer Brushes	11007
6.2. Polymer Brushes Based on Bactericidal Polymers	11007
6.3. Polymer Brushes Functionalized with Antibacterial Compounds	11009
6.4. Antifouling Polymer Brushes with Respect to Bacterial Attachment	11011
6.4.1. Brushes with Poly(ethylene glycol) Subunits	11011
6.4.2. Zwitterionic Brushes	11014
6.4.3. Negatively Charged Brush Surfaces	11014
6.4.4. Other Neutral Antifouling Brushes	11015
7. Conclusions and Outlook	11016
Author Information	11016
Corresponding Authors	11016
Notes	11016
Biographies	11016
Acknowledgments	11017
References	11017

1. INTRODUCTION

Understanding and controlling interfaces has proven to be key to a very wide range of applications, from optical and electronic materials^{1,2} to energy storage and production,^{3–5} sensing and biosensing,^{6–9} sample purification and analysis,^{10–13} cell culture and tissue regeneration,^{14–17} antibacterial coatings,^{18–20} composites,^{21–23} catalysis,^{24,25} food industry applications,²⁶ and water purification.^{27,28} Various strategies have been developed to design and control such interfaces. In particular, polymer brushes are attractive as they allow the control of a number of important architectural features: they consist of polymer chains that are tethered at one end to an underlying, often solid, substrate, which enables the grafting density (density of polymer chains per surface area) and the thickness of the coating (via the length of the polymer chain and the grafting density) and its chemistry (via the choice of monomers that are polymerized when a brush is generated) to be manipulated very readily.^{29–32} Such flexibility allows tuning of interfacial properties such as hydrophilicity and surface energy,^{33–38} rheological and tribological behavior,^{39–42} electron and energy transfer,^{43–46} binding and adsorption of molecules and proteins,^{47–52} catalytic activity,^{53–55} diffusion of molecules and particles,^{56–59} and cell adhesion.^{60–62}

Polymer brushes can be generated via a “grafting-to” method, in which polymer chains are anchored to a surface, or via a “grafting-from” approach, in which an initiator molecule is coupled to the surface and allows the growth of a polymer chain.^{30,31} The latter method allows a closer control of the architectural features of the resulting brush and hence has recently received a lot of attention.⁶³ Advances in the design and preparation of grafted-from polymer brushes have been enabled by developments in the fields of surface science and polymer chemistry.³² First, controlled surface-initiated polymerizations required the development of a number of controlled polymerization techniques, in particular those based on radical chemistry such as atom-transfer radical polymerization (ATRP),^{64–66} reversible addition–fragmenta-

tion chain-transfer (RAFT) polymerization,^{67–69} nitroxide-mediated polymerization (NMP),^{70,71} and iniferter polymerization.^{72,73} Second, advances in surface science and chemistry have allowed the development of a wide variety of initiators for controlled surface-initiated polymerization, including from silicon^{74–78} and glass,^{79–82} gold and other metals, alloys or metal oxides,^{83–87} mica,^{88,89} graphene,^{90,91} hydroxyapatite,^{92,93} cellulose,⁹⁴ electrospun fibers,⁹⁵ fluorinated polymers,^{96,97} nylon-6,6,⁹⁸ polystyrene,^{99–101} poly(methyl methacrylate),¹⁰⁰ polypropylene,⁹⁷ polyethylene,¹⁰⁰ polyurethanes,¹⁰² polyimide,⁹⁷ poly(ethylene terephthalate),^{97,100,103} poly-caprolactone),^{104,105} poly(ether ether ketone),¹⁰⁶ poly(ether sulfone),¹⁰⁷ poly(dimethylsiloxane),¹⁰⁸ poly(2-hydroxyethyl methacrylate-*co*-methyl methacrylate) hydrogels,¹⁰⁹ polypyrrole,¹¹⁰ polythiophene,¹¹¹ poly(3,4-(ethylenedioxy)-thiophene),^{43,112} and polycarbazole.¹¹³ Hence, progress in surface-initiated controlled polymerization has enabled the applications of polymer brushes to nanotechnologies^{114–117} and for the design of biointerfaces.^{60,114,118–121} This review will focus on the properties and application of polymer brushes to the biomedical field, placing the emphasis on recent work reporting brushes generated via a grafting-from approach and controlled radical polymerizations. The synthesis and fundamental properties of polymer brushes have previously been reviewed in several excellent reviews^{31,32,63,122–130} and will, therefore, here only be briefly described with references to the most recent literature covering the subject.

2. PROTEIN INTERACTION WITH POLYMER BRUSHES AND BIOFUNCTIONALIZATION

2.1. Brush Architecture and Responsiveness

The behavior and properties of polymer brushes arise from a combination of their chemistry and architecture.^{63,122,129,131} These properties have been exhaustively reviewed elsewhere, and we direct the reader to this literature for a detailed discussion of the behavior of polymer brushes.^{32,126–129} The wealth of chemical functions that have been incorporated into polymer brushes (see Figure 1 for examples discussed in this review) has allowed the achievement of a wide variety of surface properties and bioactivity or biointeractivity, but architectural features play an important role in modulating the brush behavior.

One of the key defining features of polymer brushes is the density of chains per area (grafting density): at high density, the polymer chains tend to be extended and partially oriented to avoid excluded volume effects (the “brush” regime), whereas, at low grafting density, the chains tend to coil randomly and form isolated structures distributed over the underlying surface (the “mushroom” regime).^{32,132–134} The size and shape of these “mushrooms” and the boundary between the two regimes depend on the monomer structure as well as interaction with the solvent and underlying substrate.¹³⁵ Although at the nanoscale this behavior is well documented and supported, a clear picture of the brush structure at the atomic scale is less clear, and recent works have given a more nuanced picture of the brush architecture. Neutron reflectivity provided evidence that the brush end chains are not localized at the maximum height of the brush but are distributed throughout the brush and that this distribution is sensitive to the grafting density,¹³⁶ in agreement with predictions of brush models.^{137–140} These results are also supported by molecular dynamics simulations that also implicate the role of temperature in the chain

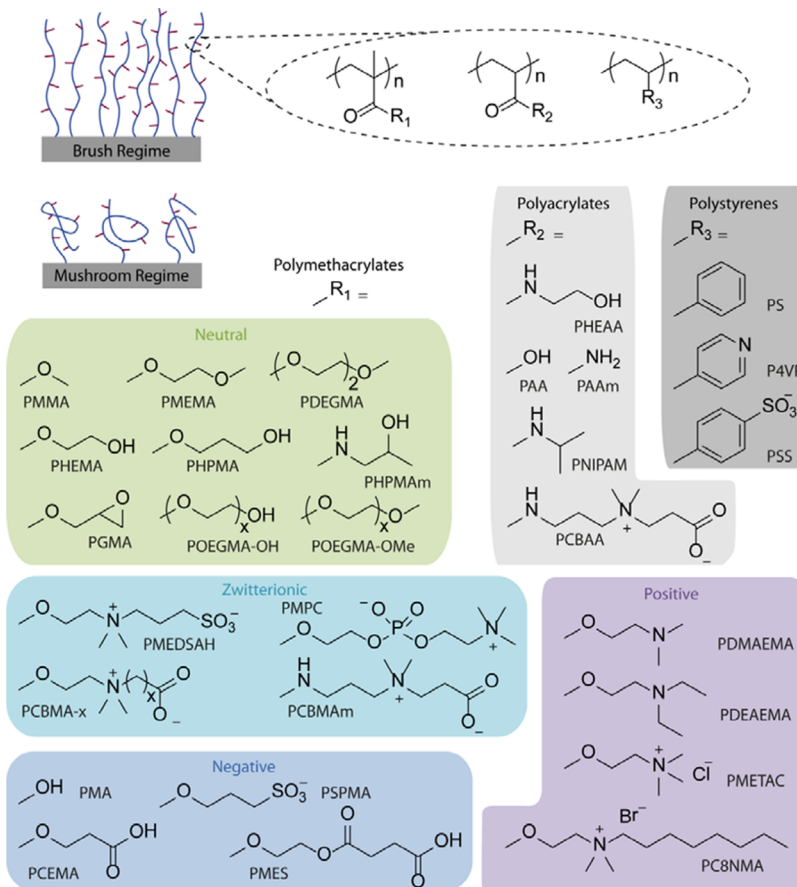


Figure 1. Chemical structures of polymer brushes most commonly used for biomedical applications.

conformation, brush swelling, and chain end distribution.¹⁴¹ Similarly, the chain conformation is strongly dependent on other structural features of the brushes: side chain branching was predicted to increase the brush density and stretching¹⁴² and the localization of branching points, and end chains in dendritic brushes are strongly affected by the grafting density.¹⁴³

Other environmental parameters such as solvent quality,^{144–146} pH,^{35,37,147} ionic strength, and the presence of specific electrolytes^{116,148} or small molecules¹⁴⁹ also influence the brush conformation and can give rise to responsive systems with controllable surface properties such as particle aggregation,¹⁴⁸ wettability,³⁵ lubrication,¹⁵⁰ and protein adsorption.¹⁵¹ Another feature of polymer brushes is the ability to generate block copolymer architectures^{56,152,153} and mixed polymer brushes,^{122,154} which can easily be designed to display stimulus-responsive behaviors. The main types of responsive behaviors that will be of interest in this review are those based on changes in pH, temperature, and ionic strength (Figure 2). Although the properties of the relevant brushes are modulated by their architecture, as described above, the chemistry of the repeat monomer unit is the key determinant of the environmental responsiveness (see Figure 1).

Systems sensitive to pH are based on polyacids or polybases such as poly(acrylic acid) (PAA) and poly(methacrylic acid) (PMAA),^{37,156} poly((dimethylamino)ethyl methacrylate) (PDMAEMA),¹⁴⁷ poly((diethylamino)ethyl methacrylate) (PDEAEMA),^{157,158} and poly(4-vinylpyridine) (P4VP).¹⁵⁹ One of the hallmarks of these systems is the high degree of swelling achieved in the fully charged state, typically ranging

from 400% to 700%,^{37,147} due to the strong intra- and interchain repulsive forces arising from the charged monomers and associated osmotic pressure. Such behavior is dependent on the ionic strength: at low ionic strength, swelling is independent of the salt concentration (the osmotic regime), whereas, at high ionic strength, swelling decreases with increasing salt concentration (the salted brush regime; see Figure 2),^{37,147} as predicted by the work of Pincus and Zhulina.^{160,161} Similarly, some zwitterionic brushes such as poly(carboxybetaine methacrylate) (PCBMA)¹⁶² and random copolymer brushes of oppositely charged monomers¹⁶³ can display responsive properties due to a change in electrostatic interactions and osmotic pressure upon deprotonation of the brush. In addition, ellipsometry measurements highlighted that brush swelling is thickness-dependent.¹⁶⁴

Temperature-sensitive brushes are based on polymers displaying a lower critical solution temperature (LCST)^{155,165} or an upper critical solution temperature (UCST)¹⁶⁶ in aqueous solutions. Above an LCST, chain solvation cannot compete with interchain interactions, resulting in a collapse (reduction of swelling) of the polymer conformation. Above a UCST, the opposite phenomenon occurs and chains open up. Poly(*N*-isopropylacrylamide) (PNIPAM) is one the most classical polymers displaying LCST properties, with a sharp transition at 32 °C for free polymer in solution, and has been employed to generate brushes with thermally responsive properties. The LCST in such brushes is typically broader and still occurs near 32 °C, with static contact angles increasing by 6–8° when the temperature is raised above the transition.¹⁶⁷ This transition decreases by ca. 2 °C when measured in cell

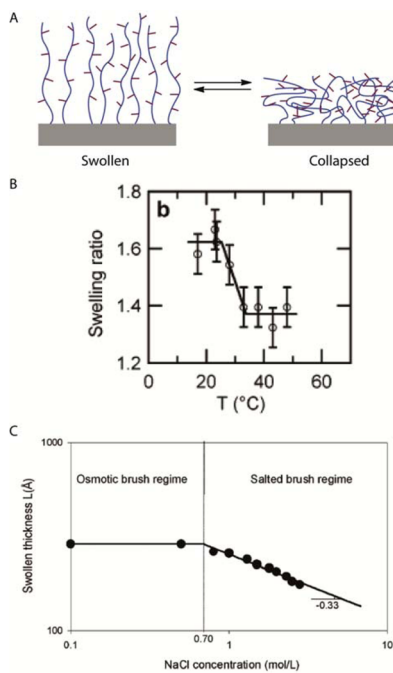


Figure 2. Responsive polymer brushes. (A) Schematic representation of polymer brushes changing conformation in response to a trigger (e.g., T , salt, pH). (B) Evolution of the swelling ratio of a PDEGMA brush in response to changes in temperature, measured by AFM. Reprinted from ref 155. Copyright 2007 American Chemical Society. (C) Effect of the ionic strength on the swelling of PMETAC brushes. Reprinted from ref 147. Copyright 2007 American Chemical Society.

culture medium, perhaps simply as a result of the change in ionic strength.¹⁶⁸ The impact of the brush thickness and grafting density is less clear. Atomic force microscopy (AFM) and quartz crystal microbalance (QCM) measurements showed that high-density brushes ($0.34\text{--}0.36 \text{ chain/nm}^2$) displayed broader transitions starting earlier and ending later than those for low-density brushes ($0.015\text{--}0.018 \text{ chain/nm}^2$; see Figure 3).¹⁶⁵ However, spectroscopic ellipsometry revealed that the collapse of PNIPAM brushes was broader for low-density brushes, which correlated with a weaker change in buffer content within the brush and a decrease of the midtemperature of the deswelling.¹⁶⁹ This behavior may be the result of complex topographical changes during the collapse of sparse brushes,¹⁷⁰ as previously proposed by the work of Williams.¹⁷¹

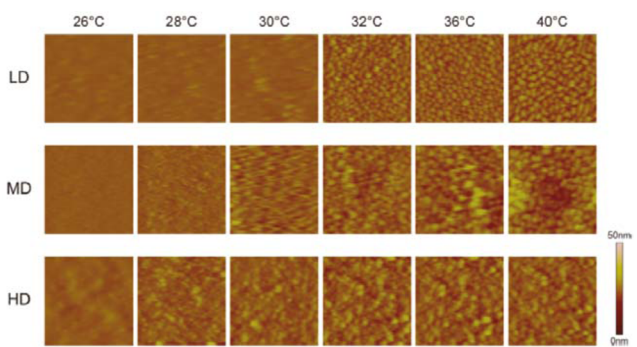


Figure 3. Impact of the grafting density on the thermal response of PNIPAM brushes, characterized by AFM. LD, low density; MD, medium density; HD, high density. Reprinted from ref 165. Copyright 2010 American Chemical Society.

It is worth noting that the strategy used for preparing PNIPAM brushes in the latter work was a grafting-to strategy. A surface force measurement study by Bureau and co-workers found that the “pull-off” force (between a PNIPAM-coated surface and a PNIPAM-coated tip) increased markedly above the LCST, but was not affected by the grafting density.¹⁶⁷ The nature of the underlying substrate was also different in these various studies and may play an important role, especially at lower grafting densities. Hence, the role of the brush architecture on the PNIPAM transition is not fully clear. Ionic strength is another parameter having a marked effect on the LCST of PNIPAM, both in bulk solution¹⁷² and in polymer brushes,¹⁶⁵ and at concentrations ranging from 10 to 100 mM, the LCST of brushes is shifted below room temperature.

Researchers have developed other systems that would either allow precise control of the position of the LCST in a wider range of temperatures or avoid the large hysteresis observed for PNIPAM. For example, poly(oligo(ethylene glycol) methacrylate) (POEGMA) and poly(bis(ethylene glycol) methyl ether methacrylate) (PDEGMA) copolymers display little hysteresis during the cooling process.¹⁷² Copolymer brushes of POEGMA and PDEGMA display an LCST that linearly increases with increasing OEGMA monomer ratio.¹⁵⁵ As for PNIPAM, this LCST correlates with a brush collapse and an increase of the water contact angle.^{35,155} Interestingly, a combination of QCM-dissipation (QCM-D) measurements and water contact goniometry revealed significant differences between the collapse temperature of bulk brush chains and that of the brush surface.¹⁷³ Jonas and co-workers found that the bulk LCST of brushes (from QCM data) was on average 8 °C below that of the surface (from variations in the water contact angle) and 5 °C lower than that of free polymer chains. Such a phenomenon may also account for discrepancies between studies reporting the behavior of PNIPAM brushes with varying grafting densities.

Some zwitterionic polymers such as poly((2-(methacryloyloxy)ethyl)dimethyl(3-sulfopropyl)ammonium hydroxide) (PMEDSAH) display UCST properties.^{166,174} In such cases, the strong dipoles arising from the zwitterionic repeat units associate at low temperature, resulting in brush collapse and surface hydrophobicity, whereas they dissociate above the UCST, inducing brush swelling and surface hydrophilicity. This transition was found to be highly dependent on the brush thickness and grafting density, occurring near 52 °C for thick dense brushes, and these parameters also influenced the magnitude of the change in water contact angle. As for PNIPAM, an increase in ionic strength resulted in lowering the UCST, as a result of the screening of dipolar interactions controlling the brush collapse and swelling.¹⁷⁵ Such salt-responsive behavior is not restricted to UCST brushes and is a hallmark of many polyelectrolyte brushes, in which the chain conformation is altered by the ionic strength as described above.^{37,147,148} The polymer brush conformation is modulated by a variety of parameters and is very dynamic, responding to multiple environmental stimuli. Such properties are essential to the understanding, design, and control of brush properties in the biomedical field, such as interaction with proteins and manipulation of cell behavior.

2.2. Infiltration of Nanoparticles and Molecules

Interfaces underlie many biomedical applications, from biosensing and medical diagnostics to protein purification, antibacterial coatings, and tissue engineering. Protein inter-

action, adsorption, and immobilization at these interfaces are often important factors governing other biochemical and biological processes such as marker detection, bacterial adhesion, and cell spreading. To use polymer brushes for the design and control of such interfaces, it is important that their interaction with proteins is understood.

From a more general point of view, several research works have focused on the interaction and infiltration of objects such as nanoparticles into polymer brushes (Figure 4). De Vos and

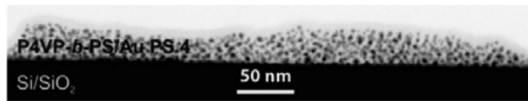


Figure 4. Infiltration of PS-coated nanoparticles in P4VP-*b*-PS brushes. Reprinted from ref 56. Copyright 2009 American Chemical Society.

co-workers investigated the importance of particle size, brush grafting density, and polydispersity on particle infiltration.¹⁷⁶ They found that small particles (for which the radius R is smaller than the distance between two polymer chains, $R < (2\sqrt{\sigma})^{-1}$, where σ is the grafting density) could penetrate deeper into sparse brushes and brushes with increasing polydispersity (e.g., potentially arising from lower control during polymer brush growth in the case of grafting-from strategies). Halperin and co-workers stressed the importance of solvent quality, which affects particle–brush interactions as well as the chain conformation.¹⁷⁷ Poor solvents, which result in chain collapse, decrease the osmotic pressure within the brush, leading to a reduction in the free energy penalty upon infiltration of a particle. In addition, solvent quality was found to impact the mode of particle adsorption: primary adsorption to the underlying substrate or ternary adsorption if sufficiently strong interactions arise between the brush and the particle (Figure 5). These observations are supported by experiments in

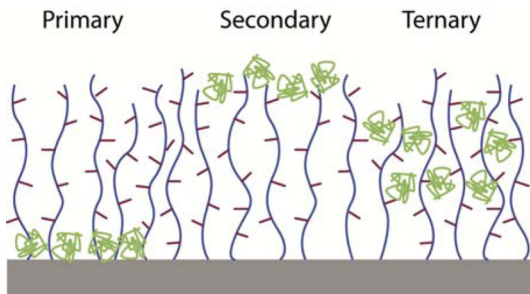


Figure 5. Modes of protein adsorption to polymer brushes.

which the localization of particles in block copolymer brushes was determined by kinetic factors, the swelling of both blocks, and the strength of interactions between the particles and the two blocks.⁵⁶ Such strong interactions can be harnessed to synthesize and load particles very stably into polymer brushes.⁵⁹

Similarly to hard particles, small molecules are reported to infiltrate brushes more easily than bulkier macromolecules. Poly(hydroxyethyl methacrylate) (PHEMA) brushes grafted on a silica monolith column gave rise to a bimodal size exclusion phenomenon, with a molecular weight cutoff below 1000 g/mol, corresponding to the infiltration of molecules within the brush.^{30,178} Such a low cutoff is surprising, especially considering the wealth of data reporting the infiltration of

proteins (with molecular weights sometimes on the order of several tens of kilodaltons) in polymer brushes, but is perhaps a result of the low swelling of PHEMA brushes under the experimental conditions used. Steroids with molecular weights near 350–400 g/mol better infiltrated PNIPAM brushes below their LCST, and this phenomenon was strongly affected by the brush grafting density.¹⁷⁹ However, in the latter case, slight changes in molecular structure had important consequences on the interaction of the steroid with the brush, beyond what would be expected from simple size exclusion and infiltration. Similarly, PNIPAM-*co*-PDMAEMA copolymer brushes led to increased infiltration of adenosine triphosphates below the LCST of the polymer, although the contribution of the increased availability of positively charged groups is less clear.¹⁸⁰ Finally, Gervasi and co-workers measured the diffusion of small-molecule probes in poly((2-(methacryloyloxy)ethyl)-trimethylammonium chloride) (PMETAC) brushes and found that the perchlorate-induced collapse of this brush significantly decreased ion motility.¹⁸¹

Several studies investigated the diffusion of larger molecules such as synthetic polymers and peptides. Rühe and co-workers studied the functionalization of copolymer brushes of poly(methyl methacrylate) (PMMA) and an *N*-hydroxysuccinimide (NHS)-bearing monomer with aminopoly(ethylene glycol) (PEG).¹⁸² A good correlation between the functionalization level and the radius of gyration (R_g) of the PEG chains was observed. The authors proposed that large polymer chains do not fully penetrate through the brush but rather remain at the upper layer. Penn and co-workers used QCM to monitor the adsorption of polystyrene (PS) and PEG polymer chains terminated with thiol groups, through PS brushes of varying sizes, to the underlying gold surface of the sensor.^{58,183} The ratio between the R_g of the brush and that of the free chains was the key parameter, whether considering the interaction of free chains and brushes of the same type or of different types. These results stress the importance of the size of free polymer chains (and hence R_g) as one of the key parameters controlling the infiltration of free polymer chains into polymer brushes. When free chains are sufficiently small, they can penetrate the brush all the way to the underlying substrate, whereas they remain confined to the upper layer for larger sizes. Molecular dynamics simulations found that macromolecules can infiltrate a brush, even in the absence of attractive interactions with the underlying substrate and in a good solvent for both the brush and free polymer chain, providing the Flory–Huggins parameter is only slightly favorable. In addition, it was found that the amount of polymer adsorbed and its position within the brush were affected by the brush grafting density and length.¹⁸⁴ Husson and co-workers found that the diffusion of peptides (five amino acids) within POEGMA brushes was tightly controlled by the grafting density, with no detectable adsorption to the underlying substrate for dense brushes.¹⁸⁵

2.3. Interaction with Proteins

Protein adsorption to the surface of materials is the result of a combination of hydrophobic and electrostatic interactions as well as hydrogen bonding.^{120,186–188} Adsorption can be multistage, involving primary interactions, sometimes followed by conformational changes in the protein structure and possible denaturation that can reinforce the adsorption to the surface. Such behavior is also observed in polymer brushes. However, the most detailed studies investigating protein–brush interactions focus on hydrophilic brushes (or brushes that swell to

some extent in a relevant buffer). Three different scenarios have been proposed for describing the interaction of proteins with polymer brush interfaces (Figure 5).¹⁸⁹ Primary adsorption arises from interactions with the underlying substrate, providing the brush height, swelling, and grafting densities allow sufficient diffusion. Secondary adsorption is restricted to the outer part of the brush, directly exposed to the bulk solution, and can be expected to dominate in the case of large proteins and very dense and homogeneous polymer brushes. Ternary adsorption occurs when the free energy of adsorption to the underlying surface is low and the attraction energy to the brush is sufficiently high. The main forces that proteins have to overcome in primary and ternary adsorption are the brush solvation energy and the penalty in osmotic pressure of the brush, whereas the latter can be ignored in secondary adsorptions. Adsorption is also modulated by the conformation, length, and grafting density of the brush as well as the protein size.

Interactions with charged brushes occur for proteins bearing a global opposite charge, and adsorption is strongest near the isoelectric point (*pI*) of the protein. Hence, bovine serum albumin (BSA), with a *pI* near 4.6–4.7, adsorbs strongly to PAA¹⁹⁰ and cationic^{191,192} brushes near this pH (Figure 6). An

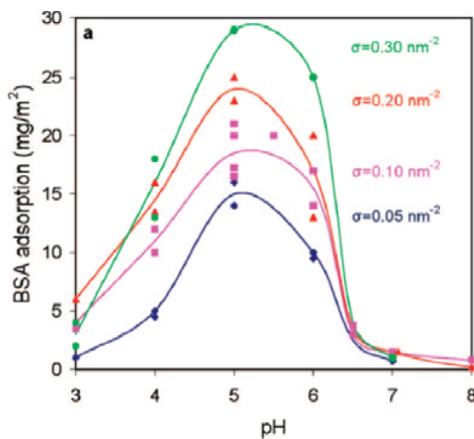


Figure 6. Impact of the grafting density and pH on the adsorption of BSA to PAA brushes. Reprinted from ref 190. Copyright 2008 American Chemical Society.

increase in chain length and grafting density resulted in higher BSA adsorption for a wide pH range. In contrast, increasing the ionic strength of the buffer had a more pronounced effect at higher pH, probably because of the stronger swelling of PAA brushes above their pK_a . These results were mirrored by QCM-D experiments studying the adsorption of human serum albumin (HSA) on PAA brushes at different pH values and ionic strengths.¹⁹³ In addition, that study showed that the combined effects of ionic strength, pH, and the presence of mixed poly(ethylene oxide) brushes can be harnessed to control the adsorption and desorption of HSA to polymer brush interfaces. High protein adsorption is not restricted to oppositely charged brushes and proteins though: proteins adsorb strongly to polymer brushes on the “wrong side” of their *pI* (at a pH for which the brush and the protein bear the same net total charge).^{190–192} To account for these observations, two mechanisms have been explored.^{194,195} The first, based on charge reversal, proposes that a local variation in the pH close to the brush results in electrostatic attraction of proteins.^{190,196}

In the second, the localization of counterions close to the brush leads to a strong osmotic pressure, which can be reduced upon interaction with protein pockets bearing charges opposite that of the brush. Hence, in this second model, protein adsorption is entropically driven and strongly depends on the buffer’s ionic strength. Evidence for the latter mechanism was recently provided by isothermal titration calorimetry.^{192,197,198} In both mechanisms, it would be expected that the strong underlying interactions with the brush and the size of the proteins result in ternary adsorption. Indeed, neutron reflectometry and small-angle X-ray scattering revealed that proteins were able to penetrate and diffuse throughout the brush^{199,200} and could even accumulate close to the core, giving rise to protein aggregation.^{201,202} This behavior was observed despite slower protein diffusion within brushes compared to that of free proteins in solution.²⁰³ Local changes in pH and interaction with the underlying substrate may contribute to shaping such a protein distribution. In comparison, proteins located in the outer part of the brush are less tightly bound and easier to displace.²⁰¹ Not surprisingly, protein adsorption from more complex protein solutions, such as blood or cell culture medium, gives rise to high protein adsorption to charged polymer brushes,^{204,205} which could be an important parameter determining cell behavior at these interfaces or for the design of biosensors and biocompatible coatings.²⁰⁶ For example, PDEAEMA brushes were shown to respond to changes in pH induced by exposure to CO₂ gases, which in turn promoted protein adsorption in a reversible manner.²⁰⁷ Similarly, lysozyme adsorption to polyampholyte brushes was found to be pH- and thickness-dependent.²⁰⁸

Neutral hydrophilic polymer brushes can similarly give rise to high protein adsorption, and thermoresponsive brushes have received particular attention. Below the LCST, PNIPAM brushes were shown to give rise to primary adsorption (Figure 5), whereas a ternary mechanism seems to prevail above this transition.²⁰⁹ This is perhaps a reflection of the balance of interactions between proteins and brushes and their underlying substrate: at low temperature, chains are hydrated and interact weakly with proteins and substrate interactions dominate (primary adsorption), whereas, above the LCST, chain hydration decreases, giving rise to stronger ternary adsorption. Hence, this highlights the importance of substrate chemistry (or functionalization, for example, using self-assembled monolayers) for controlling protein adsorption below the LCST, especially at low grafting density.^{209,210} In addition, Halperin described that, upon collapse, the brush osmotic pressure decreases, and with it the penalty of insertion of a protein within the brush.²¹¹ This results in increased protein adsorption, as observed experimentally.^{151,154,209,212} In comparison, the behavior of proteins at the interface with other neutral fouling polymer brushes (i.e., those that do not resist the adsorption of proteins) has received less attention. Gorman and co-workers studied the adsorption of BSA at the surface of polyester brushes and found that this could be restricted by simple functionalization with PEG side chains.²¹³ AFM measurements showed that concanavalin A (Con A) adheres more strongly to thinner brushes, perhaps due to the increased polydispersity characteristic of thin brushes.²¹⁴ Wang et al. also reported the impact of monomer chirality on protein adsorption, although this effect was more pronounced on spin-coated films than on brushes.²¹⁵ Specific interactions with Con A were achieved via carbohydrate-functionalized brushes: mannose- and glucose-based brushes showed high affinity,

whereas galactose brushes did not display significant Con A adsorption.²¹⁶ Such lectin-immobilized polymer brushes can in turn further interact with glycosylated peptides or glycoproteins for their immobilization or enrichment. The type of carbohydrate and its density within the brush were found to strongly impact the binding of Con A: decreasing the mannose concentration (versus galactose) resulted in a switch from multiple- to single-ligand binding, but these results perhaps also highlighted the decreasing effect of release and rebinding mechanisms.²¹⁷ Xu et al. used boronic acid-containing brushes to immobilize and purify saccharides and glycoproteins such as horseradish peroxidase.²¹⁸ This strategy led to improved retention of the enzymatic activity of the immobilized protein compared to initiator-coated surfaces. Other neutral functionalized brushes display specific adsorption of proteins, and these will be discussed in the following sections.

2.4. Protein Resistance

On the other end of the spectrum, some polymer brushes display protein-resistant properties: these coatings do not show significant protein adsorption. Although this is relatively simple to achieve for single-protein solutions, even in the case of self-assembled monolayers, it is a much harder task in the case of more complex fluids such as blood, plasma, serum, saliva, and tissue culture medium, conditions to which many biomedical platforms are routinely exposed. Exposure of polymer brushes to such complex media is commonly monitored via surface plasmon resonance (SPR) or QCM to determine protein resistance. POEGMA was the first brush for which protein resistance from sera was reported: it showed no fouling (undetected, below 1 ng/cm²) from fibronectin, lysozyme, BSA, and fetal bovine serum (FBS, an important serum for cell culture applications; see Figure 7).^{82,219} Originally anchored to

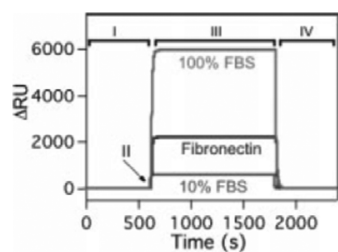


Figure 7. Adsorption of proteins to POEGMA brushes monitored by SPR. Reprinted with permission from ref 219. Copyright 2004 John Wiley and Sons.

silicon and gold surfaces, this brush was subsequently grafted from a variety of other surfaces^{98,220} without compromising protein resistance, therefore expanding its potential for biomedical applications. Similarly, PEG acrylamide brushes (with similar side chains but a polyacrylamide backbone) displayed excellent protein resistance when challenged with plasma.²²¹ Increasing the brush thickness, size of the oligo(ethylene glycol) side chains, or grafting density reduced protein adsorption.^{82,221,222} Fouling properties were very dependent on the nature of the medium used for the assay: whereas single-protein solutions and some sera (e.g., FBS) did not result in significant protein deposition (below 0.1 ng/cm²), other sera (e.g., whole horse serum, bovine serum, human serum), blood, and plasma resulted in somewhat higher protein fouling (in the range of 10–100 ng/cm²).^{223,224} However, even in contact with these more challenging media, POEGMA

brushes performed better than traditional protein-resistant self-assembled monolayers. The stability of POEGMA brushes during storage at ambient conditions and when exposed to cell culture conditions was also studied: it was found that methoxy-terminated brushes remained stable when stored for several weeks or during cell culture for more than 7 days,²²³ whereas hydroxyl-terminated POEGMA brushes showed poorer stability and detachment of the film after prolonged incubation times.²²⁵ This is perhaps a result of the presence of dimethacrylate in the commercially available hydroxyl-terminated monomers, hence producing cross-linked brushes for which stress-induced swelling in buffer may give rise to surface detachment.

Other neutral brushes displayed good to excellent protein resistance. Hence, PHEMA resisted well the adsorption of BSA, fibrinogen, and lysozyme (protein adsorption below 0.5 ng/cm²) and performed reasonably when challenged with human serum or plasma (adsorption near 5–10 ng/cm²).²²⁶ Protein deposition initially decreased with increasing brush thickness, reaching a plateau above 20 nm, before increasing again for thicker brushes (above 40–50 nm). Similar results were obtained for PHEMA-*co*-POEGMA brushes, and this trend correlated with the higher swelling and hydration of brushes of intermediate thickness (20–40 nm).²²⁷ It was found that the protein resistance of PHEMA brushes was strongly influenced by the grafting density too.^{228,229} Polyacrylamide brushes displayed a similar decrease in protein adsorption, reaching optimal antifouling properties above 30 nm (adsorption near 2 ng/cm² from human plasma and serum).²³⁰ Fibronectin adsorption to poly(oligo-2-oxazoline) brushes depended on the side chain length as well as the hydrophilicity of the brush (varied via the type of oxazoline side chain).²³¹ The adsorption of lysozyme, BSA, and fibrinogen to poly(D-gluconamidoethyl methacrylate) depended on the chain length, brush density, and protein size.²³² Similarly, fibrinogen and lysozyme adsorption to polypeptoid and PEG brushes (respectively) fell to low levels (below 10 ng/cm²) when chain packing reached a critical density, which depended on the brush length.^{233,234} Ishihara and co-workers found that the grafting density of PHEMA and PMPC brushes controlled the brush elastic repulsion and correlated well with fibrinogen repulsion.²³⁵

These results connecting brush thickness and density to protein resistance are mirrored by studies investigating the effect of dendritic coatings, suggesting that molecular crowding, brush hydration, and perhaps entanglement are important parameters preventing the infiltration of proteins through brushes,^{236,237} in the absence of strong brush–protein interactions and in line with predictions from models previously discussed.²¹¹ The impact of the brush chemical structure on the fouling properties (and even weak brush–protein interactions) is less clear though. Hence, extension of the side chain of PHEMA brushes by one methylene group increased protein adsorption from serum and blood by a factor of 2–4,^{226,238} but replacement of the methacrylate by a methacrylamide backbone and shifting of the hydroxyl to the 2-position resulted in no detectable protein adsorption from human plasma.^{224,239} Perhaps variations in brush hydration, swelling, and the associated rise in osmotic pressure are key to the understanding of such fouling behavior, as suggested by the study of related N-(hydroxyalkyl)acrylamide brushes via SPR and sum frequency generation vibrational spectroscopy.²⁴⁰

Differences in hydration have been proposed to account for the improved protein resistance of some zwitterionic polymer brushes compared to POEGMA. Low-field ¹H NMR and

differential scanning calorimetry showed that the first hydration layer was more tightly bound to free PMEDSAH chains than PEG chains, but that subsequent hydration layers were less so.²⁴² These measurements also pointed to a greater number of bound water molecules per sulfobetaine repeat unit, compared to ethylene oxide, but this may not be a fair comparison given the difference in size of the two monomers. Similarly, NMR, fluorescence spectroscopy, and AFM experiments designed to study interactions between lysozyme or bovine serum albumin and PEG and PMEDSAH polymers (free chains in solutions) provided evidence for weak hydrophobic and reversible interactions between these proteins and PEG, but not PMEDSAH.²⁴³ Molecular dynamics simulations gave further evidence of such differences in hydration between zwitterionic and oligo(ethylene glycol) repeat units as the hydration free energies of carboxybetaine and sulfobetaine are more than double that of tetrakis(ethylene glycol).²⁴⁴ In addition, the study found that the first hydration layer was more tightly bound to the negative center of carboxybetaine, compared to that of sulfobetaine, perhaps providing some insight into the superior antifouling performance of poly(carboxybetaine methacrylate) brushes PCBMA, poly(carboxybetaine methacrylamide) (PCBMAm), and poly(carboxybetaine acrylamide) (PCBAA), compared to PMEDSAH (Figure 8).²⁴¹ Similarly, sum frequency generation vibrational spectroscopy gave evidence of strong interfacial water association and ordering for PCBAA and, to a lesser extent, PMEDSAH brushes.²⁴⁵ This phenomenon was dependent on pH in the case of PCBAA and

was also strongly influenced by the presence of cations (in particular divalent cations).

Several studies found that PCBMA and its parent PCBA had superior protein-resistant properties compared to PMEDSAH and POEGMA,^{98,241,246} with protein depositions below the detection limit of SPR platforms.^{224,247} PMEDSAH, although showing excellent performance in many conditions,^{248–251} typically displays higher fouling from bovine and fetal bovine sera as well as plasma compared to PCBMA,²⁰⁴ despite their similarity of structure and hydrophilicity.²²⁴ Similarly, AFM studies also showed that strong electrostatic interactions, decreasing at high ionic strength, occur between arginine-glycine-aspartic acid (RGD) peptide-functionalized tips and PMEDSAH brushes.²⁵² Indeed, ζ -potential measurements performed on particles functionalized with PMEDSAH brushes displayed a residual negative potential, even at high ionic strength and in phosphate-buffered saline (PBS), which may account for the higher fouling of this brush.²⁰⁴ The origin of this negative potential is unclear.

QCM-D experiments also highlighted the important role of the ionic strength and the type of anions present in the medium to modulate protein adsorption on PMEDSAH brushes.²⁵³ It is also worth noting that some studies found increased adsorption to PCBMA compared to PMEDSAH using QCM to monitor the response of surfaces when challenged with FBS, hence contributing to making the structure–property relationship picture more complex.²⁵⁴ Changes in thickness had an effect on antifouling properties similar to that for neutral brushes: protein adsorption from plasma to PCBAA brushes was minimal for a thickness of 20 nm and increased again for thicker brushes.^{247,254} This increase was more pronounced than for neutral brushes though, perhaps owing to the fact that the UCST properties of some zwitterionic brushes are modulated by the brush thickness and polydispersity.¹⁶⁶ Interestingly, some correlation between the refractive index of dry PCBAA brushes and their protein resistance was observed.²⁵⁵ Although this is difficult to fully interpret, it may reflect differences in brush polydispersity and water affinity, which may play a role in controlling protein infiltration.²⁵⁶ A block copolymer architecture in which a block of PCBAA was grown over POEGMA was found to perform as well as PCBAA, suggesting that secondary adsorptions dominate in POEGMA brushes.²⁵⁷ The nature of the polymerizable group (forming the backbone of the brush) was not found to affect the fouling properties (note that this study refers to marine biofouling).²⁵⁸

The full elucidation of the proteome and nature of the macromolecules and objects that adsorb to polymer brushes should shed light on the various observations made and offer novel directions for the design of ultra-protein-resistant coatings for applications in medical diagnostics. In this respect two recent studies highlighted the importance of apolipoprotein adsorption, especially from low-density lipoprotein particles, to the fouling of polymer brushes.^{259,260} This phenomenon is important as it seems to contribute to the cooperative adsorption of other proteins such as fibrinogen and albumin. Although variations were observed when different brushes (POEGMA, PHEMA, and PMEDSAH) were compared, such a cooperative mechanism seems ubiquitous in the protein fouling of polymer brushes. Finally, other zwitterionic brushes, such as those based on poly((methacryloyloxy)ethyl phosphorylcholine) (PMPC),^{246,261} poly(serine methacrylate),²⁶² poly(lysine methacrylamide),²⁶³ poly(ornithine methacrylamide),²⁶³ and polyampholytes,^{163,246,264,265} have been reported to display low

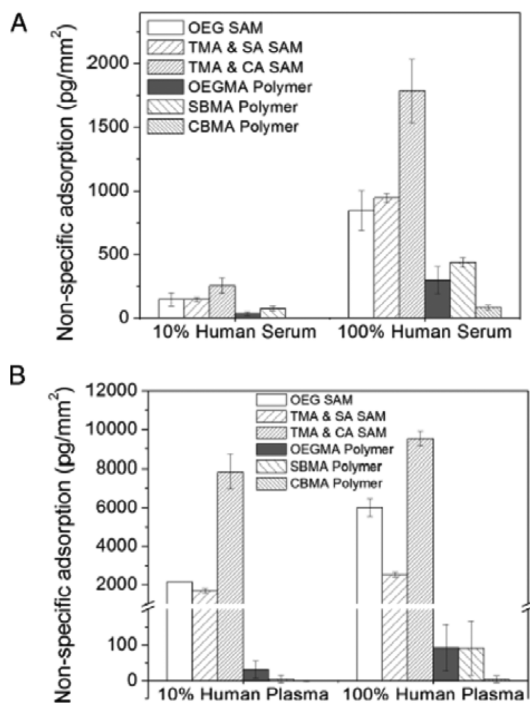


Figure 8. Protein resistance of polymer brushes when challenged with serum or plasma. OEG SAM, TMA & SA SAM, and TMA & CA SAM are oligo(ethylene glycol), 1-mercaptopro-11-N,N,N-trimethylammonium chloride/1-mercaptopro-11-undecanesulfonic acid, and 1-mercaptopro-11-N,N,N-trimethylammonium chloride/1-mercaptopro-11-undecanecarboxylic acid self-assembled monolayers, respectively; SBMA is named PMEDSAH in the present review. Reprinted from ref 241. Copyright 2008 American Chemical Society.

fouling properties similar to those of PMEDSAH. Some cationic brushes have been described to display antifouling properties, but this is surprising considering the strong adsorption of proteins at charged interfaces.²⁶⁶

2.5. Biofunctionalization of Polymer Brushes

2.5.1. Protein Adsorption. To display bioactive properties, polymer brushes typically have to be biofunctionalized with small molecules, peptides, and proteins. Some brushes display inherent bioactivity, but these are specific cases in which the brush chemical structure itself is based on bioactive repeat units, such as carbohydrates.^{206,216,267} Several strategies have been designed to achieve biofunctionalization, the simplest being to directly adsorb proteins onto brushes (Figure 9). To

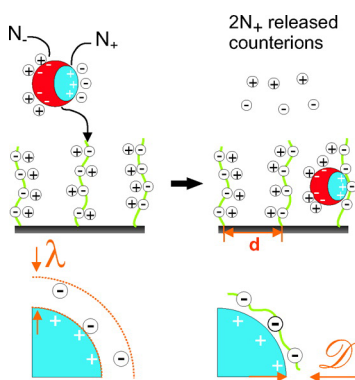


Figure 9. Adsorption of charged proteins to polyelectrolyte brushes. N_- = number of negatively charged residues at the protein surface, N_+ = number of positively charged residues at the protein surface, λ = Gouy–Chapman length, and D = thickness of the polyelectrolyte layer on the protein surface. Reprinted from ref 198. Copyright 2010 American Chemical Society.

do so robustly enough to sustain long-term immobilization, strong protein–brush interactions are required. Polyelectrolyte brushes are particularly attractive in this respect as they allow the immobilization of a very wide range of proteins without the requirement of added coupling agents. A key element is that such adsorption should preserve the protein activity, for example, to enable specific recognition or enzymatic catalysis. Ballauff and Wittemann used FTIR spectroscopy to probe the secondary structure of proteins immobilized in polyelectrolyte brushes. They found that the ratios of α -helix and β -sheets of proteins such as BSA, RNase A, and β -lactoglobulin adsorbed in PAA and poly(styrenesulfonate) (PSS) brushes remained almost unchanged compared to those of free proteins in solution.^{268,269} Importantly, the proteins displayed no further signs of denaturation after release from the brush and retained their enzymatic activity.^{270–273} However, the denaturation temperature of RNase A was decreased by 10 °C when adsorbed in PSS brushes, and this phenomenon was irreversible,²⁷⁴ suggesting that although adsorption to polyelectrolyte brushes does not directly give rise to denaturation for a wide range of proteins, it can decrease their stability. Horseradish peroxidase (HRP) activity decreased to 11% of the native enzyme activity when immobilized to PAA brushes, although such PAA-adsorbed HRP remained 1 order of magnitude more active than HRP directly adsorbed to silica.²⁷⁵ When HRP was desorbed from the brush by increasing the ionic strength of the buffer, only 52% of its activity was recovered, implying an irreversible denaturation within the

brush. Other proteins, such as bovine hemoglobin, were found to interact with the hydrophobic core of particles on which PSS brushes were grafted and subsequently denatured,²⁰² hence highlighting the influence and importance of the substrate.

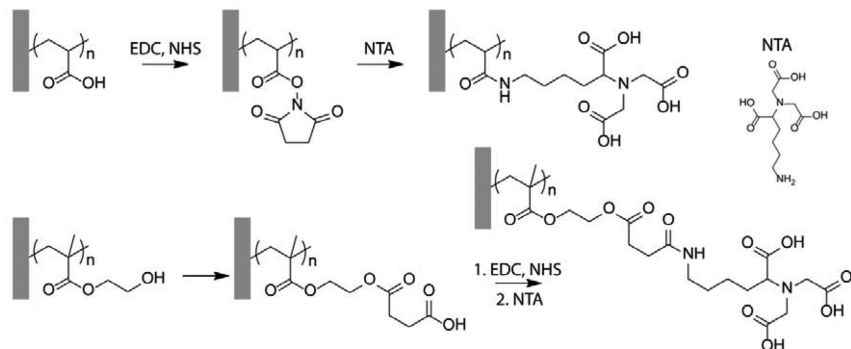
Another class of brushes that has received attention as a platform for protein adsorption is POEGMA.²⁷⁶ Interestingly, POEGMA is described as one of the ultra-low-fouling coatings, yet protein spotting followed by desiccation allows irreversible immobilization of antibodies on these brushes. This seems contradictory with the performance of POEGMA, even when challenged with undiluted serum. However, it is thought that, upon drying, dehydration of the brush and antibody results in increased protein–brush interactions and entanglement that prevent desorption of the protein when the surface is subsequently immersed in buffer. Even after sonication and washing with detergent (Tween-20), the spotted proteins remain anchored to the brush. Despite this dehydration, the protein remains functional and able to specifically recognize antigens in solution. Similarly, it was reported that collagen anchoring occurs on POEGMA brushes when a moderately concentrated collagen solution is directly removed from the brush surface without prior dilution.²²³ Although further studies are required to fully understand the nature of the protein immobilization process and how the protein conformation is preserved in dried brushes, such an immobilization platform has the advantage of being simple and versatile and has also been used for POEGMA-*co*-PGMA copolymer brushes.²⁷⁷ The intermediate hydrophobicity of POEGMA brushes, compared to other hydrophilic ultra-low-fouling brushes such as PCBA, may explain why dehydration can easily take place in mild conditions and result in immobilization while not fully perturbing the protein structure and function.

Other neutral polymer brushes such as PNIPAM also display protein adsorption above their transition temperature.^{151,209} In these cases, desiccation is not required, and it is the combination of brush collapse, the decrease in the osmotic pressure and hydrophobicity of the brush (and associated strength of protein–brush interactions) that result in protein adsorption, as discussed earlier. Hence, chain hydration also seems to be at the heart of protein adsorption to neutral LCST brushes, but the fact that such processes are reversible for LCST brushes implies weaker hydrophobic interactions, partial dehydration, less extensive chain entanglement, or a role of the osmotic pressure within the brush. Protein adsorption to PHEMA and its methoxy derivative poly(methoxyethyl methacrylate) (PMEMA) was also reported.²⁷⁸ In addition, glucosidase adsorption to PHEMA preserved its orientation and conformation, so that it was able to effectively bind Con A. It was not clear whether such behavior is preserved on PMEMA, but the difference in surface energy between these two brushes may again suggest that subtle changes in hydration are responsible for controlling protein adsorption.

2.5.2. Brush Functionalization with Small Molecules and Peptides. Simple protein adsorption does not always provide sufficient control of biofunctionality or may not be compatible with other requirements for the properties of the platform, such as low nonspecific binding of unwanted proteins and cells. Hence, it has been and is still necessary to develop selective biofunctionalization methods, compatible with charged, zwitterionic, and neutral brushes.

Functionalization of polymer brushes bearing carboxylic acids, such as PAA, or decorated with hydroxyl groups, as in PHEMA and POEGMA-OH (hydroxyl-terminated POEG-

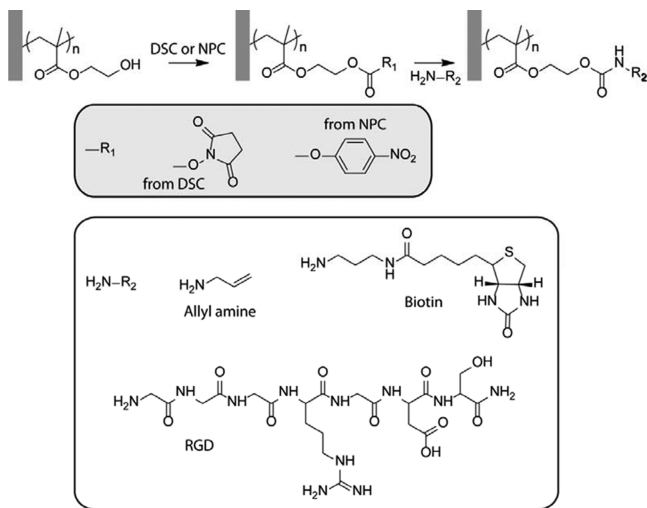
Scheme 1. Coupling of Small Molecules to Carboxylated Polymer Brushes



MA), extended with succinic or glutaric anhydrides, has most often been carried out via *N*-(3-(dimethylamino)propyl)-*N'*-ethylcarbodiimide hydrochloride (EDC)/NHS coupling (see Scheme 1). Nitrilotriacetic acid (NTA) was coupled to PAA brushes using a direct EDC/NHS coupling, which led to relatively high functionalization levels (>50%).^{279,280} Alternatively, succinic anhydride can be used to convert hydroxyl-terminated PHEMA brushes, prior to EDC/NHS coupling of NTA, to afford high-protein-binding-capacity membranes and particles.^{281,282} Alternatively, brushes such as poly(2-(methacryloyloxy)ethyl succinate) can be directly functionalized.^{283,284}

Similarly, amine-bearing small molecules, including short peptides, have been used to functionalize hydroxy-terminated brushes such as PHEMA and POEGMA-OH (Scheme 2). The

Scheme 2. Coupling of Small Molecules Bearing Primary Amines to PHEMA Brushes



two most favored coupling agents are disuccinimidyl carbonate (DSC)^{50,222,285} and 4-nitrophenyl chloroformate (NPC),^{61,286} although carbonyldiimidazole (CDI)²⁸⁷ has also been employed successfully. These coupling agents are attractive due to their availability and mild reaction at room temperature and the stability of the activated ester formed, even in contact with aqueous buffers, hence enabling efficient urethane formation.^{222,285} Biotin was coupled to POEGMA-OH brushes using DSC coupling, which led to a high biotinylation level and complete conversion of DSC-activated groups.²²² Similarly, Klok and co-workers found that NPC activation yielded high

densities of RGD peptide immobilization, and they were able to control this density via the starting concentration of peptide.⁶¹ Importantly, such functionalization was achieved with deprotected peptides. Differences in coupling efficiency between PHEMA and POEGMA are difficult to quantify on surfaces, but considering the difference in size of repeat units for these brushes, FTIR indicated comparable extents of peptide anchoring per repeat unit. Neutron reflectivity experiments revealed that functionalization of NPC-activated PHEMA brushes with amino acids (leucine and serine) depended both on the grafting density and on the brush height²⁸⁸ (Figure 10):

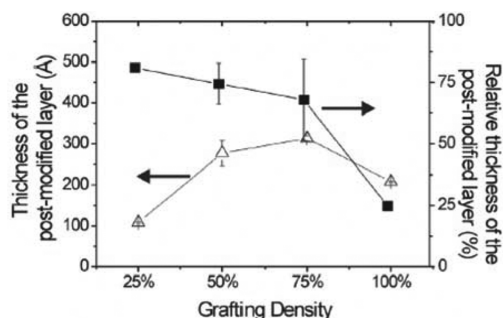
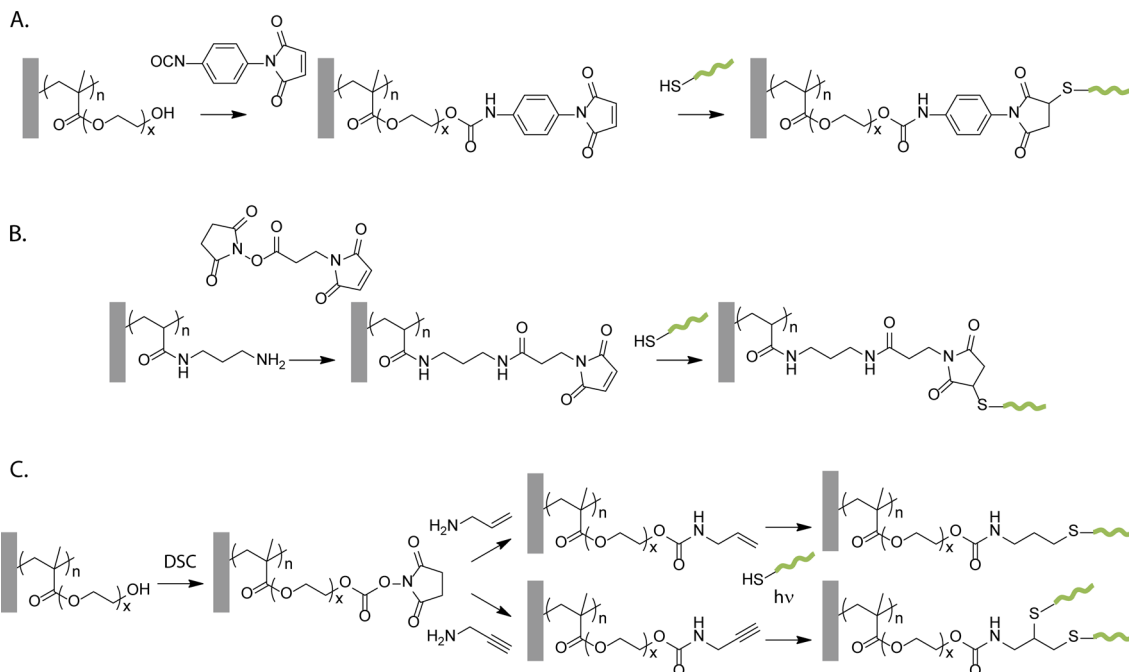


Figure 10. Impact of the PHEMA grafting density on amino acid functionalization after activation with NPC. Reprinted from ref 288. Copyright 2011 American Chemical Society.

denser brushes allowed functionalization only of the upper part of the brush (to a depth of 20 nm), whereas sparse brushes allowed more homogeneous coupling. The nature of the amino acid was also important as the bulkier and more hydrophobic leucine was found to be less reactive than serine. In contrast, the functionalization of PGMA brushes with propylamine was found to be homogeneous, as evidenced by X-ray photo-electron spectroscopy (XPS) studies.²⁸⁹ Considering that these observations were made for single amino acids, this has important implications for longer peptide sequences, which should react more slowly and should not diffuse as easily as single amino acids. Glycine-phenylalanine-hydroxyproline-glycine-glutamic acid-arginine (GFOGER), a 45-amino acid peptide, was coupled to POEGMA-OH and saccharide polymer brushes (2-gluconamidoethyl methacrylate) using NPC activation.^{286,290} Peptide densities of 20 and 8.5 ng/cm², respectively, were calculated from SPR measurements, clearly corresponding to submonolayer levels, highlighting the difficulty of functionalizing protein-resistant polymer brushes with even moderately large peptide sequences and proteins. Zhao et al. functionalized POEGMA-OH brushes with

Scheme 3. Coupling of Cysteine-Bearing Peptides to Polymer Brushes^a

^aIn (A) and (B), the peptides (in green) are coupled to brushes activated with maleimide residues. In (C), the peptide is coupled to the brush via a thiol–ene or thiol–yne reaction, mediated by UV irradiation in the presence of a photoradical generator.

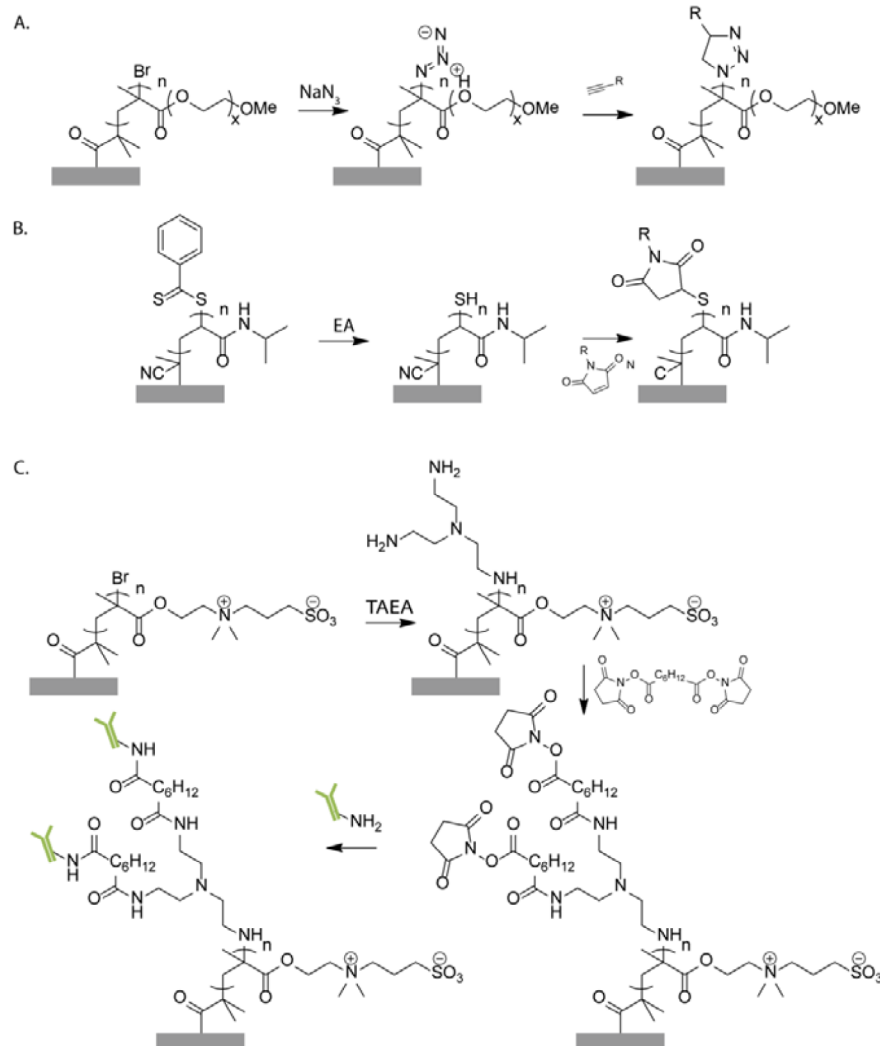
titanium phosphonate moieties via CDI coupling to allow the selective capture of phosphorylated peptides.²⁸⁷ Glinel et al. activated POEGMA-OH brushes with *N*-(*p*-maleimidophenyl)isocyanate before further functionalization with a cysteine-terminated peptide (magainin 1, 23 amino acids; see Scheme 3A).²⁹¹ An excellent correlation between the content of hydroxyl-terminated monomer and the resulting peptide density was observed. A similar maleimide–cysteine strategy was used to decorate cationic brushes with Tet-213 peptides (10 amino acids; see Scheme 3B).²⁹² In this case, primary amines on the brush side chains were functionalized with an *N*-hydroxysuccinimide maleimide linker, enabling further reaction with cysteine residues. The coupling efficiency was high (near 15 peptides/nm²), particularly at low brush grafting density. Costa et al. used thiol–ene and thiol–yne chemistry to couple peptides to POEGMA brushes functionalized with allylamine and propargylamine via cysteine residues (see Scheme 3C).²⁹³ This allowed the photoactivation of the conjugation step using a photoradical initiator. The density of tethered peptides was controlled simply via changing the peptide concentration during the coupling step. The reaction of alkyne-functionalized RGD peptides with azido-PGMA derivatives also enabled efficient peptide coupling to poly(vinylidene difluoride) (PVDF) substrates.²⁹⁴

It is also possible to exploit the residual chemistry arising from brush growth to selectively functionalize the end chains of brushes. Indeed, the ATRP process results in halogenated end chains, which can be further functionalized, in particular in the case of brominated chains, via nucleophilic substitution with sodium azide, followed by 1,3-dipolar cycloaddition with alkynes (Scheme 4A).²⁹⁵ This process allowed the efficient biotinylation of POEGMA brushes without requiring modification of the side chain chemistry. Similarly, brushes grown via a RAFT process are capped with a chain-transfer agent such as a dithiobenzoate group which can be transformed via

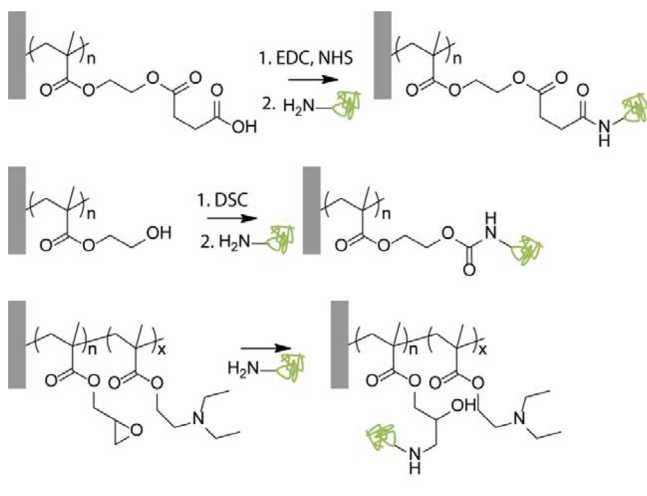
aminolysis into a terminal thiol (Scheme 4B). This thiol can then be reacted with maleimide derivatives, resulting in specific end chain functionalization.²⁹⁶

Another successful approach for brush functionalization consists of growing reactive polymer brushes. PGMA brushes have received particular attention owing to their well-controlled growth, availability of the monomer, and efficiency of functionalization. Amines, as well as other nucleophiles,^{297,298} result in efficient opening of the epoxide in mild conditions.²⁹⁹ This strategy was used to generate metal-chelating brushes after reaction of iminodiacetic acid or imidazole with PGMA.³⁰⁰ Interestingly, copolymer brushes of PGMA and PDEAEMA displayed enhanced rates of reaction with a variety of primary amines, at room temperature, in aqueous conditions.³⁰¹ Other types of chemistries have also been exploited. Patton and co-workers reported the simple functionalization of alkyne brushes with a variety of thiols, via photoirradiation,³⁰² and azidopropyl methacrylates can be functionalized with alkynes via 1,3-dipolar cycloaddition.³⁰³ The direct coupling of oligonucleotides to copolymer brushes of POEGMA, PMMA, and the bioreactive poly(formylphenyl methacrylate) has also been explored.³⁰⁴

2.5.3. Protein Coupling and Binding. Similar strategies have been used to anchor proteins to polymer brushes. As for functionalization with small molecules, brushes bearing carboxylic acids have been activated using EDC/NHS before incubation with avidin,³⁰⁵ streptavidin,²²² silk sericin,³⁰⁶ collagen,³⁰⁷ chitosan,³⁰⁸ RNase A,²⁸⁰ fibronectin,³⁰⁹ and bone morphogenetic protein 2 (Scheme 5).³¹⁰ Neutral brushes such as PHEMA and POEGMA were also activated using CDI, NPC, and DSC to couple lysozyme,³¹¹ fibronectin fragments,^{312,313} streptavidin,²²² and antibodies (Scheme 5).³¹⁴ Other strategies have consisted of direct coupling to halogenated³¹⁵ and aldehyde-functionalized^{316,317} brushes as well as poly(azlactone) (PAzL)³¹⁸ and PGMA brushes.³¹⁹ Protein coupling to negatively charged carboxylic acid brushes

Scheme 4. End Functionalization Strategies for the Generation of Biofunctional Polymer Brushes^a

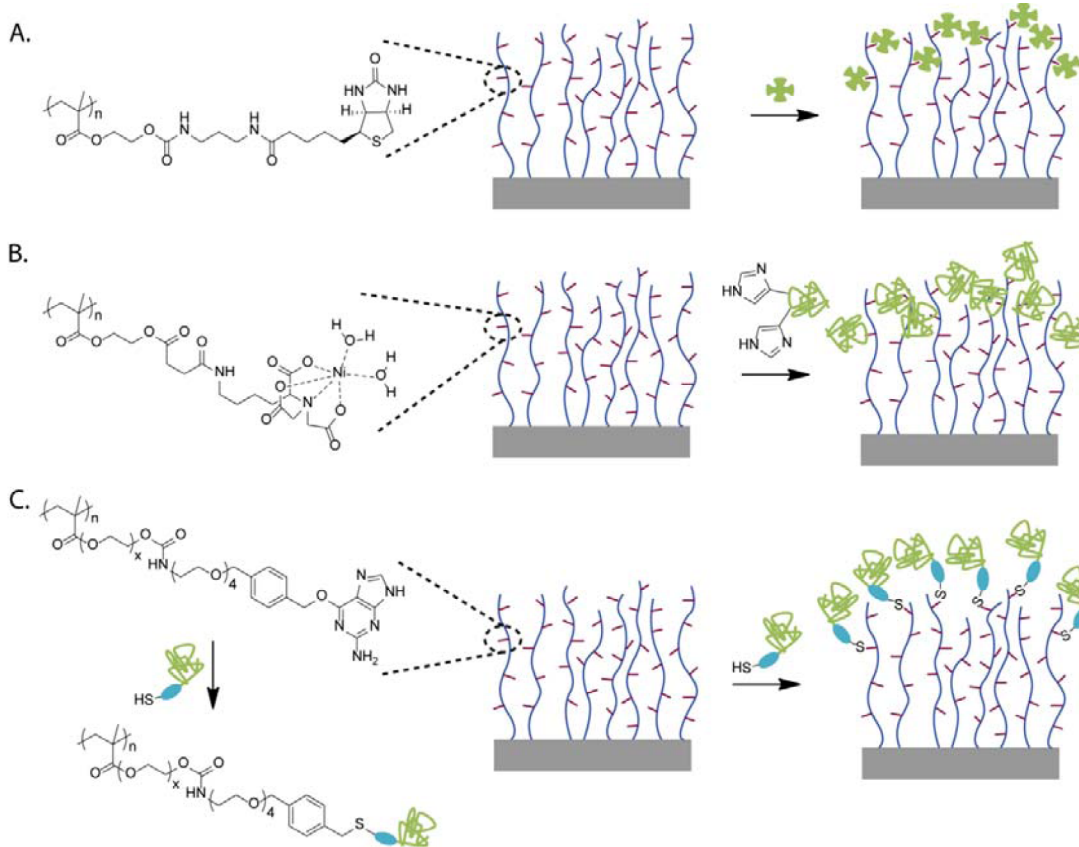
^aKey: (A) azide–alkyne click chemistry from ATRP-grown brushes; (B) thiol–maleimide coupling at RAFT-grown brushes (EA = 2-ethanolamine; (C) antibody coupling to the end chain of ATRP-grown brushes (TAEA = tris(2-aminoethyl)amine).

Scheme 5. Direct Protein Coupling to Polymer Brushes

was typically high (for example, 2–6 $\mu\text{g}/\text{cm}^2$),^{280,307} corresponding to several monolayers of proteins and implying diffusion and loading of proteins throughout the brush. This is

perhaps not surprising given the high swelling of charged brushes (e.g., PAA) and the role of electrostatic interactions in mediating protein loading into the brush. Neutral brushes were also found to give rise to high protein densities (1–10 $\mu\text{g}/\text{cm}^2$), in particular in the case of reactive brushes such as PAzL³¹⁸ and PGMA.^{319,320} When PGMA was copolymerized with PDEAEMA, protein coupling was increased as a consequence of the combined effects of protein attraction to the charged PDEAEMA and its autocatalytic effect on the opening of epoxide groups by primary amines (Scheme 5).³⁰¹ In such cases again, high protein densities suggest penetration of the brush by proteins, rather than simple surface functionalization, as further confirmed by the typical increase in bound protein mass as a function of brush thickness.^{318,319}

Protein anchoring to antifouling brushes is typically more challenging, and immobilization levels are often significantly lower (below 1 $\mu\text{g}/\text{cm}^2$) than for peptides and other small molecules.^{222,224,312} This is perhaps linked to the fact that there is no driving force to promote protein infiltration through such brushes and proteins do not spend significant amounts of time within the brush to couple to reactive groups. Hence, efficient coupling to antifouling brushes relies on two main strategies:

Scheme 6. Tethering of Proteins to Polymer Brushes via Protein Tags^a

^aKey: (A) Streptavidin capture by biotinylated brushes can subsequently allow the coupling of biotinylated proteins. (B) Nitrilotriacetic acid-functionalized brushes allow capture of histidine-tagged proteins. (C) Benzylguanine-functionalized POEGMA brushes allow the selective coupling of AGT-tagged proteins.

(1) the use of coupling agents stable enough in aqueous buffers to allow longer incubation times with moderate hydrolysis;²²² (2) the generation of temporary charges after activation of polyzwitterionic and polyampholyte brushes.^{321,322} In the latter case, the attractive electrostatic force between the brush and protein allows sufficient local protein concentration to achieve coupling before hydrolytic deactivation of the coupling agent (e.g., it was reported that NHS esters on PCBA have a half-life of 10 min).^{321,323} It is therefore not surprising that protein coupling is sensitive to the buffer pH and potentially pI of the protein to be anchored.³²³ In both cases, the protein densities achieved are typically in the range of 100–500 ng/cm², corresponding to monolayers or bilayers of proteins. Such extents of coupling imply poor protein infiltration and only surface functionalization for dense antifouling brushes. Results obtained for block copolymer brushes, for which the second block has a lower grafting density, typically show increased functionalization, which supports this view.^{324,325} In addition, the protein density does not increase significantly when the brush thickness is increased without changing the brush density.³²²

Finally, to control the orientation of the proteins when anchored to the brush and maximize the specificity of the coupling, several approaches have been designed that make use of protein tags already ubiquitous in biochemistry (Scheme 6). Hence, biotinylated and streptavidin-loaded brushes have been used to immobilize biotinylated proteins and antibodies.^{50,222,295} This typically resulted in relatively high protein

loading, even when incubation was performed at low concentration (below 10 µg/mL), with buffer also containing other proteins. Another popular anchoring method is via the use of metal complexes that can selectively bind oligohistidine residues (His-tag), a tag that is commonly used for the purification of recombinant proteins. Copper and nickel complexes of NTA have been coupled to PAA,²⁸⁰ PMAA,³²⁶ poly(2-(methacryloyloxy)ethyl succinate) (PMES),²⁸⁴ PHEMA,²⁸¹ POEGMA,⁵¹ and PAzL³¹⁸ brushes to capture enzymes and His-tagged proteins (Figure 11). Remarkably, charged PAA and PMES brushes which swell to high degrees were able to bind high densities of proteins (>10 µg/cm²), whereas immobilization on neutral brushes was lower (near or below 1 µg/cm², corresponding to 1–3 monolayers of densely packed adsorbed proteins). Although neutral brushes also bear a negative charge after NTA functionalization, their conformational change remains limited (swelling below 100%) compared to that of the highly charged PAA and PMES brushes.⁵¹ Such low swelling may not be sufficient to enable extensive infiltration of proteins. Klok and co-workers functionalized PHEMA and POEGMA brushes with benzylguanine residues, which can subsequently allow the coupling of alkylguanine–DNA–alkyltransferase (AGT) fusion proteins.³²⁷ Although AGT is a relatively bulky tag and requires the preparation of specific recombinant proteins, this approach offered an excellent control of protein orientation in mild and dilute conditions.

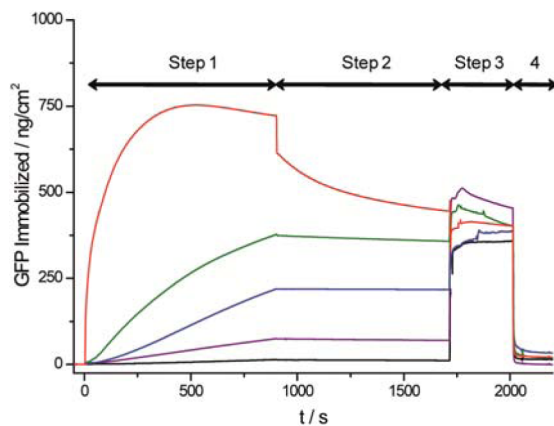


Figure 11. Stable immobilization of His-tagged green fluorescent protein (GFP) onto NTA-POEGMA brushes. His-GFP concentrations were 13.4 $\mu\text{g}/\text{mL}$ (red), 6.7 $\mu\text{g}/\text{mL}$ (green), 1.34 $\mu\text{g}/\text{mL}$ (blue), 335 ng/mL (purple), and 67 ng/mL (black). Reprinted from ref 51. Copyright 2010 American Chemical Society.

Hence, a variety of biofunctionalization strategies have been developed to confer bioactivity to polymer brushes, making use of the brush chemistry and architecture and the introduction of selective tags. Such brush-based platforms have been designed for applications in biosensing, cell culture, and tissue engineering, as antibacterial coatings, and for protein purification and membrane technologies. Examples of such platforms are discussed in the remaining sections of this review.

3. APPLICATIONS TO MEMBRANE SCIENCE AND SAMPLE PURIFICATION

3.1. Surface Coating for Membrane Applications and Sample Purification

3.1.1. Polymer Brushes Grown from a Variety of Membranes. The ability to functionalize a wide range of surfaces with polymer brushes has been particularly useful for modifying the properties of membranes and stationary phases used for sample purification (Table 1). Hence, both polymeric, such as PVDF (see Figure 12),^{220,328–330} poly(ether ether ketone) (PEEK),¹⁰⁶ hydroxylated nylon,²⁸³ polyester,³³¹ cellulose,^{332,333} poly(ether sulfone),¹⁰⁷ and poly(ether sulfone ketone),³³⁴ and inorganic (anodic alumina²⁸¹) membranes have been used as supports for the growth of polymer brushes. In the case of surfaces presenting reactive hydroxyl groups, the initiator function for the ATRP process was coupled to the membrane via silanes or acyl bromides, a standard approach in this field. Membranes lacking such reactive groups were functionalized via a polyelectrolyte multilayer assembly terminated by the deposition of a cationic macroinitiator^{107,335} or after activation using ozone/oxygen,^{220,336} 3,4-dihydroxyphenylalanine (DOPA),³²⁸ sodium borohydride,¹⁰⁶ or formaldehyde.²⁸³

3.1.2. Performance and Application of Brush-Functionalized Membranes for Sample Purification, Separation, and Filtration. Primarily, POEGMA has been grown from these membranes to confer antifouling properties. PHEMA-based,^{107,328,338} PMES-based,²⁸³ PMEDSAH-based,³³⁹ and PNIPAM-based³³² systems were also developed to allow further functionalization, improve the hydrophilicity of the coatings, or confer temperature responsiveness. For example, zirconium oxide membranes functionalized with

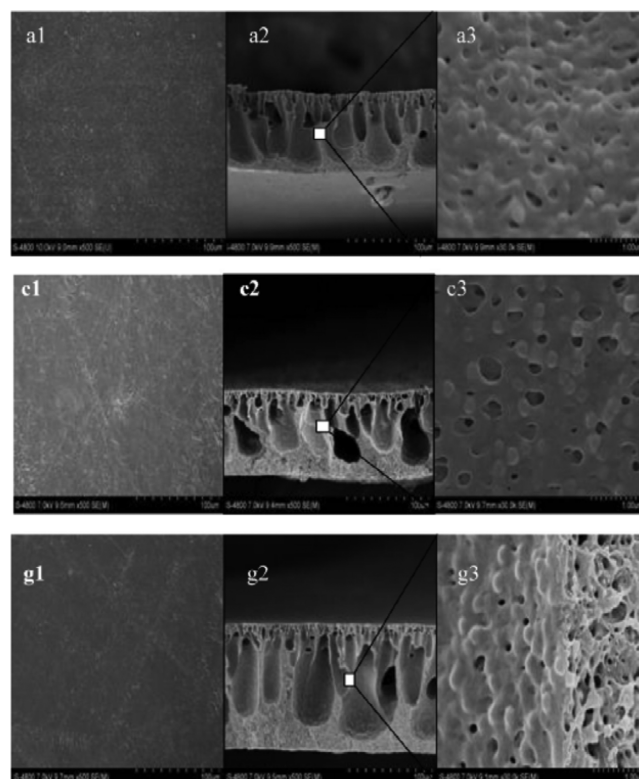


Figure 12. Morphology of PVDF membranes (top row) and PVDF membranes modified with PHEMA and PDMAEMA-*b*-PHEMA brushes (middle and bottom rows, respectively). Reprinted with permission from ref 328. Copyright 2012 Elsevier.

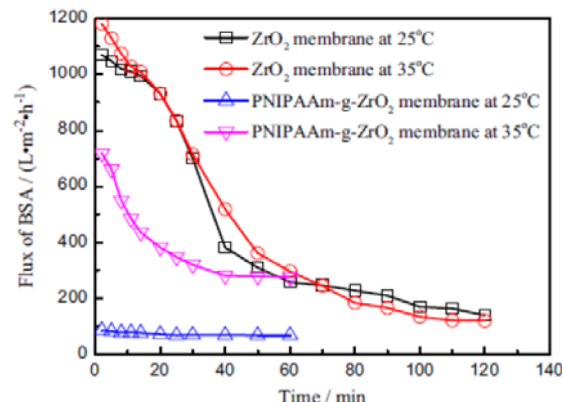


Figure 13. Variation in filtration flux of a BSA solution using zirconium oxide membranes functionalized with PNIPAM. Reprinted with permission from ref 337. Copyright 2014 Elsevier.

PNIPAM displayed antifouling properties at low temperatures and self-cleaning properties with good flux recovery (near 80%, Figure 13).³³⁷ The resulting membranes were used for sample purification and filtration: the effect of the grafting of brushes on initial sample flux was ambiguous as the associated increase in membrane hydration and reduction in pore size had opposite effects on the flux through the membrane.^{328,334,336,340,341} However, in all cases, flux recovery was significantly increased (above 90%) and the stability of the system over repeated or prolonged filtration cycles was greatly improved.^{328,332,334,336} Such performance is proposed to be the result of the marked reduction in protein adsorption to POEGMA surfaces, preventing gradual clogging of the membrane. Hence,

Table 1. Polymer Brushes Applied to Membrane Science and for Sample Purification^a

brush	substrate	initiator	application	assay	ref
POEGMA	PVDF	ozone treatment, BiBB	ultrafiltration	monitoring of permeation flux	250
PHEMA, POEGMA, PDMAEMA	PVDF	directly from PVDF	ultrafiltration	monitoring of permeation flux	329
PBVbpy	PVDF	ozone, then BIEM	microfiltration	monitoring of permeation flux	330
POEGMA, PNIPAM, PSPMA	PEEK	NaBH ₄ , then BiBB	microfiltration	membrane preparation only	106
POEGMA, POEGMA- <i>co</i> -PDEGMA	PETE	ethane/ammonia plasma	controlled delivery	permeation profile	331
PNIPAM, PNIPAM- <i>b</i> -POEGMA	cellulose	BiBB	ultrafiltration	monitoring of permeation flux	332
PHEMA	PES	cationic macroinitiator	sample purification	membrane preparation only	107
POEGMA	PPESK	chloromethylation in sulfuric acid	ultrafiltration	monitoring of permeation flux	334
PMES	hydroxylated nylon	cationic macroinitiator	sample purification	hydraulic permeability, protein binding	335
POEGMA, PMMA	PVDF	UV, air	microfiltration	monitoring of permeation flux	336
PHEMA, PDMAEMA, PDMAEMA- <i>b</i> -PHEMA	PVDF	PDOPA, then BiBB	ultrafiltration	monitoring of permeation flux	328
PHEMA	PES/silica	APTMS, RAFT agent	ultrafiltration	monitoring of permeation flux	338
PNIPAM	ZrO ₂	silane methacrylate	sample purification	monitoring of permeation flux, protein adsorption	337
POEGMA	PVDF	plasma	blood-compatible membranes	protein adsorption, blood compatibility	340
POEGMA	cellulose	BiBB	ultrafiltration	monitoring of permeation flux	341
PAAm	glass	TCCMPE	protein separation	capillary electrophoresis	342
POEGMA	glass	APTES, then BiBB	protein separation	capillary electrophoresis	343
PMEDSAH	SiO ₂ particles	RAFT silane	sample purification	protein binding	344
PNIPAM- <i>co</i> -PAEMA	gold	AIBN thiol derivative	sample purification	protein binding	345
NTA-PAA	gold	MUBiB	sample purification	protein binding	279
NTA-PAA	silicon	silane ATRP initiator	sample purification	protein binding	280
NTA-PHEMA	alumina	silane ATRP initiator	sample purification	protein binding	281
NTA-PMES	gold	MUBiB	sample purification	protein binding	284
NTA-PMES	nylon	formaldehyde, then silane ATRP initiator	sample purification	protein binding	283
NTA-PHEMA	magnetic nanoparticles	silane ATRP initiator	sample purification	protein binding	282
NTA-PAA	silicon	silane ATRP initiator	sample purification	protein binding	318
NTA-PHEMA, NTA-POEGMA	gold	MUBiB	sample purification	protein binding	51
POEGMA	magnetic nanoparticles	APTES, then BiBB	phosphopeptide enrichment	MALDI-TOF	287
PGMA	magnetic nanoparticles	silane ATRP initiator	glycopeptide enrichment	MALDI-TOF	346

^aAbbreviations: PVDF, poly(vinylidene difluoride); BiBB, 2-bromoisobutyryl bromide; PBVbpy, *N*-benzyl-*N*-(4-vinylbenzyl)-4,4'-bipyridinium dichloride; BIEM, 2-((2-bromoisobutyryl)oxy)ethyl methacrylate; PEEK, poly(ether ether ketone); PETE, track-etched polyester; PES, poly(ether sulfone); PPESK, poly(phthalazinone ether sulfone ketone); PDOPA, 3,4-dihydroxy-L-phenylalanine; APTMS, (aminopropyl)trimethoxysilane; TCCMPE, 1-(trichlorosilyl)-2-(*m,p*-(chloromethyl)phenyl)ethane; PAEMA, poly(2-aminoethyl methacrylate hydrochloride); MUBiB, 11-mercaptop-1-undecyl 2-bromoisobutyrate; NTA, nitrilotriacetic acid; PMES, 2-(methacryloyloxy)ethyl succinate; MALDI-TOF, matrix-assisted laser desorption/ionization time of flight.

polymer-brush-functionalized membranes may be useful for the purification of complex and concentrated samples such as blood³⁴⁰ in hemodialysis. In addition, eluted proteins could be separated on the basis of their size and charge^{178,329,341,342} following the change in pore size distribution and surface chemistry of the membrane or stationary phase since these parameters alter the molecular weight cutoff. This offers interesting opportunities for the design of improved chromatography and electrophoresis systems for protein separation and purification. For example, POEGMA coatings were used to decrease nonspecific binding and improve protein separation in capillary electrophoresis.³⁴³ PMEDSAH brushes were also used for the purification of glycopeptides.³⁴⁴

3.2. Protein Capture with Binding Elements

Although nonbiofunctionalized cationic brushes have been used for nonspecific protein fractionation,³⁴⁵ the ease with which polymer brushes, including those displaying low fouling, can be

functionalized has led to the development of several platforms for reversible protein capture, for protein purification, even from complex protein mixtures such as serum (Table 1). Ni-NTA has been the most extensively studied system, owing to the simplicity of the chemistry involved, the efficiency of the protein capture and its reversibility, and the ubiquity of His-tagged proteins in recombinant protein synthesis and purification (Figure 14). The brush 3D architecture offers an important advantage in terms of maximum loading level, especially in the case of negatively charged brushes characterized by higher swelling. Hence, high binding capacities (1–10 µg/cm² for 2D support substrates and near 100 mg/cm³ for 3D membranes) were typically measured.^{280,281,283,318,335} Such systems are particularly attractive for protein purification, even from complex protein solutions such as serum. In addition, adaptation of these brushes to magnetic particles allowed magnetic purification of proteins directly from cell lysates.²⁸² Neutral-brush-based systems are characterized by

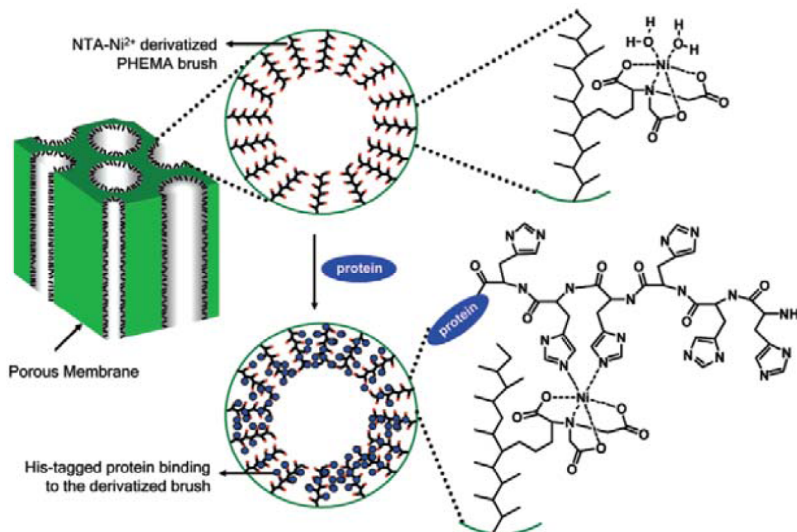


Figure 14. Polymer-brush-functionalized membranes for His-tagged protein purification. Reprinted from ref 281. Copyright 2007 American Chemical Society.

lower capacities (below 1 $\mu\text{g}/\text{cm}^2$), owing to a combination of modest swelling and reduced NTA ligand density. However, their systems displayed excellent capture stability as a result of rebinding and retained their protein resistance, hence allowing specific protein immobilization and patterning.⁵¹ Similarly to these Ni–NTA systems, titanium phosphate-functionalized brushes have been explored for the specific binding of phosphorylated peptides, which could be extended to proteins, for the detection and purification of phosphorylated species and proteomics (Figure 15).²⁸⁷ Hydrazine-functionalized PGMA brushes were developed for the enrichment of glycosylated peptides.³⁴⁶

4. POLYMER BRUSH-BASED BIOSENSING PLATFORMS

4.1. Types of Polymer-Brush-Based Sensing Platforms

Polymer-brush-based biosensing platforms fall into three main categories (Figure 16): (1) label-free detection systems in which an analyte is directly bound and sensed; (2) label-based systems in which the brush allows the binding of an analyte, with subsequent detection using a labeled molecule such as an antibody; (3) mass-amplification systems in which detection of a surface-bound analyte is amplified via the mass gain associated with surface-initiated polymerization.

4.1.1. Label-Free Biosensing. Label-free detection of analytes is particularly interesting for sensing applications as it allows fast detection of pathogens or biomarkers, potentially live, with minimal sample handling and incubation steps. Such detection methods rely on the sensing of mass or refractive index changes at the surface of the biosensor, and thus, the brush architecture and nonspecific protein adsorption to its surface (or the underlying substrate) are critical to the sensor performance, in addition to the affinity and selectivity of the sensing motif. Label-free detection platforms in which polymer brushes have been employed include QCM,³⁴⁷ SPR,^{247,277,321,324} localized surface plasmon resonance (LSPR),³⁴⁸ pulsed streaming potentiometry,³⁴⁹ and voltammetry.³⁵⁰ Among these techniques, QCM offers advantages as it has a wider sensitivity depth (with an extinction depth near 250 nm, compared to 70–150 nm for SPR^{50,351}) and provides

information on bound mass as well as the viscoelastic properties of the adsorbed layer (via the dissipation energy data).³⁵¹ SPR detection offers the advantage of being compatible with protein microarrays, hence potentially enabling parallel detection of several analytes.³⁵² It is disputable whether polymer brushes are appropriate for LSPR applications as this technique is typically associated with a short extinction depth.⁹ Nevertheless, platforms based on protein-fouling boronic acid-based brushes

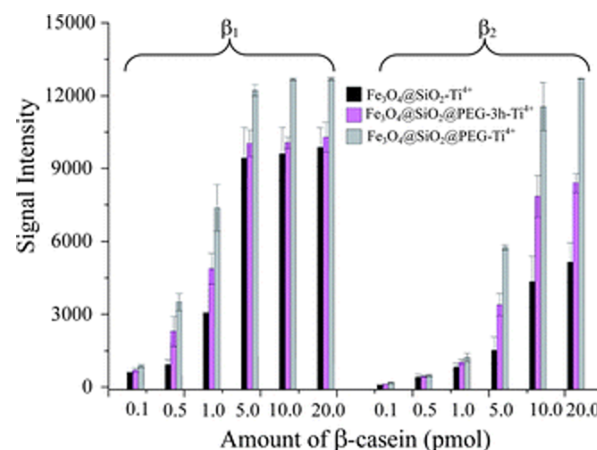


Figure 15. Enrichment of phosphopeptides using titanium phosphate-functionalized brushes. Reprinted with permission from ref 287. Copyright 2012 The Royal Society of Chemistry.

suggest LSPR displays a useful sensing range for detecting the binding of ovalbumin and avidin (limit of detection, LOD, of 100 nM and 1 μM , respectively) and subsequent antibody-based assay.³⁴⁸

4.1.2. Biosensing Based on Immunoassays and Fluorescent Tag Labeling. Other detection methods such as enzyme-linked immunosorbent assay (ELISA) and fluorescence microscopy offer advantages in terms of detection sensitivity and specificity. These techniques are less affected by the nonspecific binding typically occurring in complex samples from blood, serum, or saliva, owing to a combination of antibody specificity and the ability to use blocking steps during

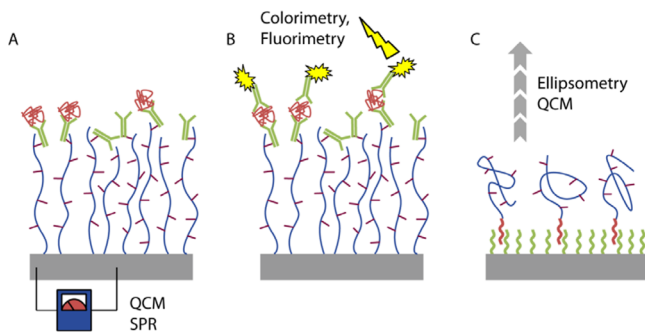


Figure 16. Three main categories of polymer-brush-based biosensing platforms: systems relying on label-free detection (A), label-based detection (B), and mass amplification (C). The binding of analytes can be detected by a number of techniques (typical examples are indicated next to each panel).

the assay. Polymer brushes have been utilized to develop such ELISA^{295,353} and fluorescence^{354,355} assays. Such platforms have been described to capture relatively high levels of

antibodies, preserve their specificity, and confer improved signal-to-noise ratios. In addition, these platforms are particularly amenable to microarraying^{276,319,356} for parallel detection of several biomarkers. Ober and co-workers used 2,4-dinitrophenyl (DNP)-functionalized POEGMA brushes to capture anti-DNP antibodies and detect their adsorption via the generation of hydrogen peroxide catalyzed by the antibody using voltammetry.³⁵⁰ Others have used a fluorescence reporter (PicoGreen) to measure the pairing of single-stranded DNA immobilized on PDMAEMA brushes.³⁵⁷ Concentrations of single-stranded DNA down to 30 pM were measured, but the limit of detection of the sensor in serum was more modest (micromolar range). A similar approach was reported, this time using streptavidin–horseradish peroxidase detection, for the identification of single-base mismatch, down to concentrations of 10 fmol.³⁵⁸

The process of surface-initiated controlled radical polymerization itself also presents interesting features for biosensor design: it is specific to a certain type of function (e.g., halogenated initiators in the case of ATRP), can tolerate a wide range of chemistries, and results in high mass amplification. In

Table 2. Polymer Brushes Used for Biosensing Applications^a

brush	substrate	initiator	biofunctionalization	assay	LOD	ref
PGMA- <i>co</i> -PDEAEMA	Ta ₂ O ₅	silane ATRP initiator	direct coupling to PGMA via primary amines	fluorescence (biotin–streptavidin and immunoassay)	~1 nM	319
PGMA- <i>co</i> -POEGMA	gold	cysteamine, then BiBB	direct coupling to PGMA via primary amines	SPR	20–100 ng/mL	277
POEGMA- <i>co</i> -PAA	cyclic olefin copolymer	NA	NHS-activated PAA	fluorescence (immunoassay)	~1 ng/mL	359, 360
POEGMA- <i>co</i> -PGMA	glass	APTES, then BiBB	direct coupling to PGMA via primary amines	fluorescence (competitive immunoassay)	3–4 pg/mL	361
POEGMA	glass	silane ATRP initiator	infiltration into POEGMA brushes and partial dehydration	fluorescence (immunoassay)	1–10 pg/mL	276
POEGMA	PDMS	alkene-functionalized ATRP initiator	bromoacetic acid, then EDC/NHS coupling of antibody	ELISA	20–700 pg/mL	362
POEGMA	magnetic nanoparticles	silane ATRP initiator	azide–alkyne click chemistry	DNA hybridization with fluorescence detection	0.5 pM	363
POEGMA	gold	MUBiB	DSC-mediated coupling of streptavidin	DNA hybridization and antibody capture, SPR	NR, clinical samples	364
PNIPAM	ITO	silane RAFT initiator	azide–alkyne click terminal functionalization with antibody	electrochemical detection of CdSe conjugate	1–10 pg/mL	365
PCBAA	gold	MUBiB	EDC/NHS coupling of antibody	immunoassay, SPR	NR, <5 ng/mL in blood serum	247, 321, 323
PCBAA, PHEMA	gold	MUBiB	EDC/NHS or DSC coupling of antibody	immunoassay for detection of bacterial strain, SPR	~6 × 10 ⁴ cells/mL	366
PHPMAm	gold	MUBiB	DSC coupling of antibody	immunoassay, SPR	NR, <600 ng/mL	224
PCBAA	gold	photoiniferter thiol, MUBiB	EDC/NHS coupling of antibody	SPR	<1 μg/mL	324, 325, 367
PMAMPC	gold	NA	biotinylation via EDC/NHS coupling	SPR	1.5 nM in blood plasma	368
POEGMA- <i>b</i> -PAA	cycloolefin polymer	photoiniferter	EDC/NHS coupling of antibody	fluorescence (immunoassay)	<50 μg/mL	369
POEGMA	photopolymerized polymer	photoiniferter	PEGylated antibody monomer used during brush growth	ELISA	1 pM	355
POEGMA, PHEMA	gold	MUBiB	coupling of streptavidin via a range of reagents	SPR and immunoassay	1 ng/mL	222
PAA	gold and silicon	MUBiB	biotinylation	SPR	NR	370
PMPC	gold	MUBiB	none	LSPR	50 ng/mL	371
PAA- <i>co</i> -PDMAEMA	graphene	none (UV)	EDC/NHS coupling	FET	NR	372
PGMA	glass	APTES, then BiBB	direct antibody capture (via boronic acids)	fluorescence (immunoassay)	10 pg/mL	373

^aAbbreviations: LOD, limit of detection; BiBB, 2-bromoisobutyryl bromide; NA, not applicable; APTES, (aminopropyl)triethoxysilane; MUBiB, mercapto-1-undecyl 2-bromoisobutyrate; NR, not reported; PMAMPC, poly(methacrylic acid-*ran*-2-(methacryloyloxy)ethyl phosphorylcholine); FET, field effect transistor.

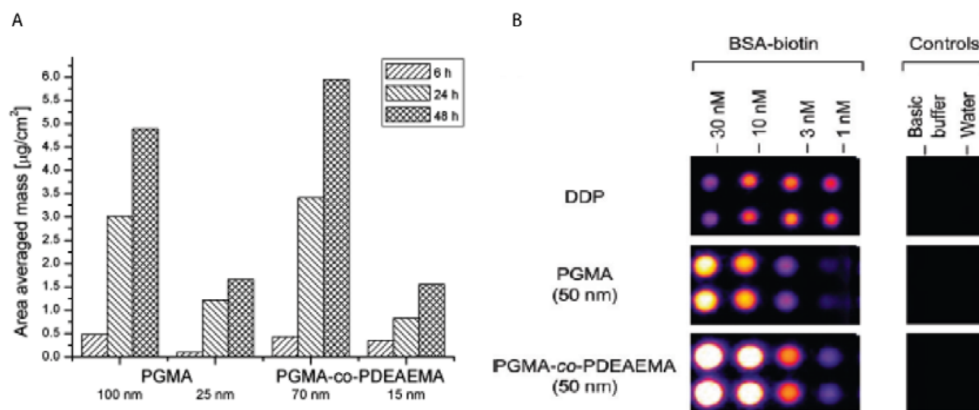


Figure 17. Polymer brush platforms for protein microarrays: (A) impact of the brush type and thickness on protein adhesion; (B) effect of the coating type and loading on the intensities detected (DDP is dodecyl phosphate). Reprinted from ref 319. Copyright 2010 American Chemical Society.

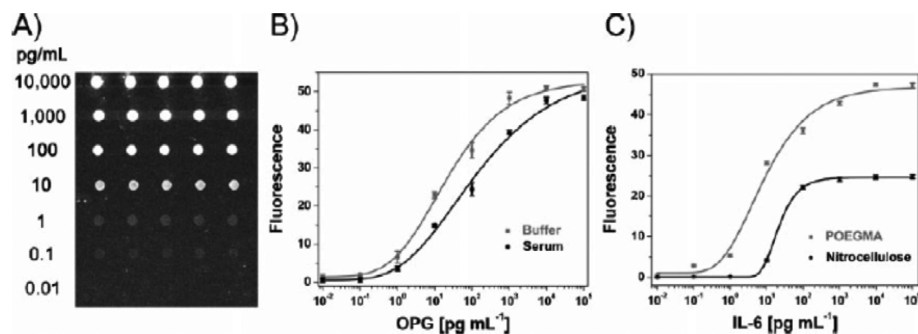


Figure 18. Example of POEGMA-based antibody microarrays (A) and their performance for the detection of analytes in buffer and serum (B, C). Reprinted with permission from ref 276. Copyright 2009 John Wiley and Sons.

the case of relatively low molecular weight analytes, or at low concentrations, this is an important advantage as a low signal (for example, arising from SPR detection) can be amplified by 3–4 orders of magnitude. Such a strategy was used for the detection of single-mismatch mutations in DNA³⁷⁴ and Con A binding³⁷⁵ using an ATRP-coupled DNA probe and a very mild activator generated by an electron-transfer approach for triggering ATRP. However, it was important to ensure that the dissociation constant of the different recognition partners used was minimal to avoid chain detachment during polymerization, with associated loss in sensitivity.³⁷⁶ Other systems, not based on radical polymerizations, such as rolling-circle DNA amplification³⁷⁷ may also be used for similar purposes.

4.2. Impact of Protein Resistance on Sensing Specificity

Biosensors should ideally allow the detection of analytes over a wide range of concentrations, without interference from other species present in the sample, such as proteins in blood or saliva. The performance of sensors is not only determined by the method of detection and its sensitivity, but also by the strength of interaction between the analyte and sensor surface and the absence of unwanted nonspecific binding. In that respect, the polymer brush chemistry is not only important to ensure efficient coupling of biomacromolecules enabling sensing of analytes, but also to prevent adsorption of proteins and other molecules to the sensor surface.

4.2.1. Low-Fouling Brushes for Biosensing. PGMA-*co*-PDEAEMA copolymer brushes, which allow high levels of protein binding compared to monolayer systems (e.g., dodecylphosphate monolayers), give rise to increased fluo-

rescence signals in protein microarrays (Table 2).³¹⁹ Consistent with the role of the 3D architecture of the brush that enables higher protein loading, an increased brush thickness resulted in a higher fluorescence intensity and an improved signal-to-noise ratio (Figure 17). A proof-of-concept microarray carried out using tumor necrosis factor α (TNF α) and a corresponding antibody revealed signal-to-noise ratios that were above 10 even for an antibody concentration of 1 nM and showed that the dynamic range of concentrations was substantially increased compared to that of a monolayer control. However, despite the increase in protein coupling density observed and the associated signal-to-noise ratios, PGMA-*co*-PDEAEMA also showed an increased nonspecific (negative control) signal, suggesting that the detection range and sensitivity of the assay could be further improved by using antifouling surfaces. Hu et al. used a similar coupling strategy, combining PGMA with the protein-resistant POEGMA to generate protein microarrays for SPR imaging, and observed limits of detections for assays in a biomedically relevant range of 20–100 ng/mL.²⁷⁷ Sung et al. microcontact-printed antibody arrays on the surface of grafted-to POEGMA-*co*-PMA³⁵⁹ (PMA = poly(methyl acrylate)) (after NHS activation) or POEGMA-*co*-PGMA³⁶⁰ brushes and reported a limit of detection below 10 ng/mL for the former brush. A similar strategy was used to create competitive mycotoxin assays, with limits of detection reaching 3–4 pg/mL.³⁶¹ Interestingly, Hucknall et al. showed that PGMA was not necessary to generate stable protein arrays and that spotting followed by controlled drying of proteins directly on POEGMA brushes was sufficient, resulting in microarrays with limits of detection near picogram per milliliter concentrations. Such a

detection limit is 1 order of magnitude lower than those measured for nitrocellulose, and the platform offered an increased dynamic range of sensing (Figure 18).²⁷⁶ It could be argued that the lower limit of detection observed for pure POEGMA arrays is a combination of the improved protein resistance of POEGMA (compared to PGMA-*co*-POEGMA) and the type of assay used (immunofluorescence). Similarly, carboxylated POEGMA-functionalized poly(dimethylsiloxane) (PDMS) platforms resulted in limits of detection in the subnanogram per milliliter range using ELISA assays.³⁶² POEGMA-coated particles were also used to detect attomolar DNA concentrations in serum.³⁶³ Riedel and co-workers used streptavidin-functionalized POEGMA brushes to capture oligonucleotide-coupled antigens of the Epstein–Barr virus (Figure 19).³⁶⁴ This allowed the detection of antibodies

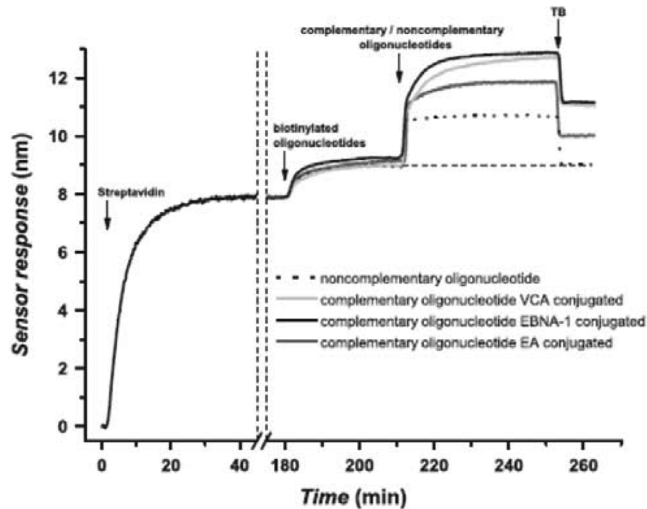


Figure 19. Functionalization of POEGMA brushes with biotinylated oligonucleotides, followed by the association of complementary oligonucleotides presenting antigens for markers of the Epstein–Barr virus. Reprinted with permission from ref 364. Copyright 2014 Elsevier.

expressed by patients infected by this virus directly from blood serum samples. Interestingly, this approach also enabled the sensing surfaces to be regenerated by melting of the oligonucleotide constructs. Other neutral brushes such as PNIPAM were used in electrochemical immunosensors and allowed the detection of mesothelin, an ovarian and pancreatic cancer marker, down to 10 pg/mL.³⁶⁵

4.2.2. Development of Brush-Based Label-Free Sensors for Detection in Serum and Plasma. Making use of the exceptional protein resistance of some zwitterionic brushes, Jiang and co-workers designed sensing platforms based on PCBAAs and SPR detection. They showed clear detection of streptavidin, spiked into undiluted plasma,³²³ and found that the activated leukocyte cell adhesion molecule (ALCAM) could be detected down to 10 ng/mL concentration in undiluted plasma using PCBAAs-coupled antibody assays.^{247,321} Similarly, PHEMA and PCBAAs brushes functionalized with antibodies were able to detect analytes from the buffer.³⁶⁶ Protein resistance from food or plasma samples was preserved in the case of PCBAAs brushes, making this type of brush a good candidate for biosensing directly from unprocessed samples. Hence, the excellent protein resistance of PCBAAs brushes, even in undiluted plasma, can be exploited

to directly detect relevant biomedical markers from undiluted samples. Similarly, poly(hydroxypropyl methacrylate) (PHPMA) brushes, which displayed no measurable nonspecific binding from plasma via SPR even after antibody coupling, allowed the sensing of a peptidoglycan antigen down to a concentration of 600 ng/mL.²²⁴ In the latter case, a sandwich assay with a secondary antibody allowed amplification of the response of the detector. Interestingly, zwitterionic PMPC brushes were shown to allow the detection of C-reactive protein (which has a high binding affinity for phosphorylcholine residues) using a localized SPR sensor without any further biofunctionalization.³⁷¹

4.3. Impact of the Coupling Chemistry and Brush Architecture

4.3.1. Impact of the Brush Architecture. Independently of the affinity and specificity of an antibody or a biomacromolecule for an antigen, the architectural features of brushes, in addition to the brush chemistry and coupling strategy, have an impact on the limit of detection achievable and the dynamic range for detection. The architecture of the brush seems to be important to achieve a high detection range and low nonspecific binding. Jiang and co-workers, following from their work on simple PCBAAs brushes, showed that a bilayer architecture displaying a sparse PCBAAs upper layer grown from a dense PCBAAs brush had improved antibody coupling, while ultralow protein fouling from serum was preserved^{324,325} (Figure 20). The brush synthesis conditions (in

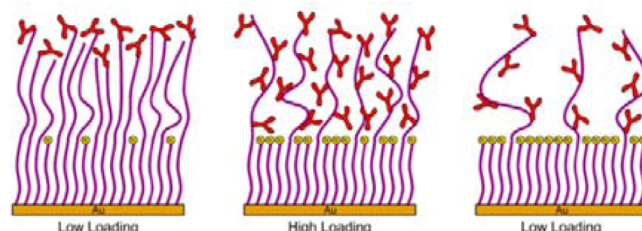


Figure 20. Schematic representation of the impact of the polymer brush architecture on antibody loading. Reprinted from ref 325. Copyright 2012 American Chemical Society.

particular the solvent composition) were essential to achieve low nonspecific binding while promoting high antibody coupling to the upper brush layer. Two strategies were directly compared: ATRP followed by partial deactivation with sodium azide and reinitiation and photoiniferter-mediated polymerization followed by deactivation with a disulfide and reinitiation.³⁶⁷ The latter method was found to yield higher levels of antibody loading (ca. 800 ng/cm²) and antigen detection (ca. 130 ng/cm²) while retaining good antifouling properties. Further studies of antigen sensing of such bilayer platforms could show whether this architecture indeed has an impact on the limit of detection from serum or plasma. Another example of copolymer brush architecture, based on first a PMPC block followed by an upper PMA block, allowed some retention of nonspecific protein resistance while increasing the level of selective protein loading.³⁶⁸ The size of the respective blocks was found to be particularly important to optimize the signal-to-noise ratio of selective protein anchoring compared to nonspecific binding from plasma. Similarly, Ma et al. used POEGMA-*b*-PAA polymer brushes for antibody-based assays and the detection of a labeled antigen.³⁶⁹ It was found that the POEGMA block was sufficient to reduce nonspecific protein

Table 3. Polymer Brushes Used as Cell Culture Platforms^a

brush	substrate	biofunctionalization	cell type	assay	ref
POEGMA	TCPS	peptides: cRGDfK, cRADfK	HeLa	CA (1 day)	387
POEGMA	PET	peptide: REDV	HUVECs, HASMCs	CA and P (2–48 h), CV (2 days)	388
POEGMA	gold	peptide: GRGDS	MC3T3 fibroblasts	CA (8 h)	185
PAAm	TCPS	RGD-functional monomer	L929 mouse fibroblasts	CA and P (24 h)	389
PHEMA	silicon	fibronectin	MC3T3-E1 osteoblasts	CA (1–2 days)	381, 390
PHEMA	silicon	fibronectin	NIH-3T3 fibroblasts	CA and P (8 h)	382
PAA	PET	collagen	human bladder smooth muscle cells	CA and P (6 h)	391
PDMAA- <i>co</i> -PNAAPBA	glass	carbohydrate	murine hybridoma cells M2139 and human myeloid leukemia cells KG1	CA (1 h), CV and P (2–4 days)	392, 393
POEGMA	titanium	none	3T3 fibroblasts	CA (4 h to 77 days)	380
POEGMA	titanium	protein fragment: FNIII _{7–10}	hMSCs	CA, D (2 weeks)	313
POEGMA	gold nanoparticle	vitronectin, fibronectin	L02 and BEL-7402 cells	CA (1 day)	394
POEGMA	titanium	peptide: GFOGER	MC3T3-E1 osteoblasts	CA (2 weeks)	286
POEGMA	gold nanoparticle	peptide: GRGDY	L929 mouse fibroblasts	CA and P (1–5 days)	395
PGAMA	titanium	peptide: GFOGER	MC3T3-E1 osteoblasts	CA (1 h)	290
PGMA, PDMAEMA	TCPS	none	L929 mouse fibroblasts	CA (1–24 h)	101
POEGMA- <i>co</i> -PHEMA	titanium	fibronectin, rhBMP-2	MC3T3 fibroblasts	CA, P, D (1–7 days)	310
PMPC	silicon	none	L929 mouse fibroblasts	CA (20 h)	261
PMA	gold	peptide: RGD	MG63 human osteoblasts	CA and P (3 weeks)	153
PMA, PDMAEMA	gold	mineralization with calcium phosphate	MC3T3-E1 preosteoblasts	CV (1–3 days)	396
POEGMA, PHEMA	glass slide	peptide: RGD	HUVECs	CA (4 h), P (4 h to 2 days)	61
PMEDSAH	TCPS	none	hESCs (BG01 and H9)	CA and P (2 days)	397
chiral poly(amino acid)s	silicon	none	kidney fibroblast cells COS-7 and mouse brain endothelial cells bEnd.3	CA (1 h to 2 days)	398
PGMA	PCL	gelatin	HUVECs	CA, P (7 days)	399
PGMA	PCL	collagen	3T3 fibroblasts	CA, P (48 h)	104
PMAA	PCL	collagen	HUVECs	CA, P (7 days)	307
POEGMA	PCL	fibronectin	hMSCs	CA (4 h)	400
PNIPAM	PCL	collagen	3T3 fibroblasts	CA, P (48 h)	105

^aAbbreviations: PET, poly(ethylene terephthalate); PDMAA, poly(*N,N*-dimethylacrylamide); PNAAPBA, poly(*N*-acryloyl-*m*-phenylboronic acid); PGAMA, poly(2-gluconamidoethyl methacrylate); PCL, poly(ϵ -caprolactone); rhBMP-2, recombinant human bone morphogenetic protein 2; HUVECs, umbilical vein endothelial cells; HASMCs, human aortic smooth muscle cells; hMSCs, human mesenchymal stem cells; hESCs, human embryonic stem cells; CA, cell adhesion; P, proliferation; CV, cell viability; D, differentiation.

adsorption and improve the detection of the antigen, even in the presence of fibrinogen (at concentrations up to 200 μ g/mL).

4.3.2. Choice of Biofunctionalization Strategy. The methods used for biofunctionalization were also found to impact the recognition of biomarkers. Direct immobilization of antibodies and proteins on brushes with relatively short side chains such as PHEMA was shown to have a detrimental effect on the activity of enzymes and the sensing of antigens.^{355,378,379}

This is perhaps a result of the combined effects of denaturation and the lack of accessibility to proteins when immobilized in dense nonswollen brushes. The choice of coupling strategy and the use of spacers such as PEG between the brush backbone and the coupled biomacromolecule have had a beneficial impact on the retention of antibody affinity,³¹⁴ giving limits of detection in the picomolar range.³⁵⁵ Similarly, direct brush biotinylation, rather than streptavidin coupling, resulted in increased initial biofunctionalization, but subsequently lower antibody and antigen capture, perhaps due to the saturation of biotin-binding pockets.²²² Such phenomena, together with poor protein infiltration within brushes, were also reported for biotinylated PMA brushes.³⁷⁰ The effect of the PEG side chain

length was more pronounced on antibody immobilization than on subsequent antigen binding levels, perhaps as a result of hindered antigen diffusion through low-swelling brushes (compared to charged and zwitterionic brushes). A relatively wide dynamic range was observed via immunofluorescence assay, with a limit of detection near 1 ng/mL; however, similar platforms showed a higher limit of detection via label-free SPR sensing (closer to 0.1–1 μ g/mL). It was also found that increasing the PEG side chain length improved the resistance of the coatings to nonspecific binding. A related system, using Ni-NTA ligands and His-tag proteins as a coupling mechanism, showed a similar impact of the brush chemistry on the antifouling properties, but also demonstrated that the high densities of Ni-NTA complexes in polymer brushes resulted in particularly stable protein immobilization, perhaps due to fast rebinding.⁵¹ Other coupling strategies, such as the reaction of benzylguanine residues with AGT fusion proteins,³²⁷ enabling the oriented and selective coupling of proteins, using other tags available in protein engineering and purification could play an important role in the future development of polymer brushes for biosensing platforms.

Polymer brushes also allow the immobilization of several types of functional groups in the vicinity of the surface of a sensor and enable the systematic variation of the chemistry and composition of such coatings without altering the chemistry of the sensor substrate itself. Hess et al. developed graphene-based field effect transistors in which the PAA-*co*-PDMAEMA brush provided a simple way of altering and controlling the graphene chemistry without introducing defects into the graphene structure.³⁷² The acid groups of the PAA segments allowed biofunctionalization of the brush with acetylcholinesterase, whereas the PDMAEMA moieties provided basic residues able to modify the local charge density close to the graphene surface. Hence, in the presence of the neurotransmitter acetylcholine, the change in local pH triggered by the enzymatic reaction altered the charge density close to the graphene sheet, resulting in a shift of its Fermi level, detectable in a field effect transistor device.

5. POLYMER BRUSH-BASED PLATFORMS FOR CELL CULTURE AND REGENERATIVE MEDICINE

The biofunctionalization of implants and devices to alter interfaces between a material and surrounding cells or a tissue is an important element of design in bioengineering. Such a biointerface should allow the control of behaviors such as cell recruitment, adhesion, spreading, motility, matrix deposition, proliferation, and differentiation. The biofunctionalization of materials with extracellular matrix molecules or fragments, growth factors, and drugs is essential, and polymer brushes are particularly well suited to do so without altering the bulk properties of such materials. Similar strategies are also employed to design new generations of cell culture systems and cell-based assays.

5.1. Biofunctional Brushes for Controlling Cell–Materials Interfaces

5.1.1. Importance of Brush-Based Low-Fouling Coatings for Cell Culture and Implant Design. POEGMA brushes, which are typically protein- and cell-resistant, have been biofunctionalized to be used to coat titanium substrates for applications in implants such as hip and knee joint replacements, dental implants, and cardiac pacemakers, as these require some level of integration with the surrounding bone to avoid implant failure (Table 3).³¹⁰ Shorter oligo(ethylene glycol) in POEGMA brushes was found to allow partial antifouling properties for only short periods of time, but was still able to sustain cell spreading for longer term cultures.³⁸⁰ Similarly, sparse brushes allowed nonspecific adsorption of fibronectin, which resulted in cell spreading,^{381,382} and gradient PHEMA brushes allowed the control of cell spreading. More generally, peptide or protein adsorption and cell attachment occurred preferentially at low grafting density, in the mushroom regime, while slight or no peptide attachment and cell adhesion were observed for denser brushes.^{383,384} Other low-fouling brushes such as poly(glycerol monomethacrylate) similarly displayed cell resistance,¹⁰¹ but allowed cell spreading when copolymerized with PDMAEMA. The protein and cell antifouling properties of polymer brushes such as PMEDSAH can be useful for coating poly(caprolactone) to improve hemocompatibility³⁸⁵ and metal stents to avoid restenosis and thrombosis.³⁸⁶ Indeed, platelet adhesion and hemolysis were decreased on PMEDSAH-coated stents.

5.1.2. Impact of the Brush Chemistry. The brush chemistry itself has been shown to impact cell behavior. In

such systems, deposition of biomolecules from the medium is thought to be important for the observed bioactive properties.

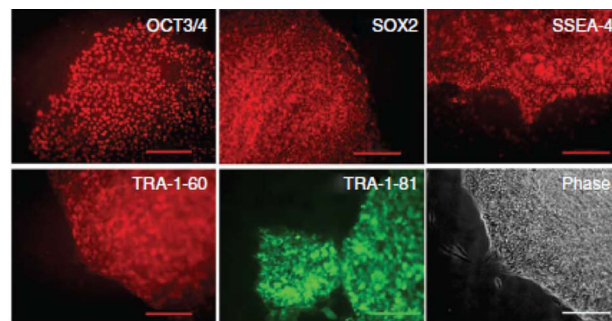


Figure 21. hESC colonies cultured on PMEDSAH and expressing stem cell markers. Reprinted with permission from ref 397. Copyright 2010 Nature Publishing Group.

Nonfunctionalized PMEDSAH was shown to promote attachment and proliferation of undifferentiated human embryonic stem cells (hESCs; see Figure 21),³⁹⁷ despite its reported protein and cell resistance in other systems.⁴⁰¹ It was reported that this coating was not fully protein resistant, which could perhaps account for the observed behavior of stem cells.²⁰⁴ The absence of strong cell adhesion and spreading may be beneficial in the specific case of ESCs. Furthermore, UV exposure used for sterilization of substrates may lead to the deterioration of antifouling properties, thus enabling sufficient adhesion of hESCs. The chirality of polymer brushes was also shown to trigger differential cell behaviors. This was illustrated by enantiomeric surfaces that modulated cell spreading. Cells adhering at high densities formed cell–cell adhesions and generated large interconnected clusters on the L-films, while nearly rounded cells in segregated stacks were observed on D-films.³⁹⁸ Topography was also shown to alter cell behavior and had an impact on the cell resistance of POEGMA brushes. The long-term adhesion of human hepatocyte and human carcinoma cells was improved when the roughness of the surfaces was modified using gold nanoparticles, compared to smooth controls.³⁹⁴ Selective cell adhesion has been obtained using moderately specific interactions, such as those mediated by boronate-containing brushes which can bind to glycoproteins on the surface of cell membranes.³⁹² Cells were shown to detach from these surfaces on demand when treated with fructose solutions. In addition, copolymers of *N,N*-dimethylacrylamide (DMAA) and *N*-acryloyl-*m*-phenylboronic acid (NAAPBA) were shown to distinguish between different cell lines,^{392,393} where complex formation between boronates and glycoproteins and glycolipids at the cell surface gave rise to stronger binding between DMAA-*co*-NAAPBA brushes and murine hybridoma cells (M2139) than between these brushes and human myeloid leukemia cells.

5.1.3. Peptide-Functionalized Brushes for Promoting Cell Adhesion and Culture. Although some nonfunctionalized systems allow cell adhesion, spreading, and culture, in the vast majority of cases neutral polymer brushes require functionalization with adhesive peptides or proteins. For example, RGD and proline-histidine-serine-arginine-asparagine (PHSRN) peptides, derived from the cell attachment domains of fibronectin,^{61,185,294,389,402,403} and GFOGER peptides, derived from collagen,^{60,286,290} are all known to bind to integrin heterodimers and promote cell adhesion on brush-

coated surfaces. The GFOGER peptide has been used to promote cell adhesion and osteoblast differentiation, and arginine-glutamic acid-aspartic acid-valine (REDV) was used to promote the adhesion and migration of endothelial cells.³⁸⁸ The density and spatial arrangement of these peptides in the brush affected cell adhesion. A vitronectin peptide was used to functionalize copolymer brushes of POEGMA and PHEMA and allow the long-term culture of human induced pluripotent stem cells (hiPSCs; see Figure 22) in a defined medium.⁴⁰⁴ The density of the peptide was found to affect cell proliferation and colony formation. After 10 cell passages on such surfaces, hiPSCs retained the expression of important stem cell markers (Nanog, Oct-4, and Sox-2).

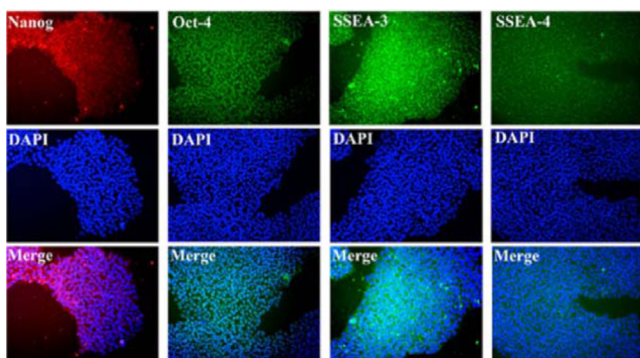


Figure 22. hiPSC colonies cultured on POEGMA-*co*-PHEMA brushes functionalized with vitronectin peptides for 10 passages. Reprinted with permission from ref 404. Copyright 2013 Elsevier.

Furthermore, the architecture of peptide-functionalized brushes was found to impact cell spreading. Higher peptide ligand densities achieved for RGD-functionalized POEGMA brushes with shorter side chains enabled the formation of focal adhesions and subsequent cell spreading.⁶¹ Focal adhesions were larger and more mature on PHEMA brushes compared to a brush with a longer side chain, POEGMA. In addition, human umbilical vein endothelial cells (HUVECs) remained responsive to flow and oriented when exposed to shear stress mimicking arterial blood flow. Adhesion of human aortic smooth muscle cells (HASMCs) and endothelial cells to REDV-functionalized brushes was investigated by Ji and co-workers.³⁸⁸ The ratio and length of OEGMA moieties in the brush had a marked effect on the adhesion of HASMCs and to a lower extent on that of endothelial cells. This offers opportunities for selective cell adhesion and manipulation

through tailored brush composition. The spacer length between the peptide and polymer chain was also found to alter the cellular response in the case of RGD ligands. When POEGMA brushes were functionalized with cyclic RGD peptides, longer oligo(ethylene glycol) spacers resulted in increased cell adhesion, with little contribution from proteins adsorbed due to nonspecific binding.³⁸⁷ The position of the adhesive peptide within the brush (upper part vs buried peptides) had a marked impact on cell spreading. It was observed that burying the peptide sequence within a PMAA brush resulted in decreased cell spreading, with vinculin staining only showing in the cytosol of the cell, while peptides at the surface of the brush promoted cell spreading with defined focal adhesions.¹⁵³ Surface roughness also played a role in modulating cell-specific interactions,³⁹⁵ and rough surfaces reduced cell adhesion and spreading on RGD-functionalized POEGMA brushes. Other chemical functions such as phosphate groups from 2-(methacryloyloxy)ethyl phosphate promoting calcification have been introduced to improve biomaterialization⁴⁰⁵ (Figure 23). It was found that MC3T3-E1 preosteoblast cells differentiated well to osteoblast lineages and that matrix mineralization was improved when RGD peptides and phosphate groups were both present.

5.1.4. Brush Coatings Functionalized with Protein Fragments, Proteins, and Growth Factors for Cell Culture and Regenerative Medicine. Protein immobilization is particularly useful when peptide sequences mimicking specific natural biomacromolecules are not known or are difficult to synthesize on a large scale. Hence, a wide variety of proteins and protein fragments have been coupled to polymer brushes. Garcia et al. functionalized POEGMA brushes with FNIII_{7–10}, a fibronectin fragment that was shown to promote cell adhesion and increase osteoblast differentiation.^{60,290,313,406,407} Although the density of ligands achieved via the immobilization of such fragments is lower than that of shorter peptide sequences (for example, 6 pmol/cm² for RGD peptides vs 1 pmol/cm² for recombinant FNIII_{7–10} fragments), the higher specificity and binding affinity of protein fragments, especially in the case of multimeric molecules, make them more attractive for promoting cell adhesion and cell differentiation. Compared to the immobilization of smaller peptides, this protein fragment approach often does not offer the same control of the coupling site and motif orientation, but this could potentially be achieved using tagged fragments. Garcia and co-workers utilized such a protein fragment strategy for the implantation of titanium rods *in vivo* and observed that the osseointegration of implants coated with such brushes was

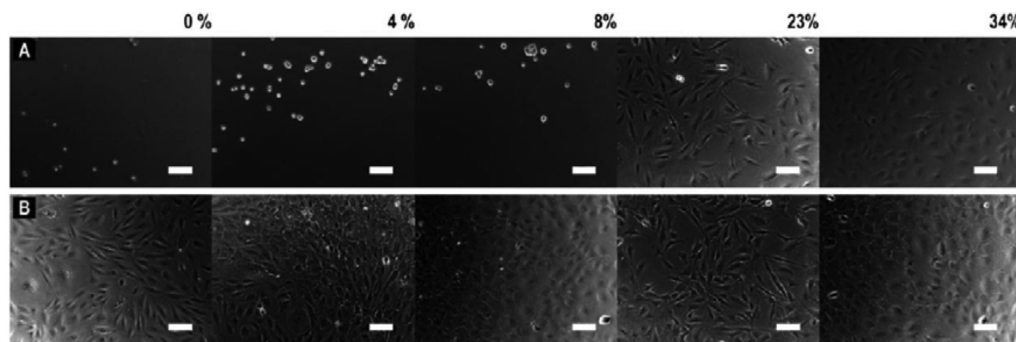


Figure 23. Cell response to PHEMA-*co*-MEP (A) and RGD-functionalized PHEMA-*co*-MEP (B) brushes for different 2-(methacryloyloxy)ethyl phosphate (MEP) concentrations. Reprinted with permission from ref 405. Copyright 2012 The Royal Society of Chemistry.

improved, illustrating their potential for bone repair (Figure 24).^{312,313}

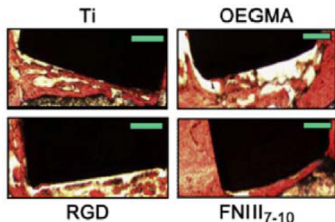


Figure 24. Osseointegration of titanium implants coated with POEGMA brushes and POEGMA brushes functionalized with an RGD peptide or an FNIII₇₋₁₀ fibronectin fragment. Reprinted with permission from ref . Copyright 2008 Elsevier.

Full-length extracellular matrix proteins have also been coupled to polymer brushes. Collagen was coupled to PAA brushes grafted from poly(ethylene terephthalate) to allow the expansion of human smooth muscle cells on these otherwise relatively bioinert polymer coatings.³⁹¹ However, simple incubation of these substrates in culture medium supplemented with serum resulted in efficient cell adhesion, suggesting that protein deposition from the medium was sufficient to promote cell anchorage. Gelatin and collagen were directly coupled to PGMA and PMAA brushes to promote cell adhesion to poly(caprolactone),^{104,307,399} allowing for improved cell spreading and proliferation. POEGMA brushes functionalized with fibronectin were used to decouple the nano- and microtopographical cues of poly(caprolactone) substrates, which altered human mesenchymal stem cell behavior.⁴⁰⁰ Similarly, collagen was immobilized to PNIPAM brushes grown from poly(caprolactone) substrates.¹⁰⁵

Growth factors are essential components of the cell microenvironment and important cues controlling cell motility, proliferation, and differentiation. Their role is sometimes associated with matrix adhesion, and strategies have been developed to couple them to brushes, either covalently or using weak electrostatic interactions. For example, fibronectin and recombinant human bone morphogenetic protein- 2 (rhBMP-2) were covalently immobilized onto low-density P(OEGMA-*r*-HEMA) copolymer brush surfaces.³¹⁰ This induced the adhesion of mouse preosteoblast cells MC3T3 on titanium surfaces and enhanced cell differentiation compared to that on a pristine Ti surface at similar cell proliferation rates. These results highlight the potential of brush coatings for the generation of Ti-based biomedical devices with bioadhesive and osteogenic properties.

Charged glycosaminoglycans such as heparin can bind growth factors via electrostatic interactions. Poly(styrenesulfonate) brushes were used to mimic such interactions with basic fibroblast growth factor (bFGF) and vascular endothelial growth factor (VEGF), two factors that stimulate cell adhesion, proliferation, and migration, wound healing (for the former), and angiogenesis (for the latter). PSS-*co*-POEGMA copolymer brushes were found to bind and protect these growth factors, with good retention of bioactivity.⁴⁰⁸ Hence, patterned surfaces based on these brushes enabled extracellular matrix (ECM) binding of these growth factors to be mimicked and could be used and exploited further to probe and control cell behavior.

5.2. Polymer Brushes for Drug and Gene Delivery

Brush coatings are promising vectors and carriers for gene and drug delivery.⁴⁰⁹⁻⁴¹² The delivery of plasmids into various types of cells can be achieved, while ensuring low cytotoxicity, using cationic polymeric vectors such as the gold standard polyethylenimine (PEI) or those obtained by controlled radical polymerizations. Such cationic materials constitute interesting alternatives to viral vectors.⁴¹³⁻⁴¹⁵ Polymer brushes allow the design and coating of a variety of nanoparticles such as nanodiamond, gold, magnetic, and silica nanoparticles, with well-defined core–shell architecture and chemistry and hence are of high interest as vectors and carriers for gene and drug delivery.⁴⁰⁹⁻⁴¹² Cationic polymer brushes such as PDMAEMA have the ability to condense DNA and enable cell uptake of nanodiamond–PDMAEMA vectors while protecting DNA from enzyme degradation (Figure 25).⁴¹⁶ Hence, nanoparticles

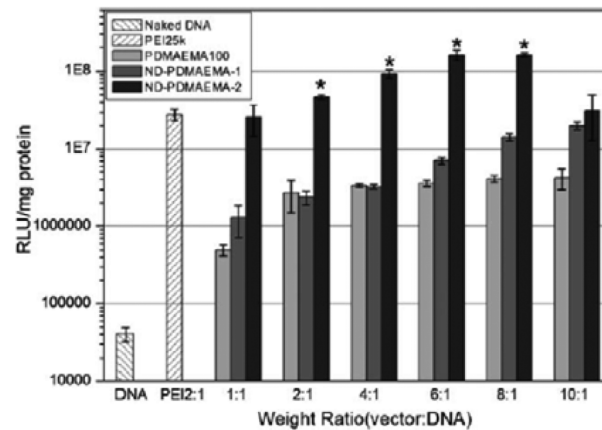


Figure 25. Evaluation of the transfection efficiency using PDMAEMA-coated nanodiamond. Reprinted with permission from ref 416. Copyright 2011 The Royal Society of Chemistry.

decorated with PDMAEMA brushes have been used for pDNA and siRNA delivery.⁴¹⁶⁻⁴¹⁸ Compared to branched PEI, these vectors were reported to perform better and to be less toxic to cells. The transfection of hard-to-transfet cells, including differentiated cells and human primary T lymphocytes, was also reported, and it was proposed that the core–shell architecture was key to such performance.⁴¹⁹ In addition, the core–shell approach allows the use of cores with diagnostic ability (e.g., MRI or fluorescence), making brush-decorated particles useful to the field of theranostics. Protein-resistant brushes have also been used as protective coatings for the stabilization of superparamagnetic particles for MRI imaging.⁴²⁰ An interesting feature of polymer-brush-functionalized nanoparticles is that the chemistry of the core and its shape can be varied independently of the chemistry of the brush. For example, gold nanorods decorated with PDMAEMA brushes were reported to give rise to high transfection efficiencies in COS-7 and HepG2 cells.⁴²¹

Gold nanoparticles have been functionalized with PEG to allow reversible drug adsorption and photodynamic therapy of cancer.⁴²² They displayed good biocompatibility in vitro and in vivo, and their cellular internalization correlated well with their surface chemistry and size.⁴²³ The integration of a receptor-specific targeting ligand to the design of such carriers could further improve their potential. Temperature- and pH-sensitive polymer brush coatings are also used for delivery of drugs as

Table 4. Thermoresponsive Brushes Utilized for Single-Cell and Cell-Sheet Recovery^a

brush	substrate	cell type	single cell/cell sheet	LCST (°C)	assay	ref
PNIPAM	TCPS/glass coverslip	bovine carotid artery endothelial cells	cell sheet	32	CA, CD	450
PNIPAM	TCPS	BAECs	cell sheet		CA, CD	451,452
PNIPAM	gold-coated glass slide	NIH-3T3 fibroblasts	single cell	32	CA, CD	209
PNIPAM	glass	BAECs	cell sheet	32	CA, CD	449
PNIPAM	silicon	NIH-3T3 fibroblasts, BAECs	single cell	32	CA, CD	453
PNIPAM	glass coverslip	bovine carotid artery endothelial cells	cell sheet	25	CA, CD	454
PNIPAM	silicon	human hepatoma cell line (HepG2)	single cell	32	CA, CD	455
PNIPAM	silicon	3T3 fibroblasts	single cell	32	CA, CD	456
PTEGMA	silicon/glass wafer	human fibroblasts	cell sheet	23	CA, CD	457
PNIPAM- <i>co</i> -PAA	TCPS	HepG2, L929 fibroblasts	single cell	32	CA, CD	458
PNIPAM- <i>b</i> -PAA	silicon	HepG2	single cell		CA, CD	459
PNIPAM	TCPS	myoblasts/cardiomyocytes	cell sheet		CA, CD	439,460
PNIPAM	PS	bovine carotid artery endothelial cells	cell sheet	32	CA, CD	442
PNIPAM	TCPS	oral mucosal epithelial cells	cell sheet	32	CA, CD	440
PNIPAM	PS	epithelial cells, hepatocytes	single cell	32 (deionized water), 25 (PBS)	CA, CD, P	461
PDEGMA- <i>co</i> -POEGMA	glass slide	L929 mouse fibroblasts	single cell	34	CA	462
PNIPAM	glass	smooth muscle cells	cell sheet	32	CA, CD, P	463
PNIPAM, PNIPAM- <i>co</i> -PAPTAC, PAPTAC- <i>co</i> -PBAAM	polystyrene beads	Chinese hamster ovary (CHO-K1) cells	single cell	32	CA, CD, P, CV	464,465
PNIPAM- <i>co</i> -PMEDSAH	glass	NIH-3T3 fibroblast cells	single cell		CA, CD	444
PNIPAM- <i>co</i> -POEGMA	gold	fibroblasts, human osteosarcoma cells	single cell	36	CA, CD	447
PNIPAM-POEGMA	silicon	3T3-Swiss albino	single cell	32	CA, CD, P	446
PNIPAM- <i>b</i> -PS	silicon	LL929 fibroblasts	single cell	32	CA, CD	466
PNIPAM, PNIPAM- <i>co</i> -PBAAM	parylene C surface	human skin fibroblast	single cell	22–29	CA, CD	445

^aAbbreviations: PAPTAC, poly((3-acrylamidopropyl)trimethylammonium chloride); PBAAM, poly(*N*-*tert*-butylacrylamide); TCPS, tissue culture polystyrene; BAECs, bovine aortic endothelial cells; CA, cell adhesion; CD, cell detachment; P, proliferation; CV, cell viability.

they allow reversible entrapment and release and consequently enable on-demand delivery.^{331,424–426} The excellent protein resistance of polymer brushes may also be used to control the pharmacokinetics of particles⁴²⁷ in drug delivery or imaging applications, in particular if combined with targeting strategies. For example, lanthanide-doped nanoparticles with a POEGMA shell functionalized with Con A were used for targeting and fluorescence imaging of cancer cells in vitro and tumors in vivo.⁴²⁸

Although the potential of polymer brushes has not been extensively investigated in drug delivery, perhaps due to the fact that thin brushes do not allow a high density of drug immobilization or controlled long-term release, these coatings may still find application in this field. Potentially, brushes could be combined with hollow cores such as carbon nanotubes^{429,430} or other porous structures used for drug delivery applications to modify their surface properties and drug release profile. Polymer-brush-decorated nanocapsules, for example, have been shown to alter the release kinetics of doxorubicin.⁴³¹

5.3. Responsive Brushes for Controlled Cell Adhesion and Detachment

Switchable surfaces enabling reversible cell adhesion are attractive for tissue engineering applications as they allow the generation of epithelial cell sheets that can be detached without requiring the use of digestive enzymes.^{432,433} Cell-sheet engineering uses a scaffold-free technology⁴³⁴ and has been

successfully used in clinical applications such as in the treatment of patients with severe disorders of the cornea,^{435,436} to capture lymphocytes,⁴³⁷ and for periodontal regeneration,⁴³⁸ impaired myocardium repair,⁴³⁹ and the treatment of esophageal ulcerations in a canine model.⁴⁴⁰

5.3.1. General Considerations for the Design of Brush-Based Responsive Substrates for Cell and Cell-Sheet Harvesting. Thermoresponsive polymer brushes are particularly well suited for such platforms as they enable the control of spatial features and display tunable LCST transitions at physiologically relevant temperatures (Table 4). In addition, other stimuli such as light, electric fields, and magnetic fields can potentially be used to control cell adhesion and detachment from these biointerfaces.^{17,441} Detachment of cultured cell layers from thermoresponsive polymer brushes such as PNIPAM,^{296,442} poly(2-alkyloxazolines),⁴⁴³ and various copolymers such as PNIPAM-*co*-PMEDSAH,⁴⁴⁴ PNIPAM-*co*-poly(*N*-*tert*-butylacrylamide),⁴⁴⁵ PNIPAM-*co*-POEGMA,^{446,447} and POEGMA-*co*-PDEGMA^{155,448} has been particularly successful. Polymer brushes are advantageous over bulk matrixes as the latter give incomplete and slow detachment of adhered cells. The development of switchable coatings requires the maximization of cell proliferation while still allowing effective detachment without cell death or destruction of the cell sheet. The key advantage of thermoresponsive platforms for cell-sheet engineering is that they do not require digestion with enzymes

that may harm and dissociate cells, but provide a mild method of detaching fully cohesive cell sheets of relatively large size. The degree of brush swelling at the LCST, the rate at which this swelling occurs and its reversibility, and the number of cycles a switchable surface can sustain are all important factors to be considered for the function and application of these stimulus-responsive matrixes.

A general method used for the detachment of cells and cell sheets from thermoresponsive brushes consists of culturing cells at high density (confluence or just subconfluence) in a tissue culture dish grafted with the thermoresponsive polymer of interest.^{17,451,454,467} The temperature of the culture is then decreased by exchanging the medium to medium at a temperature below the LCST of the brush (usually ca. 20 °C for PNIPAM or below 18 °C for poly(ethylene glycol) monoethyl ether methacrylate) (PTEGMA)) and incubating the cells at that temperature until the cells have detached.^{457,468,469} Hence, compared to other more invasive methods such as mechanical scraping or enzymatic digestion, which give rise to separation of the cells and poor integrity of the cell sheet, detachment from thermoresponsive substrates is particularly mild.⁴⁵² A membrane such as PVDF, chitin, or gelatin is overlaid over the confluent cell sheet in the dish to prevent cell sheets from shrinking or folding after detachment. The membrane supporting the cell sheet is then transferred to a new dish or tissue to be treated.^{444,468–471}

5.3.2. Mechanism of Cell Detachment and Parameters Affecting the Performance of the Coatings. Differences between cell-sheet and single-cell detachment have been observed on polymer brushes. With single cells, it has been reported that detachment can be obtained even with short PNIPAM brushes or at a low grafting density. This was not possible with cell sheets, which only exhibited an enhanced rate of detachment with a higher grafting density and a longer chain length (Figure 26).⁴⁴⁹ This has to be balanced by the longer incubation times required for initial cell adhesion when the molecular weight and chain density of the brushes are raised. Lopez and co-workers proposed the use of nanopatterned PNIPAM brushes to enable efficient cell detachment at low temperature while enabling fast initial cell adhesion.⁴⁵³ Contractile forces exerted at cell–cell junctions in cell sheets,

however, can result in accelerated rates of detachment from the surface compared to those of single cells. In addition, grafted layers also required longer incubation times to enable cell proliferation to reach a confluent monolayer.⁴⁴⁹ Such differences in behavior between single-cell and cell-sheet harvesting could be explained by the mechanism of cell detachment. This mechanism was proposed to occur via first a passive step during which hydration of the polymer chains occurs, followed by an active step during which cells undergo changes in shape and cytoskeleton organization, with associated changes in cell–matrix and cell–cell traction forces, together with altered metabolic activity requiring ATP consumption.^{433,461,470,472} In addition, examination of the generated cell sheet showed that although fibronectin, laminin, and collagen remain associated with the cell sheet, some collagen may remain linked to the brush surface. This was confirmed by TOF-SIMS (SIMS = secondary ion mass spectrometry) showing amino acids present on the PNIPAM surface after cell lift-off.⁴⁵¹ However, full desorption of extracellular matrix proteins from the brush does not seem to be required to promote cell detachment and sheet harvesting. Bureau and co-workers showed that micropatterned single cells (adhering to ECM protein patches defined by patterns of PNIPAM brushes) detached upon lowering the temperature below the LCST, although they could still adhere to areas not protected by brushes.⁴⁷³ Similarly, cell sheets adhering to micropatterned stripes of PNIPAM brushes detached below the LCST.⁴⁶³ Different shrinking rates were observed parallel and perpendicular to the orientation of the pattern, presumably as a result of cell orientation within the sheet. Hence, simple brush swelling, and potentially changes in its interaction with the cell membrane, may be sufficient to account for cell detachment from thermoresponsive polymers. Recent AFM measurements highlighted the importance of fast changes in polymer conformation and hydration to maximize cell detachment.⁴⁷⁴

5.3.3. PNIPAM- and PDEGMA-Based Brushes for Cell and Cell-Sheet Harvesting. PNIPAM has been the most extensively studied brush for thermally controlled cell detachment and cell-sheet generation (Table 4),^{466–469} and it has been applied to a wide range of cell types, including fibroblasts, epidermal cells, chondrocytes, aortic endothelial cells, muscle cells, kidney cells, cardiac myocytes, and hepatocytes. PNIPAM has been shown to display some protein resistance below its LCST, especially at high grafting densities. Above this transition protein adsorption and cell adhesions are promoted,^{209,210} hence enabling the use of PNIPAM brushes as thermoresponsive tissue culture substrates, especially considering their good biocompatibility and apparent lack of toxicity (some reports of cytotoxicity exist, perhaps due to the presence of unreacted monomers).⁴⁷⁵ A variety of copolymers of PNIPAM have also been generated, with a controlled LCST between 20 and 42 °C,^{445–447,476,477} and have found application for selective cell detachment.^{444,478} Copolymers of PNIPAM with 2-lactobionamidoethyl methacrylate (LAMA) were able to bind hepatocytes above the LCST and release them only on brushes where LAMA monomers were presented as a top layer of the copolymer.^{479,480} Oligo(ethylene glycol)-based copolymer brushes have also attracted some attention for controlling cell adhesion as they are biocompatible and their LCST can be controlled over a relatively wide range of temperatures.^{155,172,481–483} In particular, it was reported that PNIPAM experiences hysteresis during the heating and cooling process, while POEGMA copolymers did not show such phenomena

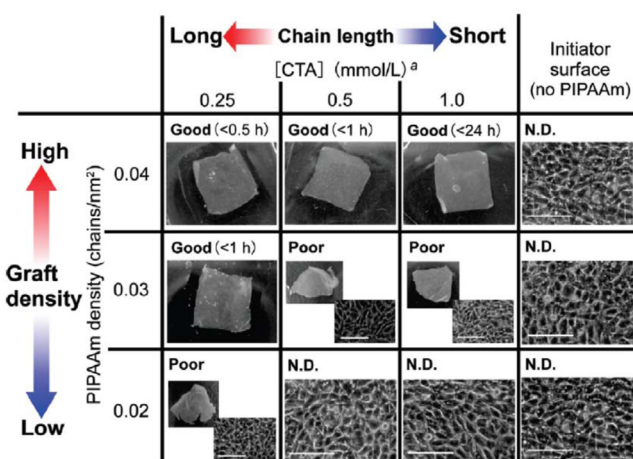


Figure 26. Quality of cell sheets generated from PNIPAM brushes of varying grafting densities and thicknesses. CTA = chain-transfer agent used during brush growth, and ND = not detached. Reprinted from ref 449 Copyright 2010 American Chemical Society.

and therefore allow more precise prediction of the temperature at which cells will detach.¹⁷² It was found that cell adhesion to these surfaces initially required more surface conditioning than for PNIPAM brushes (e.g., preincubation with cell culture medium) and that cells spreading on such copolymer brushes upregulated fibronectin production, perhaps to further remodel the brush–cell interface.⁴⁸⁴ PTEGMA also showed good thermoresponsive properties for cell detachment applications and provided a better control over the exact position of the LCST, as it is less sensitive to the monomer composition in the starting mixture.⁴⁵⁷

5.3.4. Impact of the Underlying Substrate. Successful grafting of the various thermoresponsive polymer brushes discussed above was achieved on a variety of solid substrates such as tissue culture polystyrene,⁴⁵⁰ glass coverslips,^{296,456,474} gold,²⁰⁹ silicon,^{455,459} poly(dimethylsiloxane),⁴⁸⁵ and titanium.⁴⁸⁶ The chemistry of the underlying substrates on which the polymer brushes were tethered also played a role in facilitating cell adhesion/detachment and hence the reversibility of these processes. Variations in the hydrophobicity and hydrophilicity of these substrates induced changes in primary protein adsorption, an effect that seemed more pronounced at a low brush grafting density.^{151,209} Hydrophobic surfaces such as PS enhanced the dehydration of the polymer chains, depending on the grafting density, which in turn influenced the surface chain mobility and protein adsorption.⁴⁵⁰ Similarly, the work of Wischerhoff et al. on charged polyelectrolyte multilayers functionalized with an ATRP macroinitiator highlighted the importance of the morphology of the macroinitiator layer deposited on the thickness of the brush subsequently grown from it. This was found to be important to promote sufficient cell adhesion above the LCST of the polymer (in this case POEGMA-*co*-PDEGMA) and cell detachment below this transition (Figure 27).^{448,462} Aside from substrate interactions, the thickness of the brushes, grafting density, and position of cell adhesive sites within the brush⁴⁷¹ were reported to impact cell detachment.^{168,442,455,464,474} This is perhaps a result of greater osmotic pressure in the swollen state.⁴⁷¹ Investigation of ultrathin PNIPAM brushes showed differences in surface morphology, hydration, and protein

adsorption compared to those of dense and thick brushes.⁴⁵⁴ Consequently, the density of the brushes should be carefully chosen depending on the application of the surfaces of interest (single cell or cell sheets) and the type of substrates required. Terminal functionalization of the brushes has also been reported to influence cell adhesion and detachment from thermoresponsive brushes.⁴⁸⁷ Overall, brushes and underlying substrates favoring ternary protein adsorption over primary adsorption performed better for efficient cell attachment and detachment. However, this behavior depended on the specific protein (promoting cell anchorage) being adsorbed prior to cell adhesion and in particular how temperature modulated protein–brush interactions.⁴⁵⁶

5.3.5. Brush Functionalization. Another strategy to control cell adhesion and detachment without requiring the control of protein–brush interactions consisted of the conjugation of responsive brushes with cell-adhesive peptide sequences (such as RGD).^{433,459} Providing the peptide is located at or close to the brush surface, this strategy allowed cell adhesion in serum-free conditions. The brush was shown to be collapsed above the LCST, exposing the hydrophilic peptides and facilitating cell adhesion, while below the LCST the hydrated polymer brushes swelled and shielded the peptide from integrin access, causing disruption to cell anchorage to the surface and detachment.⁴⁵⁹ Finally, phenylboronic acid-based brushes have been used to capture cells expressing highly glycosylated membrane proteins.⁴⁸⁸ The use of nanotextured substrates (silicon nanowires) enhanced such capture, and glucose was used to induce cell release. This provided a simple method for cell purification.

5.4. Patterned Brushes for Controlling the Cell Microenvironment

Factors affecting cellular processes in the cell microenvironment are not efficiently captured under classic culture conditions and therefore give rise to artifacts and irreproducibility. This is because cells encounter a homogeneous adhesion substrate that is flat, rigid, and vast and thus does not represent the characteristics of the *in vivo* microenvironment. Microengineering techniques, however, allow subcellular-scale manipulation of the chemical properties of cell culture substrates.⁴⁸⁹ Engineered micropatterns offer micrometer-scale, complex, and dynamic microenvironments for individual cells or multicellular assemblies, as the fabrication of culture substrates with microscopic features provides defined cell adhesion and biofunctional geometry. These platforms allow the reconstitution of more complex microenvironments allowing the design of assays to probe cellular mechanisms or the testing of drugs and the systematic quantification of the expression of markers and their localization.^{489,490}

5.4.1. Strategies Developed for the Micropatterning of Polymer Brushes for Cell Patterning and Culture. A range of methods have been used to achieve micropatterning of polymer brushes for cell patterning applications (Table 5). A straightforward approach consists of using conventional photolithography to deposit the ATRP initiators ((3-((2-bromo-2-methylpropionyl)oxy)propyl)trichlorosilane or 3-(chlorodimethylsilyl)propyl 2-bromo-2-methylpropionate) between areas protected by a photoresist (Figure 28).^{491,501} After removal of the photoresist and subsequent surface-initiated ATRP, polymer brush patterns with micrometer-sized resolution were obtained. Although this method generated clean patterns on silicon oxide and glass (and potentially other

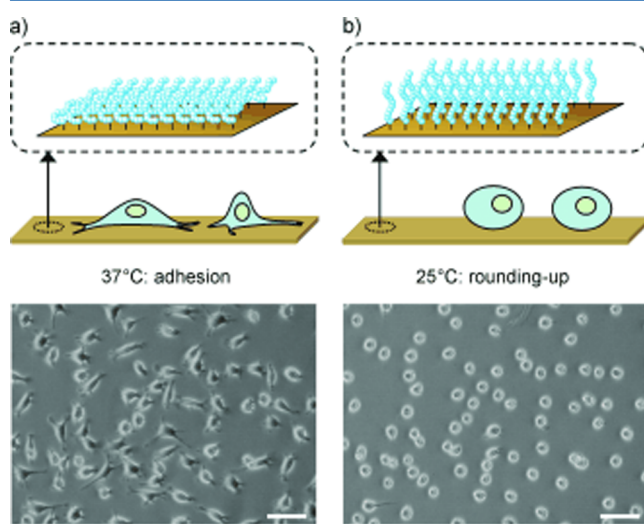


Figure 27. Cell adhesion and detachment from POEGMA-*co*-PDEGMA brushes. Reprinted with permission from ref 448. Copyright 2008 John Wiley and Sons.

Table 5. Polymer Brushes for Cell Patterning Applications^a

brush	patterning	substrate	initiator	cell type	assay	ref
PMEDSAH	photoresist AZ-5214	silicon	ATRP silane	3T3 fibroblasts	long term (29 days), pattern stability	491
PMEDSAH	deep-UV photopatterning	glass	ATRP silane	MC3T3-E1 osteoblasts	long term (21 days), mRNA levels (pS3, Ki67, H4)	492
PMPC	deep-UV photopatterning	silicon	ATRP silane	L929 mouse fibroblasts	short term (1 day)	261
POEGMA	microcontact printing	gold	ATRP thiol	3T3 fibroblasts	long term (28 days), pattern stability	219
POEGMA	microcontact printing	gold/glass	ATRP thiol, silane, macroinitiator	epidermal stem cells	medium term (7 days), pattern stability and cell polarization	223
POEGMA	photopatterning	PE	isopropylthioxanthone	MG63	live/dead assay	493
POEGMA	photoresist NR9-1500PY	silicon, PS, PMMA, PET, PE	ATRP silane, PVBC, P2-CEMA	human umbilical vein endothelial cells	short term (12 h)	100
POEGMA	macroinitiator dewetting	PS	ATRP macroinitiator	L929 mouse fibroblasts	short term (1 day)	494
POEGMA	microcontact printing	gold-coated glass	ATRP thiol	epidermal stem cells	cell differentiation, mechanotransduction mechanism	495, 496
POEGMA	microcontact printing	gold-coated glass	ATRP thiol	epidermal stem cells	multicellular clusters, microepidermis formation	497
POEGMA-biofunctionalized	microcontact printing	gold-coated glass	ATRP thiol	hNECs, HUVECs	cell viability, long term (31 days)	498
PNIPAM	deep-UV photopatterning	glass	APTES, then BMPB	mouse embryonic fibroblasts	single-cell spreading, F-actin organization, detachment	473
PHEMA-biofunctionalized	reactive ion etching	silicon	APTMS, then BiBB	MC3T3-E1 osteoblasts	cell spreading	499
PMAA (RGD-functionalized)	photopatterned gradient brushes	silicon	iniferter photoinitiator (SBDC)	3T3 fibroblasts	gradient cell culture (cell density assay)	500
PAA	photoresist LOR 5A	silicon	ATRP silane	2H3 RBL mast cells	cell spreading, mechanism of adhesion	501
PMETAC	photoresist LOR 5A	silicon	ATRP silane	rat hippocampus neuronal cells	cell adhesion, neurite length	502
POEGMA- <i>co</i> -PMETAC	photoresist S1813	silicon	ATRP silane	mouse hippocampal neuronal cells	cell density, viability, neurite length	503
POEGMA, PMEDSAH, PMETAC, PSPMA	microcontact printing	gold-coated glass	ATRP thiol	epidermal stem cells	cell viability, patterning efficiency, differentiation, FA formation	204
PMAA, PMEDSAH, PSPMA	deep-UV photopatterning	silicon, glass	ATRP silane	hMSCs	short term 1–4 (days)	504

^aAbbreviations: PET, poly(ethylene terephthalate); PE, polyethylene; PVBC, poly(vinylbenzyl chloride); P2-CEMA, poly(2-chloroethyl methacrylate); hNECs, human neuroepithelial cells; HUVECs, umbilical vein endothelial cells; APTES, (3-aminopropyl)triethoxysilane; BMPB, 2-bromo-2-methylpropionyl bromide; APTMS, (3-aminopropyl)trimethoxysilane; BiBB, 2-bromo-2-methylpropionyl bromide; SBDC, ((N,N-(diethylamino)-dithiocarbamoyl)benzyl)trimethoxysilane; FA, focal adhesion; hMSCs, human mesenchymal stem cells.

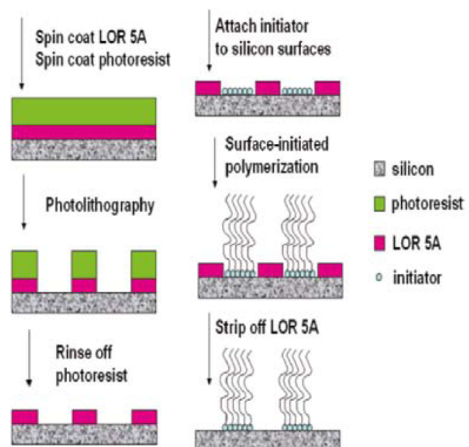


Figure 28. Patterning of polymer brushes using photolithography. Reprinted from ref 501. Copyright 2011 American Chemical Society.

substrates compatible with photolithography procedures), it required multiple patterning steps. Patterning of gold substrates (including ultrathin gold coatings on transparent glass slides)

using microcontact printing of a thiol initiator monolayer proved to be an excellent alternative: the clean and fast patterning of thiol molecules onto gold substrates allowed the generation of large numbers of patterned substrates required for biological experiments.⁵⁰⁵ Hence, POEGMA brushes have been patterned on gold substrates with excellent reproducibility and control of micrometer-sized features.^{219,223} Although AFM imaging showed that the edge contrast of such gold-patterned brushes was sharp, it was found that thick brushes (100 nm) lead to poor protein adhesion and cell patterning.²²³ This was perhaps a result of some polymer chains being initiated from the nonprinted areas. This problem was not observed for thinner coatings (20 nm), and given the excellent protein resistance of POEGMA brushes of this height, they were favored for high-quality cell patterning. Microcontact printing has also been reported on a variety of other substrates, including the deposition of silanes onto silicon and glass substrates.⁵⁰⁶ However, the poorer contrast associated with the patterning of these molecules resulted in graded edges and poor protein and cell adhesion, presumably owing to initiator diffusion away from the areas of contact between the stamp and the substrate.²²³ To reduce such effects, a polyelectrolyte

macroinitiator was printed instead of a silane initiator. This improved the profile of the patterned brush, protein adsorption, and cell adhesion, but required fresh stamps to be generated regularly as the plasma treatment used to improve the hydrophilicity of the stamp typically damaged it after a few rounds of printing.

Other works have used direct photopatterning to control brush growth at the micrometer scale. This offers the advantage of being compatible with a wider range of substrates while potentially retaining good control of the pattern resolution and not requiring photoresist-based lithography prior to brush growth. Li et al. used the adsorption of isopropyl thioxanthone onto plastic substrates to generate photoinitiating sites for polymer brush growth.⁴⁹³ They showed that this resulted in cell patterning to the unexposed areas. Deep-UV curing was also used to directly etch initiator monolayers deposited on glass or silicon substrates.^{261,492} This offers the advantage of avoiding diffusion of initiator molecules in the patterning step, although incomplete etching may result in a loss of pattern contrast. In addition, large-area patterning and the use of a wider range of substrates, including flexible polymers, should be possible using this method. A similar approach consists of deep-UV curing the polymer brush coating itself. Hence, Ahmad et al. found that irradiation of polymer brushes at 244 nm induced progressive etching of the exposed brush.³¹⁷ This correlated with an increase in protein adsorption, presumably because of chemical modification of the remaining brush (however, the loss in brush height was not sufficient to expose the underlying surface). A similar strategy was used by Mandal et al. to etch PNIPAM brushes (this time fully exposing the underlying substrate) before protein deposition and cell seeding.⁴⁷³ It was also found that local heating of a PNIPAM brush with a laser (wavelength 461 or 588 nm) was sufficient to induce the collapse of the coating and adsorption of proteins, resulting in easily programmable multifunctional protein patterns.⁵⁰⁷ Alternatively, Hucknall et al. used reactive ion etching to degrade POEGMA brushes, but this required the use of a photoresist as a mask.¹⁰⁰ Yang and co-workers similarly used reactive ion etching, combined with colloidal lithography, to degrade PHEMA brushes.⁵⁰⁸ Li et al. used reactive ion etching to pattern the initiator monolayer at the nanoscale before brush growth.⁴⁹⁹

Photopatterning was also used to directly control the initiation and brush growth of PMAA brushes.⁵⁰⁰ In this case, a self-assembled monolayer of the photoiniferter ((*N,N*-(diethylamino)dithiocarbamoyl)benzyl)trimethoxysilane was used to functionalize the substrate and patterning was achieved by varying the exposure time across the sample, thereby achieving a gradient brush. Alternatively, visible light was used to cleave polymer brushes from their substrates when a photolabile initiator was used.⁵⁰⁹ This allowed multicomponent protein patterning, but also potentially the direct writing of patterns during cell culture. Interestingly, recent development in photocontrolled ATRP, using an iridium complex (*fac*-[Ir(2-pyridylphenyl)₃]), has been used to control the patterning of polymer brushes and the generation of gradient brushes.^{510,511} In this system, visible light is used to activate the iridium complex and the redox ATRP process, hence enabling the reaction to start and stop depending on the illumination of a sample. Such photocontrolled surface-initiated ATRP should be well suited for cell patterning studies. Finally, another approach has exploited the dewetting of macroinitiator molecules to generate micropatterned areas that support the growth of

POEGMA brushes. The resulting substrates allow control over protein localization on the exposed substrates and guidance of fibroblast adhesion inside the dewetted areas.⁴⁹⁴ This substrate-independent method offers the advantage of being scalable and of low cost, although it does not control the geometry of the patterns generated.

5.4.2. Impact of the Brush Chemistry on Cell Patterning. Aside from the patterning methodology, the brush chemistry is also an important aspect of the design of a cell pattern assay. The high protein resistance of POEGMA and its chemical stability during storage and cell culture have made it particularly attractive for simple assays where the control of single-cell spreading, cell shape, and cell cluster size and geometry are of interest.^{219,223} POEGMA brushes allow simple deposition of ECM proteins such as collagen, laminin, and fibronectin directly from solution, just prior to cell seeding, hence ensuring the deposition of high-quality, freshly prepared protein patterns for fast cell adhesion. This is particularly important for the development of assays based on stem cells that initiate differentiation when they remain in suspension for too long prior to adhesion. Hence, the robustness of brush-based micropatterns offers interesting advantages compared to direct microcontact printing of ECM proteins. Other neutral polymers have similarly been used for protein and cell patterning. For example, PHEMA brush gradients have been used to control cell spreading and guide cell motility.⁵¹² The stability of zwitterionic PMEDSAH brushes was also compared with that of POEGMA brushes. Choi and co-workers found that the cell resistance of PMEDSAH was preserved up to 19 days, despite prior partial degradation of the brush coating.⁴⁹¹ Proliferative patterned cell cultures (3T3 fibroblasts) were not found to invade nonadhesive PMEDSAH areas until day 19, whereas POEGMA fully restricted cell spreading only until day 4, a difference that may be ascribed to the increased hydrophilicity of PMEDSAH brushes, despite similar or even slightly inferior protein resistance.²⁰⁴ However, this behavior is likely to be substrate-, cell-type-, and density-dependent as human primary keratinocytes remained constrained on POEGMA micropatterns for at least 7 days (last time point).²²³ Hence, for shorter studies, the patterning efficiency of PMEDSAH and POEGMA brushes was almost identical and the response of keratinocytes to changes of adhesion geometry was not altered.²⁰⁴ Other neutral brushes, such as the zwitterionic PMPC,²⁶¹ also showed protein and cell resistance, which makes them suitable for cell patterning. Finally, neutral thermosensitive brushes such as PNIPAM can also be used for cell patterning, providing their density is sufficiently high (protein resistance to such brushes is density-dependent),⁴⁷³ and it was found that single cells (mouse embryonic fibroblasts) could adhere to and spread well on PNIPAM patterns above the LCST of this polymer. Upon decreasing the temperature of the culture below the LCST (20–30 °C), cell detachment was observed only in patterns in which the cell membrane was overlapping brush-coated areas (e.g., for cells spreading on adhesive rings with a brush also grown in the center of the pattern). The authors proposed that this was a result of a net repulsive force generated on the cell membrane by the brush swelling below its LCST. However, work carried out with *Streptococcus mutans*⁶² suggests that interactions between cell membranes (although bacterial in that example) and swollen brushes are not necessarily repulsive, and hence, the cell response to patterned thermoresponsive systems is likely to be cell-dependent.

Neutral polymer brushes are not the only systems that have been explored for cell patterning. Anionic brushes such as poly(3-sulfopropyl methacrylate) (PSPMA) also display excellent performance for generating cell patterns, even for single-cell assays.²⁰⁴ This is surprising given the high protein adsorption levels observed to these brushes from the serum contained in cell culture media. Perhaps this is a result of the lack of specificity of the proteins adsorbed, as well as the strong negative charge characteristic of these brushes that can repel the cell membrane. Hence, with PSPMA patterns, it was possible to specifically deposit fibronectin to exposed substrate areas, and the resulting platforms allowed the control of cell spreading and shape to a level similar to that of patterns generated from neutral POEGMA or PMEDSAH brushes. Other charged brushes such as PAA displayed similar behavior; i.e., although rat basophilic leukemia (RBL) mast cells were not able to adhere to homogeneous PAA brushes, they adhered well to patterned brushes (2–10 μm square patterns; see Figure 29).⁵⁰¹ Interestingly, it was found that membrane proteins

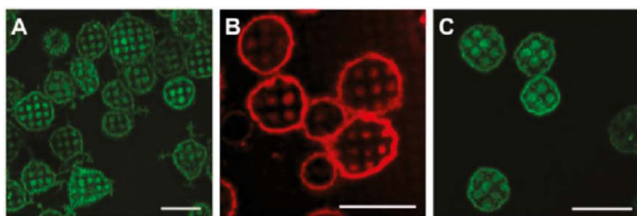


Figure 29. Patterning of RBL mast cells using PAA brushes and fluorescence imaging of membrane accumulation at PAA patches. Reprinted from ref 501. Copyright 2011 American Chemical Society.

accumulated at the PAA patches in that case, a phenomenon that correlated with fibronectin deposition to these brushes and which was inhibited by the presence of soluble RGD peptide or treatment with the F-actin disrupter cytochalasin D. Hence, despite the apparent cell resistance, PAA brushes can contribute to cell adhesion on patterned substrates.

Positively charged coatings such as poly(lysine) are often used for culturing or directing the growth of neuronal cells.

Ober and co-workers developed the use of PMETAC brushes for such applications.^{502,503} They patterned PMETAC or copolymers of PMETAC and POEGMA and found that these coatings supported well the growth of hippocampal neuronal cells, giving rise to more extended neurites and allowing the direction of their growth according to the underlying pattern. Cell viability was found to be very comparable to that measured on poly(lysine) when copolymers containing 10% PMETAC were used. This result contrasts with the high cell death reported for PMETAC homopolymer brushes when keratinocytes were seeded on this coating.²⁰⁴ Perhaps the resistance to the toxic effects is cell-dependent, but it could also be a result of differences in surface conditioning upon exposure to different cell culture media as the resistance is likely to be sensitive to surface charge densities (as for the copolymer of PMETAC and neutral POEGMA used by Ober and co-workers).⁵⁰³

5.4.3. Cell-Based Assays Developed Using Polymer-Brush-Based Platforms.

Overall, polymer brushes offer important advantages for microengineered cellular assays as they are particularly stable coatings that allow the control of the surface chemistry and geometry of adhesive or biofunctional molecules. Hence, they have been used in a variety of assays that explored the impact of the cell microenvironment on cell behavior. Poly(L-lysine) (PLL)-PEG and PMEDSAH brushes were used to control protein deposition and cell adhesion on nanopatterned substrates generated via colloidal lithography.⁵¹³ This allowed the control of the size of adhesions that keratinocytes formed with the substrates, from 100 nm to 3 μm . It was found that decreasing the size of adhesions resulted in a gradual decrease in cell spreading and correlated with an increased frequency of cell differentiation. This assay also suggested that the geometrical maturation of adhesions (from nascent adhesions to mature focal adhesions) controls the ability of cells to establish a mature actin cytoskeleton, independently of the biochemical maturation of the adhesion sites (protein recruitment and composition, phosphorylation, and matrix deposition). Connelly et al. showed that simple variation of the size of adhesive islands defined by POEGMA brushes enabled the control of cell spreading and that this had a

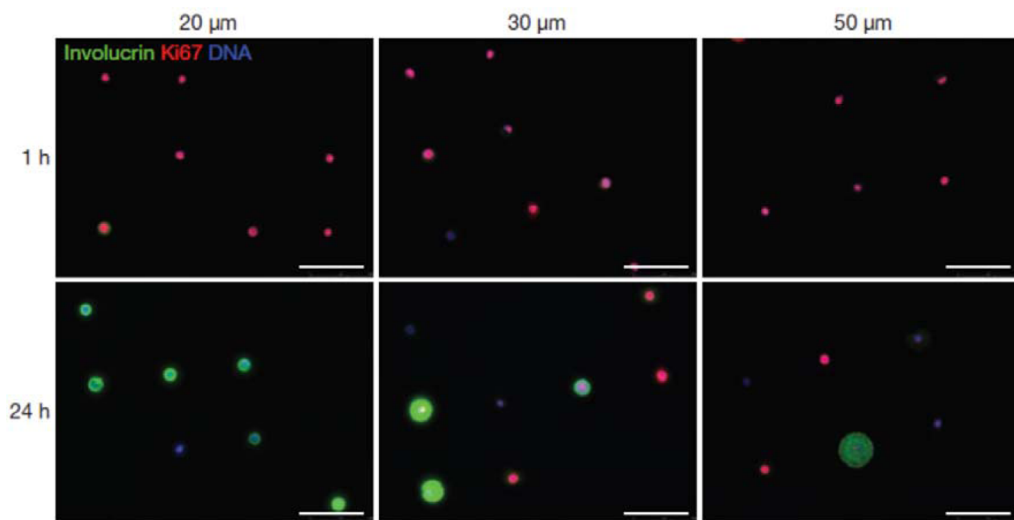


Figure 30. Examples of polymer-brush-based cell arrays for controlling the impact of the microenvironment on the fate decision of epidermal stem cells. Cells seeded on small islands (20 μm) differentiate more (involutrin expression in green), whereas cells allowed to spread on 50 μm islands are more proliferative (Ki67 expression in red). Reprinted with permission from ref 495. Copyright 2010 Nature Publishing Group.

direct impact on the keratinocyte fate decision (Figure 30).⁴⁹⁵ Restricting cell spreading and forcing rounded cell morphologies increased the incidence of differentiation, whereas allowing full spreading allowed the cell to remain proliferative and express stem cell markers. It was found that the pattern geometry, and in turn cell shape, controlled the remodeling of the F-actin cytoskeleton, inducing a shift in the balance of F- to G-actin and downstream megakaryoblastic leukemia 1–serum response factor (MAL–SRF) signaling mediated by AP1 and histone acetylation.^{495,496} Aside from cell spreading, micro-patterned substrates also allowed the control of cell polarization and orientation,²²³ as well as systematic quantification of this phenomenon and the molecules that mediate it. Although it was found that cell spreading and the cell projected area were the main determinants of keratinocyte fate decision, the chemistry of the brush coating had an impact on cell differentiation too.²⁰⁴ Cells spreading on arc-shaped patterns defined by negatively charged PSPMA brushes differentiated more frequently than those spreading on neutral PMEDSAH or POEGMA patterns of the same shape. Hence, polymer brushes allow the exploration of the coupling between geometrical adhesive cues and physicochemical surface properties. Brush-based micropatterns have also been used to generate multicellular cluster arrays. It was found that the geometry of larger adhesive islands ($100\text{ }\mu\text{m}$) allowed multiple keratinocytes to adhere and self-organize into compartmentalized tissue-like structures (“microepidermis”, Figure 31).⁴⁹⁷ Using this platform

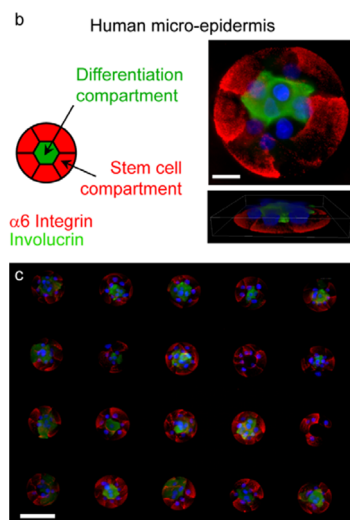


Figure 31. Probing the level of cell differentiation and the respective positioning of stem cells and differentiated cells using arrays of cell clusters. Reprinted with permission from ref 497. Copyright 2012 Elsevier.

form, the impact of cell–matrix and cell–cell interactions on the formation of such microtissues and the disruption of this phenomenon in cancer were studied. Finally, the biofunctionalization of POEGMA brushes using thiol–ene chemistry was exploited to generate dynamically adhesive patterns.²⁹³ Such platform can be used to study how geometrical constraints of the microenvironment affect cell migration and wound healing.

Hence, compared to simple tissue culture plastics, polymer brush micropatterns are ideal platforms for the generation of cellular assays aiming to capture more complex cellular phenotypes and tissue functions and to systematically quantify these phenomena. These systems are particularly interesting for

the testing of cellular mechanisms and pathways, as well as the design of improved in vitro models for the screening of drug efficacy. Future developments in this field will no doubt add to the complexity of the current brush-based platforms, for example, enabling multiple patterning of proteins,⁴⁹⁸ peptides, and growth factors and allowing the design of dynamic, responsive substrates to improve current in vitro models of cell and tissue culture.

6. ANTIBACTERIAL COATINGS BASED ON POLYMER BRUSHES

Antibacterial coatings that prevent formation of bacterial biofilms are desirable for a wide range of applications.^{514–516} Bacterial biofilms on surfaces can, for example, cause problems in healthcare by medical-device-associated infections, in the shipping industry through increased friction on ship hulls or biocorrosion, and in water or food storage. Although biofilm formation is sometimes desirable, for example, for producing fine chemicals or for degradation of waste, the long-term preservation of unwanted bacterial adhesion and colonization remains an important challenge. Polymer brushes have been presented as possible candidates for antibacterial coatings and have been reported to reduce the overall adhesion of bacteria for both hydrophobic and hydrophilic brushes.^{205,517} It has also been described that bacterial adhesion on “switchable” polymer brushes, such as PNIPAM, differs above and below the LCST. Below the LCST the brush is extended, which reduces the amount of adherent bacteria on the surface.^{477,518} The coatings can, as previously described in this review, be applied onto a range of different materials. In the literature, three main approaches are reported for constructing antibacterial brush coatings (Figure 32, Tables 6–8): (1) polymer brushes

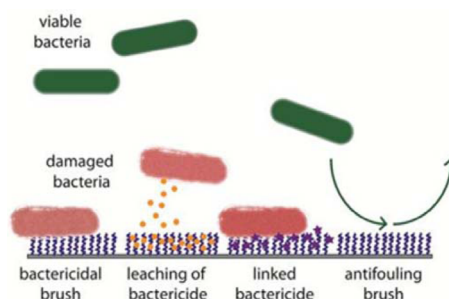


Figure 32. Schematic of common approaches described in the literature for creating polymer-brush surfaces that inhibit bacterial adhesion and biofilm formation. Viable bacteria are color-coded in green and damaged bacteria in red. Note that bacteria in this schematic (often one to a few micrometers in size) are drawn very small in relation to the brush size (often of nanometer dimensions) to more easily illustrate the brush action.

composed of a bactericidal polymer, (2) polymer brushes functionalized with a bactericidal or bacteriostatic compound, either covalently linked to the brush or embedded in the brush film to allow subsequent diffusion, and (3) nonfouling polymer brushes that aim to repel bacterial adhesion and subsequent biofilm formation. This section will especially emphasize what is known about the mechanisms via which brush coatings prevent biofilm formation, and bacterial attachment, in the three approaches. However, first a brief introduction of experimental methods is given to facilitate the understanding of the tables and discussions.

Table 6. Polycationic Brushes Tested for Antibacterial Effects

brush ^a	functionalization ^b	substrate ^c	exposure time	bacterial loading used ^d ^e	assay	bacterium ^e	solution during exposure ^f	ref
chitosan	Q with METAC	SiO ₂	6 h	10 ⁴ CFU/mL {4}	S. aureus		dil brain heart infusion	539
chitosan	Q with METAC	SiO ₂	2 days	10 ⁶ CFU/mL {2, 3B, 5}	S. aureus		dil brain heart infusion	540
P4VP	Q with hexBr	PVBC micro-spheres	20 min to 2 h	10 ⁵ CFU/mL {1}	E. coli		PBS	541
P4VP	Q with hexBr	stainless steel	3–21 days	10 ⁶ MPN/mL {1B, 3C}	D. desulfuricans		SSMB	542
P4VP	Q with hexBr	polyimide	2 h	10 ⁷ CFU/mL {4}	E. coli		PBS	543
hb PBPEA	Q with pyridine	stainless steel	1 h	10 ⁸ CFU/mL {1, 4}	S. aureus		0.9% saline	544
PCBMA-1 (cationic precursor), PC8NMA, PCBMA-2 (control)		gold	1 h	10 ⁷ –10 ¹⁰ CFU/mL {4, 3B}	E. coli		N/S	545
PCBMA		PP membranes	2 h	10 ⁵ CFU/mL {1}	S. aureus		broth	546
PDMAEMA	Q with etBr	glass and paper	1 h	10 ⁴ –10 ⁹ CFU/mL {1, 2, 3C}	B. subtilis, E. coli		LB broth dil w/ buffer	533
PDMAEMA	Q with etBr	glass	30 min to 1 h	10 ⁵ –10 ¹⁰ CFU/mL {1, 2, 3B}	E. coli		LB broth dil w/ buffer	534
PDMAEMA	Q with etBr	PP	1 h	10 ⁵ CFU/mL {1}	E. coli		N/S	535
PDMAEMA	Q with etBr	glass	20 min to 1 h	10 ⁸ CFU/mL {1, 2}	E. coli		LB broth	536
PDMAEMA	Q with etBr	Fe ₃ O ₄ NPs	1 h	10 ⁵ –10 ⁶ CFU/mL {1}	E. coli		LB broth dil w/ buffer	537
PDMAEMA	Q with decBr	PP membranes	0–1 h	10 ⁵ CFU/mL {1, 3A}	E. coli, S. aureus		PBS	547
PDMAEMA	Q with benzyl halide or viologen	stainless steel	3–21 days	10 ⁶ MPN/mL {1, 3A}	D. desulfuricans		SSMB	548
PDMAEMA	Q with propargyl bromide, then click polyglycerols, click PEI, Q with hexBr	PVDF membranes	4–18 h	10 ⁸ CFU/mL {3A, 7}	E. coli, S. epidermidis		PBS then broth	549
PDMAEMA	Q with hexBr	PVDF membranes	2 h	10 ⁷ CFU/mL {4}	E. coli		PBS	550
PDMAEMA	Q with alkyl halide	PET	1 h	10 ⁵ CFU/mL {1}	E. coli		LB broth	526
PDMAEMA-co-EGDMA		silica NPs	0–60 min	10 ² –10 ⁵ CFU/mL {1, 3A, 15}	E. coli, S. aureus		water or broth	551
hb PEI	Q with octCl	stainless steel	1 h	10 ⁸ CFU/mL {1, 4}	S. aureus		saline	544
PGMA	ethylamine or diethylamine	PE membranes	0–8 h	10 ⁹ CFU/mL {2, 6}	E. coli, B. subtilis		PBS	299
PGMA	diethylamine	PE membranes	0–70 h	10 ⁸ CFU/mL {2, 3B, 7, 5, 14}	E. coli		PBS then LB	538
PGMA	diethylamine	PE membranes	0–8 h	10 ⁹ CFU/mL {3A, 6}	E. coli, P. aeruginosa, P. putida, P. fluorescens, Pa. denitrificans		PBS	552
PHEMA	chitosan	stainless steel	4 h	10 ⁶ or 10 ⁸ CFU/mL {1, 2}	E. coli		PBS	308
PMETAC		glass	0–72 h	10 ⁹ CFU/mL {2, 3B, 7, 8, 14}	P. aeruginosa		saline then isosensitest	205
PMETAC		glass	24 h	10 ⁷ CFU/mL {1, 3A}	Pseudomonas sp., S. aureus		simul seawater and PBS	517
PMETAC		stainless steel	4 h	10 ⁷ CFU/mL {1, 3A}	E. coli, S. epidermidis		PBS	553
PMETAC		PES membranes	filtering of 3 L	10 ⁶ CFU/mL {2, 3B}	E. coli		PBS	554
PIL	exchange of counterions	TiO ₂ NPs	24 h, 3 days	10 ⁶ CFU/mL or 10 ⁶ spores/mL {1, 3B}	E. coli, S. aureus		PBS or artif seawater	555

^aAbbreviations: P4VP, poly(4-vinylpyridine); hb, hyperbranched; PIL, poly(ionic liquid); EGDMA, ethylene glycol dimethyl acrylate.

^bAbbreviations: Q, quaternized; hexBr, hexyl bromide; etBr, ethyl bromide; decBr, decyl bromide; octCl, octyl chloride. ^cAbbreviations: PP, polypropylene; PVBC, poly(4-vinylbenzyl chloride); PVDF, poly(vinylidene fluoride); PET, poly(ethylene terephthalate); PE, polyethylene; PES, poly(ether sulfone); PBPEA, poly(2-(2-bromopropionato)ethyl acrylate). ^dAssays: 1, plating for CFU; 1B, plating for MPN; 2, live/dead or other staining; 3, microscopy imaging (3A, scanning electron microscopy; 3B, optical or fluorescence microscopy; 3C, atom force microscopy); 4, CFU counts on the surface of the sample; 5, shear stress or detachment study; 6, OD monitoring (optical density at 600 nm) or luminescence; 7, flow cell setup; 8, motility assay; 9, disk diffusion study; 10, CD spectroscopy studies; 11, in vivo studies; 12, surface plasmon resonance studies; 13, gravimetric studies; 14, biofilm quantification; 15, MIC determination; 16A, static exposure; 16B, dynamic exposure. ^eS. aureus = *Staphylococcus aureus*, E. coli = *Escherichia coli*, D. desulfuricans = *Desulfovibrio desulfuricans*, B. subtilis = *Bacillus subtilis*, S. epidermidis = *Staphylococcus epidermidis*, P. aeruginosa = *Pseudomonas aeruginosa*, P. putida = *Pseudomonas putida*, P. fluorescens = *Pseudomonas fluorescens*, and Pa. denitrificans = *Paracoccus denitrificans*. ^fAbbreviations: dil, diluted; N/S, not specified; SSMB, seawater-based modified Baar's medium.

6.1. Examples of the Experimental Setup for Determining the Antibacterial Properties of Polymer Brushes

A classical experiment used for quantitative data on bacterial attachment is to determine the number of remaining viable bacteria after exposure to a surface. This is done by monitoring the amount of colony-forming units (CFU), i.e., bacteria viable enough to reproduce either at the surface or in surrounding solution after a specified exposure time. Each viable bacterium will give rise to one colony on an agar plate. Serial dilutions of the bacterial suspension of interest enable counting of colonies. The amount of CFU/mL is obtained when the dilutions performed are taken into consideration. One important consideration for this method is that if antibacterial agents are leached from a surface into the solution, it is likely that they will have a continued effect throughout the incubation on agar plates, which prolongs the real exposure time. Furthermore, it is important (as with all methods) to have relevant reference surfaces since detachment methods, e.g., using sonication, can damage cells.⁵¹⁹ Viable counts can also be made directly on surfaces after exposure to a bacterial suspension or a bacterial aerosol.⁵²⁰ For sulfate-reducing bacteria a method called most-probable number (MPN) is often used and is based on specific enumeration media where bacterial counts are estimated from secondary processes in the media.⁵²¹

Viability is also often studied through staining using a live/dead stain.⁵²² This stain generally consists of two fluorescent dyes, Syto-9 and propidium iodide. As the two dyes do not penetrate membranes equally, cells with a compromised membrane stain red from propidium iodide and viable cells stain green with Syto-9. Syto-9 stains both live and dead bacteria, whereas only dead or damaged bacteria are stained with propidium iodide. It should be noted that propidium iodide can also stain negatively charged structures such as extracellular DNA or polyanionic polymer chains.

To determine the antibacterial effect of compounds leaching from a surface, disk diffusion (or the Kirby Bauer method) is used (described in detail in *Performance Standards for Antimicrobial Disk Susceptibility Tests*⁵²³). A large number of bacteria (enough to form a bacterial lawn) are spread onto an agar plate, and the sample is carefully placed onto the spread bacteria. After incubation overnight, the “zone of inhibition” around the sample is measured and is indicative of the toxicity of the leached compound to the bacterial strain. For soluble compounds the minimal inhibitory concentration (MIC) can be determined in solution. Serial dilutions of the compound are performed in growth medium, and bacteria are subsequently inoculated. After incubation, the minimal inhibitory concentration can be read as the first vial without visible growth.⁵²⁴ However, it is important to remember that the MIC obtained is often sensitive to the culture medium used, etc.⁵²⁵

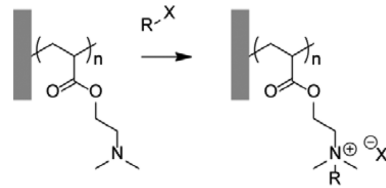
For studies performed during longer time spans, it is generally best to have a continuous flow system where medium with nutrients can be supplied to bacteria at a desired flow rate. If bacteria are kept for long periods of time in the same medium or in saline, they will likely be damaged irrespective of what type of surface or compound they are exposed to and the testing will be performed on bacteria that are weakened by the lack of nutrients. Thus, if appropriate controls are not used, misleading conclusions can be drawn from such data.

6.2. Polymer Brushes Based on Bactericidal Polymers

Bactericidal polymer brushes presented in the literature (Table 6) are almost exclusively from quaternary amines forming

polycationic surface coatings. The vast majority of publications on polycationic bactericidal polymer brushes deal with PDMAEMA that is quaternized using an alkyl halide (Scheme 7). Several lengths of alkyl halide have been used to quaternize

Scheme 7. Quaternization of PDMAEMA Using Alkyl Halides (RX)



PDMAEMA brushes, and lengths of six or seven carbons or more have been reported to increase the antibacterial efficiency,^{526,527} similar to reports for bulk polymers from polyethylenimine.⁵²⁸

The bactericidal mode of action of polycationic brushes on cell membranes has, so far, not been completely understood. However, it is likely that the mechanisms are similar to what has been proposed for other free polycationic polymers and substances. For these, most authors agree that the polycations interact in some way with the membrane and that this causes leakage of cell compounds. However, the exact sequence of events is not clearly determined, and a couple of hypotheses exist. Vooturi and Firestone reviewed the literature between 2004 and 2010 for membrane-targeting antibiotics.⁵²⁹ They did not find a fully determined mechanism but stated that cationic charge and amphiphilicity are important parameters and that this was due to insertion of substances into the membrane depolarizing it and causing release of ions and metabolites. For phosphatidyl glycerol lipid membranes it has been shown that association of cationic polyelectrolytes leads to conformational changes.⁵³⁰ These changes were interpreted as insertion into the membrane, and it was found that bulkier polymers displayed a reduced insertion.⁵³⁰ This hypothesis about insertion can also be found in publications from Klibanov et al.⁵³¹ Another group studied the effect of polyethylenimine on the permeability of several Gram-negative bacterial strains and found effects similar to those of EDTA. They also found that the effect could be damped by additions of MgCl₂.⁵³² The hypothesis brought forward was that the polycations permeabilize and destabilize the membrane through depletion of cations “cross-linking” the lipopolysaccharide (LPS) membrane in Gram-negative bacteria.⁵³² Thus, the two main hypotheses for membrane interactions with polycationic substances are insertion of the substance into the membrane and/or removal of stabilizing counterions.

The group of Matyjaszewski performed several studies investigating the importance of charge density to the antibacterial effect of PDMAEMA brushes quaternized with ethyl bromide.^{533–537} They observed that with different loadings of cells they reached an upper limit of efficiency of around 10⁹ CFU/mL for *Escherichia coli* and 10⁶ CFU/mL for *Bacillus subtilis* and that cells died quite rapidly, i.e., within 15 min.⁵³³ The most biocidal surfaces had more than 1–5 × 10¹⁵ charges/cm², and the maximum killing capacity of a surface was reached at 8 × 10¹⁵ charges/cm² (with bacterial loadings of 10⁷ and 10⁸ CFU/mL and incubation times of 30 min; see Figure 33). However, they did not find chain length or chain density to be important. The authors noted that the surface charge of *E.*

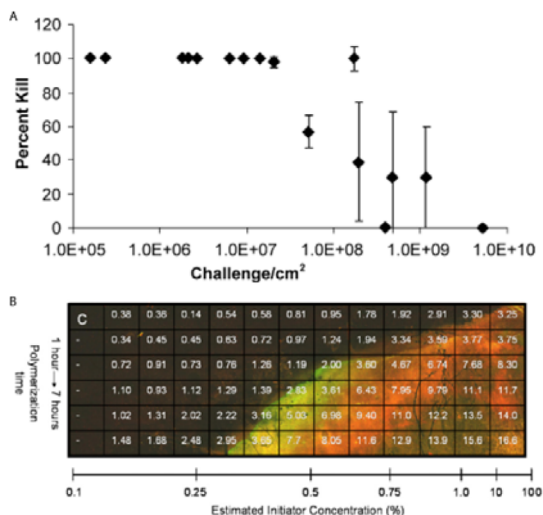


Figure 33. (A) Percentage of killed *E. coli* cells as a function of bacterial load (challenge) on glass surfaces with a high density of cationic charge, i.e., 8×10^{15} charges/cm². (B) Mosaic of live/dead staining of *E. coli* cells made from 500 images of a glass slide with a gradient polycationic brush. The charge densities in positive charges/cm² ($\times 10^{15}$) are superimposed and shown as numbers. Reprinted with permission from ref 534. Copyright 2007 Elsevier.

coli cells has been reported as 5×10^{14} to 5×10^{15} charges/cm² depending on the growth phase of the cell, corresponding well to the number of charges required at the surface for good efficacy.⁵³⁴ The maximal bacterial loadings corresponded roughly to a monolayer of cells at the surface of the sample. This was later confirmed in experiments showing that polymer brush surfaces with quaternary amines kill the first monolayer of cells but that excess cells, or longer incubation times, give surviving cells a chance to grow and form a biofilm on top of the layer of dead bacteria.^{205,538}

Matyjaszewski's group also investigated the differences in bactericidal efficacy between grafted-to and grafted-from surfaces.⁵³⁶ They found similar killing efficacy; however, the grafting-to polymers gave rise to heterogeneous surfaces with patches of more dense polycationic film and higher charge density. Also here charge density was a more important factor than chain length or chain density. In grafting-to approaches the charge density was found to be lower overall (6×10^{14} vs 10^{16} charges/cm²) and did not reach the maximum killing efficiency of the grafting-from brushes. However, due to the heterogeneities at the grafted-to surfaces, they were more efficient at equal charge density (Figure 34).⁵³⁶

In repeated bacterial exposures, polycationic surfaces were reported to become covered with extracellular substances and/or cell debris that reduce the antibacterial efficacy unless removed through thorough washing with sodium dodecyl sulfate (SDS)⁵³³ or by shaking if the brushes were grown on nanoparticles.⁵³⁷ This is in accordance with studies showing that polycationic brush surfaces adsorb large amounts of substances from growth media, producing conditioning films that can reduce their biocidal effect,^{204,205} possibly explaining why biofilms have been reported on polycationic surfaces after time periods of a few days.^{205,538} Many studies have been performed in relatively clean buffer solutions and during short time periods (Table 6), and it can be expected that the efficacy of the surfaces would have been lower in more complex media. However, Lee et al. found that biofilms formed on quaternized

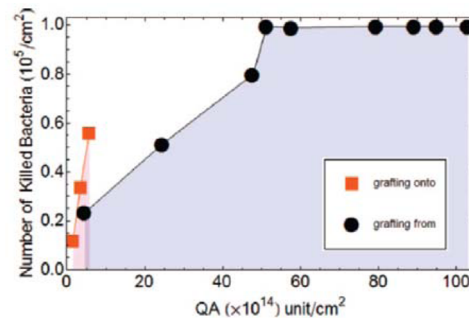


Figure 34. Difference in biocidal activity on *E. coli* between grafted-from and grafted-to polycationic brushes. QA = quaternary amine group. Reprinted from ref 536. Copyright 2008 American Chemical Society.

chitosan were more easily removed by shear stress than biofilms on pure chitosan^{539,540} and suggest this was due to more pronounced swelling in the charged quaternized brushes.⁵⁴⁰ This could perhaps indicate that even if biofilms are formed on polycationic surfaces, they will be more easily removed thanks to the layer of debris between the biofilm and the swollen polymer brush, although the opposite observation was reported by Terada et al., who found biofilm on polycationic surfaces to be quite resistant to shear forces.⁵³⁸

A hypothesis for the biocidal mechanism of polycationic brushes was proposed by Matyjaszewski and co-workers. It was based on the high killing efficiency of short polymer chains that should not be able to penetrate the bacterial cell wall and the lack of importance of chain length for efficacy. This hypothesis suggests destabilization of the membrane from a process of cation exchange, leading to loss of important metal ions cross-linking the LPS membrane in Gram-negative bacteria and stabilizing its negative charge.^{534,536}

A few examples of "smart surfaces", allowing controlled cell attachment and release, have also been presented using polycationic brushes. Irreversibly switchable surfaces were synthesized in the form of zwitterionic PCBMA brushes with cationic derivatives.^{545,546} These surfaces were designed to first immobilize and kill bacteria and then, through hydrolysis release of the top layer of cationic polymer and dead bacteria, to expose an antifouling surface beneath. The surfaces managed to reduce the number of *E. coli* by 3 orders of magnitude and release 98% of them during hydrolysis. The hydrolysis of a surface exposed to 10^{10} cells/mL took 8 days, and that of a surface exposed to 10^7 cells/mL took 48 h.⁵⁴⁵ A more reversible surface was created by the same group using acrylate copolymers of (2-(acryloyloxy)ethyl)trimethylammonium chloride (AETAC, the acrylate equivalent of (2-(methacryloyloxy)ethyl)trimethylammonium chloride, METAC) and 2-carboxyethyl acrylate (CEA, the acrylate equivalent of 2-carboxyethyl methacrylate, CEMA).¹⁶³ At low pH, when the carboxylate groups were protonated, the surface was positively charged, and at neutral or high pH, the surface became antifouling. These surfaces adsorbed bacteria at low pH to a higher extent than corresponding zwitterionic homopolymers, and there was a release of bacteria at higher pH.¹⁶³ Another version of a switchable surface was constructed using a patterned surface where some areas were made biocidal using quaternary ammonium salt with thermoresponsive PNIPAM occupying the space between these areas.⁵¹⁸ Above the LCST, when the brush was collapsed, the biocide was exposed,

resulting in bacterial attachment and killing. However, when the temperature was lowered using cold water, the brush swelled, causing detachment of the majority of dead bacteria (Figure 35).⁵¹⁸

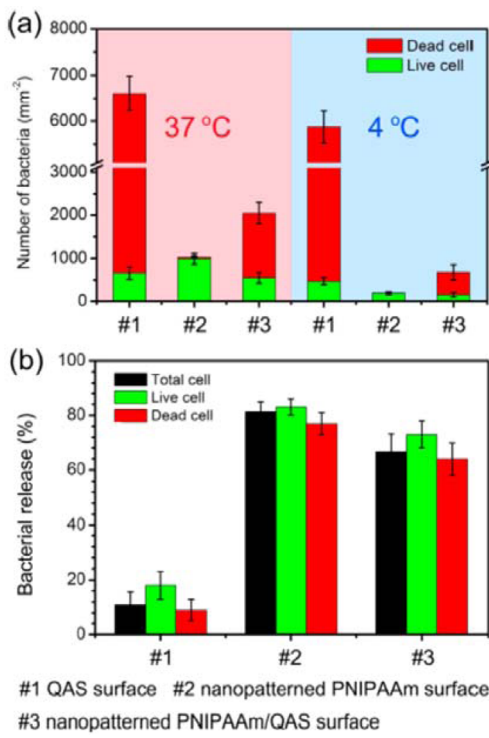


Figure 35. (a) Attachment of *E. coli* onto a patterned PNIPAM/polycationic surface and control surfaces after 2 h at 37 °C, as well as after subsequent rinsing with saline and water at 4 °C. (b) Percentage of bacterial release in (a). Reprinted from ref 518. Copyright 2013 American Chemical Society.

The differences in experimental conditions and choice of bacterial strains make it very difficult to compare and draw general conclusions about the efficacy of different polycationic surface compositions (Table 6). However, it is clear that the killing efficiency of these types of surfaces is dependent on the charge density at the surface, the surrounding solution composition, the bacterial loading, and the strain of bacteria chosen. However, it can be concluded that polycationic brushes are bactericidal under optimal conditions (e.g., low bacterial loadings in saline or water) but that their efficacy is lowered with time due to debris accumulating at the surface from dead cells and/or from the surrounding solution. Consequently, a suggestion for future work on polycationic surfaces is that antibacterial effects are monitored for longer time intervals and/or through repeated exposures and that the possibility of formation of conditioning films from complex growth media and from bacterial debris is well investigated.

6.3. Polymer Brushes Functionalized with Antibacterial Compounds

Brushes functionalized with antimicrobial agents follow two main types of design. Either a substance is incorporated into a brush to give a surface that releases it into the surrounding solution, or the antimicrobial compound is covalently linked to the brush (Figure 31). Both approaches have advantages and disadvantages.

Surfaces that leach antibacterial agents are less sensitive to deposition of surface debris since antimicrobials often diffuse through an overlayer of material. However, since the active ingredient is leached, the surfaces will have a limited lifetime and the active ingredient can possibly cause unwanted effects on the surrounding host cells. The amount of substance that leaches out also must be concentrated enough to have the expected effect. In the literature, common examples of this approach make use of the diffusion of silver ions from charged brushes or brushes with trapped silver halide salts or silver nanoparticles.^{525,559,560,569,570} In general, most studies find that silver ions and silver compounds are very efficient against both Gram-negative and Gram-positive bacteria (reducing bacterial growth by several logarithmic units), but only if they are used in very clean systems, e.g., distilled water, saline, or buffer solutions, which lack substances with an ability to chelate silver ions (Table 7). However, in the presence of, e.g., serum proteins, the antibacterial effect is much reduced or disappears completely.⁵²⁵ Furthermore, the cytotoxic effects of silver ions and silver nanoparticles observed on mammalian cells⁵²⁵ and especially nerve cells^{571–573} make it questionable if these types of surfaces are suitable for usage in medical devices. Brushes with drug release have also been constructed with the antimicrobial peptide nisin^{562,574} or with traditional antibiotic substances such as triclosan, bromopol, benzalkonium chloride, and chlorhexidin being trapped in a polymer brush.^{557,558} Although the surface with triclosan displayed antibacterial properties in disk diffusion studies, it was not able to reduce bacterial colonization during a time span of 24 h. The other surfaces with traditional antibiotics reduced colonization of *E. coli* by less than a logarithmic unit.^{557,558} Yu et al. investigated the use of patterned PNIPAM brushes presenting areas containing surface-adsorbed lysozyme. The pattern was designed to expose surface-deposited lysozyme at 37 °C and swell to hide the enzyme at 25 °C, as well as release bacteria as the brush went through the transition. The surfaces displayed 60–70% killing efficiency and released ~70% of the attached bacteria, leading to reduced killing efficiency in subsequent exposures.⁵⁶⁶

The advantage of covalently linking an antibacterial agent to a brush is that the substance remains on the surface for longer time periods, and also it is less prone to interfere with the surrounding tissues or cells. However, the drawbacks are that if the surface is covered in debris, the substance will be buried, which can lead to a loss of function. Furthermore, this approach requires that the active target of the substance is situated on the outer surface of the bacterium. Several examples of this approach can be found in the literature (Table 7). Both antimicrobial peptides and proteins targeting the bacterial cell wall have been covalently linked to brushes and retained their antibacterial activity. However, some groups report a lower activity for the immobilized peptide compared to the soluble peptide due to lower flexibility and diffusivity.⁵⁶³ The group of Glinel et al. designed surfaces so that the antimicrobial peptide magainin I was linked to a relatively long flexible oligo(ethylene glycol) side chain to retain some of the mobility of the molecule and allow for better interactions with the cell membrane.^{291,568} They also investigated temperature-responsive brushes that would expose the peptide at 26 °C and hide it at 38 °C (Figure 36) to avoid harmful effects on mammalian cells, as well as coated magnetic beads which would allow for easy disinfection of solutions.^{567,568}

Table 7. Brushes with External Antimicrobial Agents Tested for Antibacterial Effects^a

brush	functionalization	surface	exposure time	bacterial loadings used ^b {assay}	bacterium ^c	solution during exposure	ref
PDMA- <i>co</i> -PAPMA	AMP: Tet-213, 1010cys, Tet-20, Tet-21, Tet-26, HH2, MXX226	Ti, quartz	1 h to 7 days	10 ⁵ –10 ⁸ CFU/mL {1, 2, 3AB, 6, 11}	<i>P. aeruginosa</i> , <i>S. aureus</i>	broth	556
PDMA- <i>co</i> -PAPMA	AMP: Tet-213	Ti	4 h	10 ⁵ CFU/mL {6}	<i>P. aeruginosa</i>	BM2 culture medium	292
PAA	triclosan	PVC	24 h	10 ⁸ CFU/mL {1, 9}	<i>S. aureus</i> , <i>E. coli</i>	broth	557
PAA	bronopol, benzalkonium chloride, chlorhexidine	PVC	24 h	10 ⁸ CFU/mL {1}	<i>S. aureus</i> , <i>E. coli</i>	broth	558
PAA	Ag nanoparticles	paper	29 h	{6}	<i>E. coli</i>	LB broth	559
PEG	Ag nanoparticles	PC	24 h	10 ⁸ –10 ⁹ CFU/mL {2, 3B}	<i>E. coli</i> , <i>P. aeruginosa</i> , <i>S. epidermidis</i>	saline	560
Pluronic	lysozyme	silicone rubber	0–20 h	10 ⁸ CFU/mL {1, 2, 7}	<i>B. subtilis</i>	PBS followed by broth	561
PEG	AMP: nisin	polystyrene or polyurethane	4 h to 6 days	{1, 9, 10}	<i>Pe. pentosaceus</i>	broth	562
poly(allyl glycidyl ether)	AMP: RK1, RK2	PDMS and urinary catheters	3 h to 3 days	10 ⁶ –10 ⁸ CFU/mL {1, 2, 3AB, 14}	<i>E. coli</i> , <i>S. aureus</i>	broth, PBS, or urine	563
PMA	silk sericin	Ti	5 h	10 ⁷ CFU/mL {1, 2, 3B}	<i>S. aureus</i> , <i>S. epidermidis</i>	PBS	306
PMEDSAH, PCBMA	Ag nanoparticles	gold	1 h	10 ⁷ CFU/mL {2, 3B, 4}	<i>E. coli</i>	water or PBS	564
PNIPAM	carbon nanotubes	layer by layer structure on Si wafer	2 h	10 ⁷ CFU/mL {2, 3B}	<i>Exiguobacterium</i>	PBS	565
PNIPAM	SAM of quaternary ammonium salt	Si wafer	2 h	10 ⁸ CFU/mL {2, 3A, 3B}	<i>E. coli</i> , <i>S. epidermidis</i>	saline	518
PNIPAM	lysozyme	Si wafer	2 h	10 ⁷ –10 ⁸ CFU/mL {2, 3A, 3B}	<i>E. coli</i> , <i>S. epidermidis</i>	saline or PBS	566
POEGMA-OH POEGMA-OMe HEMA	AMP: magainin I	Si wafer	3 h	10 ⁷ CFU/mL {2, 3B}	<i>L. ivanovii</i> , <i>E. coli</i>	water	567
POEGMA-OH	AMP: magainin I	Si particles	3 h	10 ³ CFU/mL {1, 3B, 2}	<i>L. ivanovii</i>	water	568
POEGMA-OMe	AMP: magainin I	Si particles	3 h	10 ³ CFU/mL {1, 3B, 2}	<i>L. ivanovii</i>	water	568
POEGMA-OH POEGMA-OMe	AMP: magainin I	Si wafer	3 h	10 ⁷ CFU/mL {1, 3B, 2}	<i>L. ivanovii</i> , <i>B. cereus</i>	water	291
POEGMA-OH poly(2,2'-bithiophene)	lysozyme	stainless steel	0–36 h	10 ⁷ CFU/mL {1, 2, 3B}	<i>E. coli</i> , <i>S. aureus</i>	PBS	311
Ag nanoparticles	Cu	30 days	10 ⁵ –10 ⁸ MPN/mL {1B, 3A}	<i>D. desulfuricans</i>	SSMB	569	
PSPMA	incorporation of Ag ⁺	Si wafer	overnight	OD ≈ 0.5 {4}	<i>P. aeruginosa</i> , <i>S. aureus</i>	water	570
PSPMA	incorporation of Ag ⁺ , AgCl, AgBr, or AgI	Si wafer	20 min to 24 h	10 ⁶ –10 ⁷ CFU/mL {1, 9, 15}	<i>P. aeruginosa</i> , <i>S. aureus</i>	several different solutions	525

^aAbbreviations: PDMA-*co*-PAPMA, poly(*N,N*-dimethylacrylamide-*co*-*N*-(3-aminopropyl)methacrylamide hydrochloride); PC, polycarbonate; AMP, antimicrobial peptide.

^bAssays: 1, plating for CFU; 1B, plating for MPN; 2, live/dead or other staining; 3, microscopy imaging (3A, scanning electron microscopy; 3B, optical or fluorescence microscopy; 3C, atom force microscopy (AFM); 3D, AFM force measurements); 4, CFU counts on the surface of the sample; 5, shear stress or detachment study; 6, OD monitoring (optical density at 600 nm) or luminescence; 7, flow cell setup; 8, motility assay; 9, disk diffusion study; 10, CD spectroscopy studies; 11, in vivo studies; 12, surface plasmon resonance studies; 13, gravimetric studies; 14, biofilm quantification; 15, MIC determination; 16A, static exposure; 16B, dynamic exposure. ^c*P. aeruginosa* = *Pseudomonas aeruginosa*, *S. aureus* = *Staphylococcus aureus*, *E. coli* = *Escherichia coli*, *S. epidermidis* = *Staphylococcus epidermidis*, *B. subtilis* = *Bacillus subtilis*, *Pe. pentosaceus* = *Pediococcus pentosaceus*, *L. ivanovii* = *Listeria ivanovii*, *B. cereus* = *Bacillus cereus*, and *D. desulfuricans* = *Desulfovibrio desulfuricans*.

Gao et al. immobilized seven different antimicrobial peptides on a copolymer brush from poly(*N,N*-dimethylacrylamide-*co*-*N*-(3-aminopropyl)methacrylamide hydrochloride) and thoroughly investigated their biological effect.⁵⁵⁶ They observed that all surfaces reduced bacterial viability but to different extents and that the biofilm formation seemed to be correlated to the hydrophobicity of the functionalized surface. The most hydrophilic surfaces displayed the lowest amount of biofilm from *Pseudomonas aeruginosa*.⁵⁵⁶ Their most efficient antimicrobial peptide (AMP)-conjugated surface (with Tet-20) was also tested *in vivo*, in rats, against *Staphylococcus aureus* infection. It was found that the antimicrobial effect of the surface resulted in more than 85% reduction in CFU in 10 out of 14 animals after 7 days.⁵⁵⁶ No activation of platelets or the

complement system was seen, nor did the surface inhibit cell growth of osteoblast-like cells.⁵⁵⁶ The postulated mechanism of action was that the local density of positive charge disturbed the surface electrostatics and triggered autolytic and/or bacterial cell death mechanisms.⁵⁵⁶ Li et al. also studied AMP-conjugated brush surfaces and showed that although bacterial cells lysed when exposed to the surface, no cytotoxic effects were detected on smooth muscle cells.⁵⁶³ Lysozyme and silk sericin have also been immobilized on brushes, and although it was reported that the immobilization of these two proteins did not reduce adhesion of bacteria to any large extent compared to reference surfaces, it reduced the number of viable bacteria at the surface.^{306,311,561}

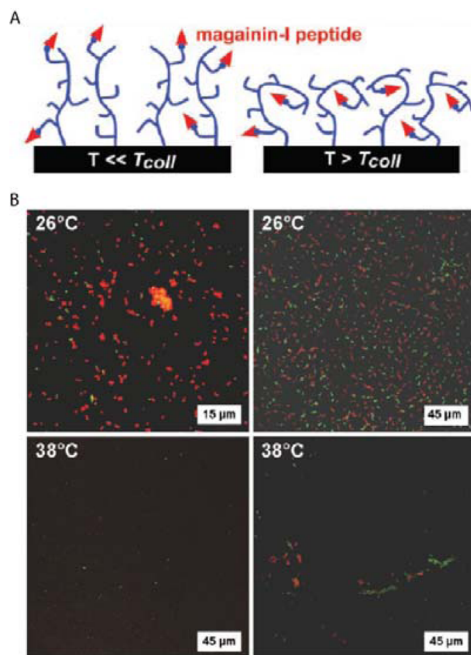


Figure 36. (A) Responsive peptide-based antibacterial brushes. (B) Live/dead staining of temperature-responsive surfaces (exposing an antimicrobial peptide at 26 °C and hiding it at 38 °C) exposed to *Listeria ivanovii* (left images) and *E. coli* (right images). Reprinted with permission from ref 567. Copyright 2010 John Wiley and Sons.

6.4. Antifouling Polymer Brushes with Respect to Bacterial Attachment

The most benign way to create antibacterial surfaces is by producing a surface where bacteria cannot attach and form a biofilm. This is a very attractive option for medical devices since it would most probably not cause any harm to the surrounding mammalian cells. In the literature these films are almost exclusively hydrophilic and, in general, overall neutral (Table 8).

As was seen in section 6.2, the presence of substances immobilized from the solution and/or dead cells can form a conditioning layer that allows bacteria to grow on hostile surfaces. Consequently, a general strategy for bacterium-antifouling surfaces has been to design surfaces that repel protein adsorption, assuming that this will also prevent bacteria from attaching. However, several researchers have reported that this is not always true.^{575–578} Gon et al. suggested that the bacteria can compress large areas of polymer brushes and interact with several attachment sites (Figure 37).⁵⁷⁶ They reported that, for bacteria, the most important factor preventing adsorption on PEG was the mass of polymer, due to brush compression and osmotic pressure.⁵⁷⁶ PEG brushes displaying patches of positive charge were found to retain some protein resistance but did not resist bacterial adhesion.⁵⁷⁶ Kingshott and co-workers found that bacteria adsorbed onto surfaces that resisted protein adsorption and discussed this in terms of medium- and/or bacterium-induced conditioning of PEG films.^{577,578} This kind of bacterium-induced surface conditioning has also recently been reported for *E. coli* and *P. aeruginosa* on other surfaces.^{579,580} Antifouling polymer brushes with respect to bacterial colonization described in the literature are here grouped into four categories: brushes with poly(ethylene glycol) subunits (PEG, POEGMA), zwitterionic brushes, negatively charged brushes, and other neutral brushes. The

two first groups are, so far, the most prevalent in the literature (Table 8).

6.4.1. Brushes with Poly(ethylene glycol) Subunits.

Several researchers have studied the bacterium-antifouling properties of brushes with poly(ethylene glycol) subunits (Table 8). Busscher, van der Mei, and co-workers followed *in situ* biofilm formation by several bacterial strains onto PEG brushes grafted to glass or silicone rubber. For the majority of strains tested they observed a reduction in biofilm formation, and a larger reduction was observed for taller brushes with a larger exclusion volume that prevented proteins and bacteria from approaching the surface.⁵⁸¹ Proteins have been described to adsorb better to poly(ethylene oxide) (PEO) brushes at higher temperatures due to increased interactions with brush segments. In contrast, no difference in biofilm formation was found between experiments at 20 and 37 °C, indicating that the bacteria did not penetrate the brush or interact strongly with it.⁵⁸¹ They observed that the biofilm developed more slowly on the brush surface and attached more weakly.⁵⁸² When an air bubble was passed through the system, bacteria were removed more easily from PEO brushes than from the control glass surface.⁵⁸¹ The same was observed for adhesive bacterial strains,⁵⁸³ which suggests that analyzing biofilms on PEO ex situ could be difficult (or prone to errors) due to detachment of the biofilm.⁵⁸¹ It was also seen that the balance between attachment and detachment at shear forces under flow was different on the brush where pieces of biofilm detached at increased shear stress, while the biofilm on the control surface was much more stable (Figure 38).⁵⁸⁴

The brush surface remained antifouling after detachment of some strains tested (*Staphylococcus epidermidis*) but not for others (*S. aureus*),⁵⁸² and XPS analyses indicated the formation of conditioning films after detachment of the latter strain. The brush coating also induced differences in the biofilm morphology (spherical microcolonies), resulting in bacteria being more viable on the PEO brush than on a control surface of silicone rubber.⁵⁸² After pre-exposure of PEO films to biological fluids, such as saliva, urine, or PBS, the efficacy of the brush films was decreased due to hydrolysis of the PEO chains and the appearance of a conditioning film.⁵⁸⁵ This effect was observed after 4 h, and after 42 h no difference was observed between biofilm formation on the control and that on the preconditioned PEO brush.⁵⁸⁵ This lack of long-term efficiency of brushes with ethylene glycol subunits has also been observed by other groups.²⁰⁵ However, despite this conditioning, *in vivo* experiments in mice showed that PEO-coated silicone rubber disks inserted into an infected site displayed less bacterial colonization compared to control disks. Antibiotic treatment also seemed to be more efficient on the brush-coated disks.⁵⁸⁶ In a similar way, the efficacy of antimicrobial cleaning solutions was also shown to be significantly higher on brush-coated cases for contact lenses than on the control. The reason suggested was that the looser bacterial attachment on brushes does not trigger bacteria into the biofilm phenotype.⁵⁸⁷

Large differences in the interactions with PEO brushes were observed for hydrophilic and hydrophobic strains of *P. aeruginosa*.⁵⁸³ This difference was also seen between different bacterial species^{581,582,595} and was not correlated to the bacterial shape (rods or cocci).⁵⁹⁵ Differences in the initial deposition rate onto PEO between Gram-positive *S. epidermidis*, *Streptococcus salivarius*, and *S. aureus* and Gram-negative strains from *E. coli* and *P. aeruginosa* were observed,⁵⁹⁵ as well as differences in adhesion strength, measured as critical

Table 8. Bacterium-Antifouling Brushes (Homopolymers or Active Block Copolymer) Tested for Antibacterial Effects^a

brush	static contact angle (deg)/functionalization	surface	exposure time	bacterial loadings and assay used ^b	bacterium ^c	solution during exposure ^d	ref
PMETAC- <i>co</i> -PSPMA	27	PP membranes	48 h	10 ⁸ –10 ⁹ CFU/mL {2, 3AB, 13}	<i>E. coli</i>	TSB broth	588
PAAm	28 ± 5	silicon wafer	0–4 h	10 ⁸ CFU/mL {3B, 5, 7}	<i>S. aureus</i> , <i>Str. salivarius</i>	PBS	589
PAAm	28 ± 2	silicone rubber	4 h	10 ⁸ CFU/mL {3B, 7}	<i>S. aureus</i> , <i>Str. salivarius</i>	preconditioning in saliva, then PBS	590
PAAm		silicon wafer	4 h	10 ⁸ CFU/mL {3B, 7}	<i>S. aureus</i> , <i>Str. salivarius</i>	preconditioning in saliva, then PBS	591
PAAm		silicone rubber	4 h	10 ⁸ CFU/mL {3B, 7}	<i>S. aureus</i> , <i>E. coli</i>	PBS	592
PCBAA-1 and PCBAA-2		gold	30 min	OD = 0.5 {12}	<i>P. aeruginosa</i> , two different strains	PBS	593
PCBMA, PMEDSAH		glass	0–10 days	10 ⁶ or 10 ⁸ CFU/mL {3B, 7}	<i>P. aeruginosa</i> , <i>P. putida</i>	PBS followed by TSB or FAB broth	594
PCBMA-1, PC8NMA, PCBMA-2	59 (PEO 526), 45 (PEO 2000), 48 (PEO 9800)	gold	1 h	10 ⁷ –10 ¹⁰ CFU/mL {3B, 4}	<i>E. coli</i>	N/S	545
PEG	41 ± 5	glass or Si	0–4 h	10 ⁸ CFU/mL {3B, 5, 7}	<i>S. epidermidis</i> , <i>P. aeruginosa</i>	PBS	581
PEG (9.8 kDa)		glass	0–4 h	10 ⁸ CFU/mL {3B, 5, 7, 8}	<i>S. epidermidis</i> , <i>S. aureus</i> , <i>Str. salivarius</i> , <i>P. aeruginosa</i> , <i>E. coli</i>	PBS	595
PEG (9.8 kDa)		glass	30 min	10 ⁸ CFU/mL {3B, 7}	six <i>P. aeruginosa</i> strains	PBS	583
PEG (9.8 kDa)					<i>S. epidermidis</i> (total of nine strains)	preconditioning in urine/saliva, then PBS	585
PEG		silicone rubber	30 min to 20 h	10 ⁸ CFU/mL {2, 3B, 5, 7}	<i>S. epidermidis</i> , <i>S. aureus</i> , <i>P. aeruginosa</i>	PBS, then 10% TSB	582
PEG		silicone rubber	0–120 min	10 ⁸ CFU/mL {3B, 5, 7}	<i>S. epidermidis</i> , <i>S. aureus</i> , <i>P. aeruginosa</i>	PBS	584
PEG		silicone rubber	5 days	{1, 11}	<i>S. aureus</i>	in vivo	586
PEG	25–40	Si nanoparticles	4 h	10 ⁸ CFU/mL {3B, 4, 5, 7}	<i>S. epidermidis</i> , <i>P. aeruginosa</i>	PBS	596
PEG	24	Si nanoparticle coating on PP	20 h	10 ⁴ CFU/mL {2, 3BD, 5}	<i>P. aeruginosa</i> , <i>S. aureus</i> , <i>Se. marcescens</i> , <i>Se. liquefaciens</i> (total of nine strains)	TSB or BHI	587
PEG (2–5 kDa)		glass	initial adhesion	10 ⁵ CFU/mL {3B, 7}	<i>S. aureus</i>	PBS	576
PEG	41	PVDF membranes	3 or 24 h	10 ⁹ CFU/mL { <i>S. epidermidis</i> }, 10 ⁶ CFU/mL (<i>E. coli</i>) {2, 3B}	<i>S. epidermidis</i> , <i>E. coli</i>	broth	597
POEGMA PHEAA	51, 52	stainless steel	4 h	10 ⁷ CFU/mL {1, 3A}	<i>E. coli</i> , <i>S. epidermidis</i>	PBS	553
PHEMA- <i>co</i> -POEGMA	~50	Au	1 h, 1–8 weeks	10 ⁷ CFU/mL {2, 3B}	<i>C. marina</i> and field experiment	artificial seawater, seawater	227
PGMA		PE membranes	0–70 h	10 ⁸ CFU/mL {2, 3B, 5, 7, 14}	<i>E. coli</i>	PBS followed by LB	538
PHEMA, PHPMA, PHEAA	31, 33, 15	Au	0–3 days	10 ⁸ CFU/mL {2, 3B}	<i>S. epidermidis</i> , <i>E. coli</i>	broth	598
PHEMA, PHPMA		Au	2 h	10 ⁸ CFU/mL {2, 3B}	<i>Cy. lytica</i>	seawater	226
PHEMA, PSS, PMEDSAH	41	glass	24 h	10 ⁷ CFU/mL {1, 3A}	<i>Pseudomonas</i> sp., <i>S. aureus</i>	simulated seawater, TSB	517
PMEDSAH		glass	1–3 days	10 ⁶ CFU/mL {3B, 7}	<i>P. aeruginosa</i>	PBS followed by TSB	599
PMEDSAH	<10	gold and glass TiO_2 , SiO_2 , Au, PC, PE, PTFE, PU	24 h	10 ⁸ CFU/mL {2, 3B, 16A}	<i>P. aeruginosa</i>	buffer, then TSB broth	600
PMEDSAH	<20	PP membranes	3 h	10 ⁸ CFU/mL {3A}	<i>E. coli</i> , <i>P. fluorescens</i> , <i>S. aureus</i>	PBS	34
POEGMA and PMEDSAH		gold	3–48 h	10 ⁸ CFU/mL {2, 3B, 7}	<i>S. epidermidis</i> , <i>P. aeruginosa</i>	PBS followed by broth	602
PPSMA, POEGMA, PMEDSAH, PMMA	<10, 49, 39, 76	glass	0–72 h	10 ⁹ CFU/mL {2, 3B, 7, 8, 14}	<i>P. aeruginosa</i> , four different strains	saline followed by broth	205

brush	static contact angle (deg)/functionalization	surface	exposure time	bacterial loadings and assay used ^b	bacterium ^c	solution during exposure ^d	ref
PAETAC- <i>co</i> -PCAA	30–40	gold	3 h and 30 min	10^8 CFU/mL {2, 3B, 5, 7} {6}	S. epidermidis	buffer	163
PMPC	~20 (adv)	PMMA	overnight	10^7 – 10^8 CFU/mL {2, 3B, 16AB}	S. epidermidis, P. aeruginosa, E. coli	Todd Hewitt broth saline	603
PNMG	14–26	TiO ₂	24 h	10^9 CFU/mL {3B}	E. coli, two different strains	HEPES buffer	604
PLL-Pox	31–50 (adv)	Nb ₂ O ₅	1 h	{2, 3B, 7}	S. epidermidis, E. coli	TSB or LB broth	605
Polypeptoids	27	TiO ₂	1 or 4 days	10^6 CFU/mL {~1}	E. coli	N/S	606
PSBVI	57, 82, 28	Si wafer	24 h	10^7 CFU/mL {1}	S. aureus	N/S	607
PTMAEMA- <i>co</i> -POEGMA, PTMAEMA- <i>co</i> -PS, PTMAEMA- <i>co</i> -PAA		stainless steel	1 h				608

^a Abbreviations: PC, polycarbonate; PE, polyethylene; PU, polyurethane; PTFE, poly(tetrafluoroethylene); PLL-Pox, copolymer poly(L-lysine)-g-poly(2-methyl-2-oxazoline); PNMG, poly(N-methylglycine) (polysarcosine); PSBVJ, poly(sulfobetaine vinylimidazole); adv, advancing contact angle. ^b Assays: 1, plating for CFU; 1B, plating for MPN; 2, live/dead or other staining; 3, microscopy imaging (3A, scanning electron microscopy; 3B, optical or fluorescence microscopy; 3C, atom force microscopy); 4, CFU counts on the surface of the sample; 5, shear stress or detachment study; 6, OD monitoring (optical density at 600 nm) or luminescence; 7, flow cell setup; 8, motility assay; 9, disk diffusion study; 10, CD spectroscopy studies; 11, in vivo studies; 12, surface plasmon resonance studies; 13, gravimetric studies; 14, biofilm quantification; 15, MIC determination; 16A, static exposure; 16B, dynamic exposure. ^c E. coli = *Escherichia coli*, S. aureus = *Staphylococcus aureus*, S. marcescens = *Staphylococcus marcescens*, S. epidermidis = *Pseudomonas putida*, P. putida = *Pseudomonas aeruginosa*, P. aeruginosa = *Cytophaga lytica*, C. lytica = *Corbetia marina*, C. marina = *Serratia liquefaciens*, S. liquefaciens = *Serratia marcescens*, and S. mutans = *Streptococcus mutans*. ^d Abbreviations: N/S, not specified; BHI, brain-heart infusion broth.

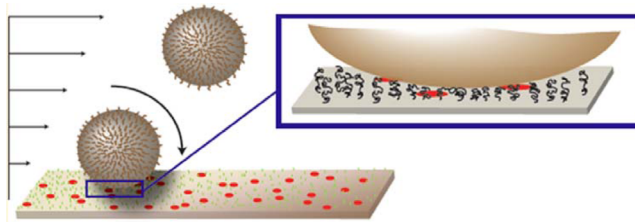


Figure 37. Initial stages of adhesion from *S. aureus* in a gentle flow, showing compression of a PEG brush coating to allow interaction with several adhesive sites (cationic patches) at the surface. Reprinted from ref 576. Copyright 2012 American Chemical Society.

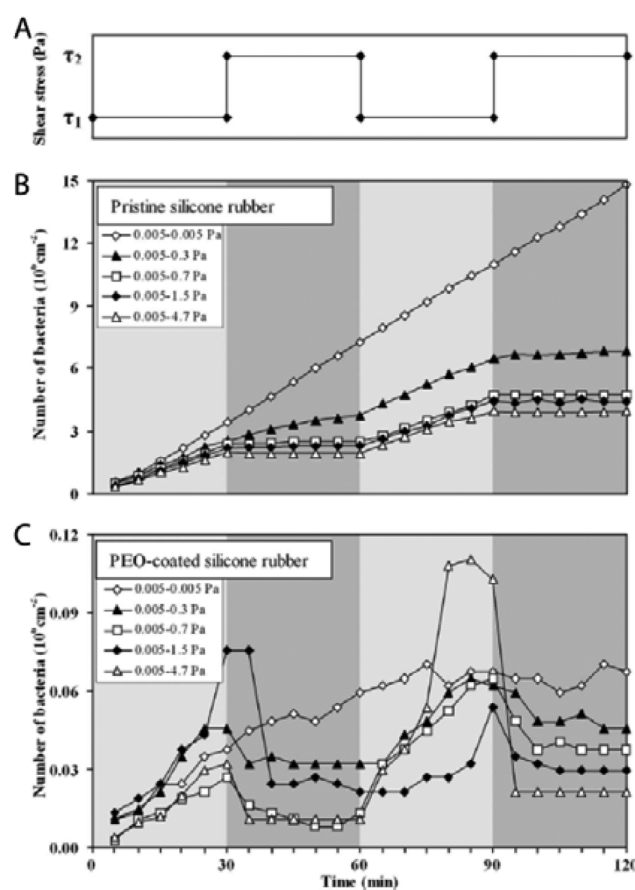


Figure 38. *S. epidermidis* attachment and detachment (shown as the number of adhering bacteria; note the difference in y-scales) during shear stress fluctuations (A), where τ_1 was 0.005 Pa and τ_2 varied according to the symbols in the legend, on pristine silicone rubber (B), and on PEO-coated silicone rubber (C). Reprinted with permission from ref 584. Copyright 2008 The American Society for Microbiology.

shear stress, among *S. epidermidis*, *S. aureus*, and *P. aeruginosa*. The critical shear stress per bacterium for staphylococci was 0.8–2.1 pN on glass and 0.1 pN on a PEO brush, and that for *P. aeruginosa* was 1.3 pN for silicone rubber and 1.6 pN for a PEO brush.⁵⁸⁴ The *P. aeruginosa* strains used were in several comparative studies the most adhesive and the most hydrophobic species of the ones tested, and the adhesion of these strains was discussed in terms of hydrophobic interactions between the bacterium and the PEO brush.^{581,583,584,595} When six *P. aeruginosa* strains of different hydrophobicities (but similar ζ potentials and motilities) were used, it was found that the adhesive strains were more hydrophobic and released more extracellular substances, some with the ability to change the

surface tension.⁵⁸³ This correlated to the free energy of adhesion to PEO coatings, calculated from contact angle measurements. The free energy was found to be attractive for the adhesive strains and repulsive for those that were nonadhesive.⁵⁸³ For glass it was attractive for all strains, although the energy gain was found to be lower for the nonadhesive strains.⁵⁸³ However, overall and even for the more adhesive strains, a reduction of adsorption was observed onto PEO brushes (33–63% of that of the control for adhesive strains).

6.4.2. Zwitterionic Brushes. Zwitterionic brushes have been described to repel proteins due to their high degree of hydration.⁶⁰⁹ Jiang and co-workers have studied bacterial adhesion onto a variety of zwitterionic brushes such as homopolymers from PSBMA (or PMEDSAH) and PCBMA or random copolymers of poly((2-(acryloyloxy)ethyl)-trimethylammonium chloride) (PAETAC) and poly(2-carboxyethyl acrylate) (PCEA) either grafted from surfaces using surface-initiated ATRP^{163,594,599,602} or grafted to a surface⁶⁰⁰ (Table 8). They found that *P. aeruginosa* and *S. epidermidis* adsorbed less to POEGMA or PMEDSAH brushes than to self-assembled monolayers (SAMs) with similar functionality and suggested this could be a result of degradation of the SAMs with time and/or the thickness of the coating produced using brushes.⁶⁰² On PMEDSAH and PCBMA brushes very small amounts of a patchy biofilm were observed, and it was suggested that the adhesion was enabled by extracellular substances secreted by the bacteria.^{594,602} Confocal microscopy enabled other researchers to establish that this type of biofilm had a mushroom-shaped morphology with a different phenotype, characterized by higher levels of the signaling molecule cyclic diguanosine monophosphate (c-di-GMP), which is known to upregulate production of exopolymers.²⁰⁵ The PMEDSAH brush reduced the bacterial adhesion of *P. aeruginosa* by 2–3 logarithmic units,^{205,599} and immersion of the brush into PBS for 42 days did not remove the antifouling effect on serum and plasma.⁵⁹⁹ Similar antifouling effects were also observed for zwitterionic surfaces made using a grafting-to approach.⁶⁰⁰ On polypropylene (PP) membranes, it was reported that brush coatings of 560 µg/cm² PMEDSAH were able to completely suppress bacterial adhesion of *E. coli* and *S. aureus* but not *Pseudomonas fluorescens* (in this study *E. coli* was the most hydrophilic followed by *P. fluorescens* and then *S. aureus*). At a coating coverage of 265 µg/cm², there was also a reduction compared to the control, and lower densities of *S. aureus* and *E. coli* than *P. fluorescens* were found (similar to the adhesive trend on the control surface; see Figure 39).³⁴

Long-term experiments of bacterial adhesion from *P. aeruginosa* and *Pseudomonas putida* onto zwitterionic surfaces at three different temperatures showed that the antifouling effect was decreased with temperature. At 25 °C the surfaces resisted biofilm formation from *P. aeruginosa* for 10 days (the control ~2 days), at 30 °C the surfaces resisted biofilm formation from *P. putida* for 8 days, and at 37 °C no biofilm from *P. aeruginosa* was observed for 2.5 days (the control ~15 h).⁵⁹⁴ When bacteria were continuously fed to the surface, biofilms formed more rapidly.⁵⁹⁴ The same was observed when the surfaces were preconditioned using 100% human plasma despite the fact that SPR measurements showed lower than 0.3 ng/cm² adsorbed substances on the surface after preconditioning.⁵⁹⁴

Preconditioning can also occur from substances other than serum proteins. Mi et al. observed that binding of alginate to

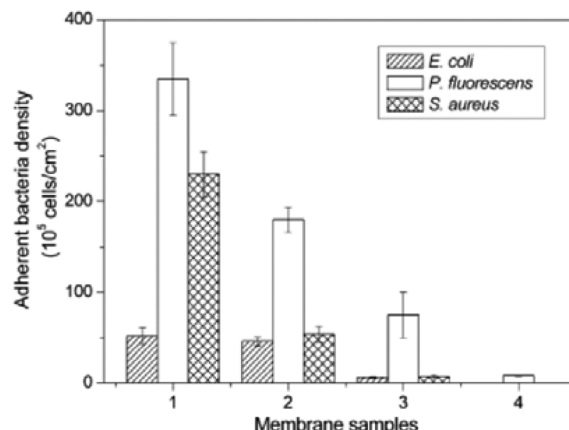


Figure 39. Density of adherent bacteria onto membranes covered with different grafting densities of PMEDSAH: 1, 0 µg/cm²; 2, 124 µg/cm²; 3, 265 µg/cm²; 4, 560 µg/cm². Reprinted with permission from ref 34. Copyright 2010 Elsevier.

some zwitterionic brushes containing carboxylic groups could be promoted by divalent cations that bridged the brush and the polysaccharide.⁵⁷⁵ They observed that 20 mM Mg²⁺ promoted alginate absorption onto PCBMA but not onto PCBA-1 and PMEDSAH, while all three brushes were equally protein resistant.⁵⁷⁵ The differences between the bridging abilities were explained as following surface charge and hydration of the anionic part of the zwitterionic moiety and correlated to the pK_a value of the anionic group.⁵⁷⁵ However, no large differences in bacterial adhesion with respect to Mg²⁺ concentrations were observed between alginate- and non-alginate-producing *P. aeruginosa* strains onto PCBA-1 and PCBA-2.⁵⁹³ Without Mg²⁺, the alginate-producing bacteria adsorbed more onto PCBA-2 surfaces than the non-alginate strain. If the concentration of Mg²⁺ was increased, the alginate-producing strain adsorbed less. The authors suggest this is due to an increased aggregation in solution and that the higher ionic strength reduced deposition of extracellular substances onto the surface.

6.4.3. Negatively Charged Brush Surfaces. Brushes that display a negative charge (for example, PSPMA and PGMA functionalized with sulfonate groups) have been shown to dramatically reduce both initial adhesion of bacteria and the mass of biofilm formed during longer time periods. They were also found to promote a biofilm architecture and physiology distinctly different from that of control surfaces for both *P. aeruginosa* and *E. coli*.^{205,538,588} It was observed that the biofilm structures formed on negatively charged surfaces were more easily removed at higher shear stress compared to a more homogeneous flat biofilm formed on a polycationic surface (Figure 40).⁵³⁸

Bacterial motility was reduced on negatively charged surfaces, and optical microscopy of bacterial cells showed that *P. aeruginosa* cells seemed to preferentially orient vertically on the surface, thereby minimizing the repulsive forces, but that mutants lacking pili and flagella did not orient and appeared further from the surface.²⁰⁵ One mechanism suggested for overcoming the electrostatic repulsion between the bacterial cell and the polyanionic surface is through the production of exopolymers that can alter the overall charge of the bacterial cell and thereby reduce repulsion with the substrate. This hypothesis was to some extent supported by the observation that the mushroom-shaped biofilm expressed high levels of the

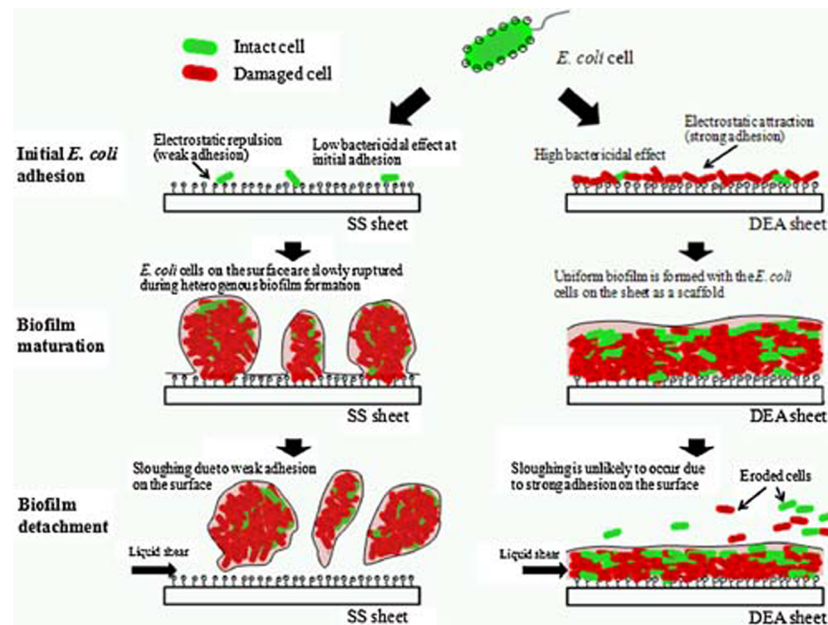


Figure 40. Suggested mechanisms for detachment of an *E. coli* biofilm from negatively charged (SS, sulfonate functionalized sheet) or positively charged (DEA, diethylamine functionalized sheet) surfaces. Reprinted with permission from ref 538. Copyright 2012 John Wiley and Sons.

signaling molecule c-di-GMP, known to promote production of exopolymers (Figure 41).²⁰⁵ However, on negatively charged

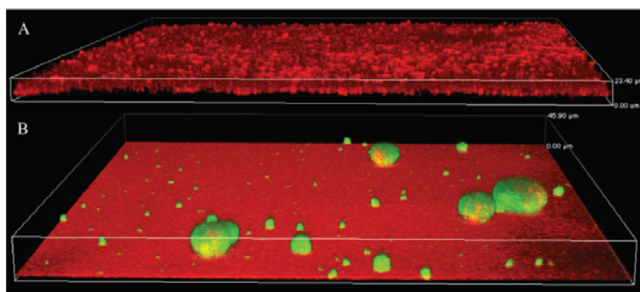


Figure 41. Biofilms with different physiologies formed by *P. aeruginosa* carrying a reporter gene expressing green fluorescent protein when c-di-GMP is expressed: (A) glass—carpet-like bacterial biofilm, (B) SPMA polymer—mushroom-shaped biofilm expressing c-di-GMP. The biofilm was counterstained with propidium iodide, which also stained the SPMA brush (thus the red background color in (B)). Reprinted with permission from ref 205. Copyright 2013 The Royal Society of Chemistry.

brush surfaces, positively charged proteins such as lysozyme can adsorb and alter the surface properties,⁵⁸⁸ which could lead to subsequent bacterial attachment and biofilm formation. This type of conditioning film could explain the bacterial attachment reported on negatively charged PSS brushes.⁵¹⁷

6.4.4. Other Neutral Antifouling Brushes. Hydroxy-terminated methacrylate brushes have been investigated as bacterium-repellent surfaces, and among PHEAA, PHEMA, and PHPMA, the best antifouling properties against both bacteria and proteins were found for PHEAA. In static bacterial adhesion studies, colonization of *E. coli* and *S. epidermidis* was reduced compared to that of a SAM control.⁵⁹⁸ Bacterial reduction of a factor of 10 was also reported for *Pseudomonas* sp. and *S. aureus* on PHEMA brushes in comparison to untreated glass.⁵¹⁷

Brushes from polyacrylamide grafted onto silicone rubber have been investigated as antifouling surfaces with respect to bacteria.^{589–592} On the brush coating, as for poly(ethylene glycol) coatings, the initial deposition rate of *S. aureus* and *Str. salivarius* was lower and bacteria detached more easily than on the control surfaces (65–87% vs 11–17% detachment).⁵⁸⁹ No preconditioning was observed with FTIR after 1 month in saliva or PBS, and bacterial adhesion did not change significantly when samples were preconditioned for 48 h or 1 month.⁵⁹¹

Dense short (2 nm) brushes from polyoxazoline were reported to repel *E. coli* strains both with and without fimbriae (long hairlike structures on the bacterial surface with adhesins at the tip) at high and low ionic strength,⁶⁰⁵ whereas less dense brushes did not repel bacteria to the same extent.⁶⁰⁵ The stabilities of these films were reported to be higher than those of the corresponding PEG graft polymer films due to a higher resistance to oxidation.⁶¹⁰

Poly-N-substituted glycine oligomers have been investigated as antifouling surfaces grafted to a surface. They differ from peptides in side chain position, which has been described to make them more stable against proteases.⁶⁰⁴ Three different polypeptoids resisted proteases to a high degree when anchored to a surface and were reported to exhibit some resistance to bacterial adhesion from *S. epidermidis* and *E. coli* as well as against *P. aeruginosa*.^{604,606}

From Table 8 it can be concluded that most of the antifouling brush surfaces presented in the literature are hydrophilic and have contact angles below the so-called Berg limit at 65°.⁶¹¹ Hydrophilicity below 65° has been described to enable water to arrange more densely at the surface of a material and repel hydrophobic interactions from, for example, proteins;⁶¹¹ however, electrostatic attractions can still occur between charged moieties and promote adhesion. Highly hydrophilic neutral surfaces seem to perform very well in long-term experiments and repel both positively and negatively charged substances, forming conditioning films. Consequently, these types of surfaces are promising candidates for bacterium-

repellent surfaces. Despite their reduced bacterial attachment, bacteria have been shown to form patches of biofilm also on these surfaces, probably with the aid of extracellular substances, but with much lower attachment strength.

From reviewing the literature, it becomes clear that, to compare the efficiency of different types of antifouling surfaces with respect to bacterial adhesion and biofilm formation, it is necessary to perform carefully designed experiments where the different surfaces are tested using the same bacterial strain and the same experimental conditions on well-characterized surfaces. It is also clear that the same species of bacterium can have strains that have very different adhesion and biofilm formation characteristics, as was shown for different *P. aeruginosa* strains on PEO brushes. Sometimes the differences between strains within a bacterial species were found to be larger than between bacterial species. The physicochemical parameters, such as hydrophobicity, of the bacterial cell wall of these strains have been given as one reason for the large differences observed, but it is possible that there are also other factors that play a role. It is clear that the time frame for the experiments very much influence the obtained result. This illustrates some of the complexity that should be taken into account in future investigations of antibacterial and antifouling brush surfaces. Ideally, the surface characteristics, in particular physicochemical properties, of both materials and bacterial strains should be carefully characterized to enable better comparisons between different studies. Several hydrophilic brush surfaces have been identified as promising candidates for antifouling surfaces (Table 8) with different advantages and disadvantages, suggesting that the type of coating could be tailored depending on the application and anticipated bacterial exposure.

7. CONCLUSIONS AND OUTLOOK

The field of polymer brush chemistry and physics is now relatively mature, and we have a good understanding of the general physicochemical properties of these coatings. As more examples of brush architectures with improved or better controlled properties are developed, these coatings enable an exquisite control of interfacial properties, in particular in the field of biosciences. These interfaces now allow the study of complex behaviors where several parameters are required to be controlled simultaneously, such as protein resistance and biorecognition and cell adhesion and detachment upon thermal stimulation. Not surprisingly, the application of these coatings to the biomedical field is progressing fast, and brush-based biomaterials are now utilized more routinely for the study of biological systems and even making their way to the market, for example, for cell and cell-sheet culture and harvesting. A number of remaining challenges should still be addressed for their use to become more widespread and to enable important biological questions to be tackled: (1) A full understanding of the protein resistance of polymer brushes and how it correlates to cell (mammalian or bacterial) adhesion is still required. This includes the study of how multiple parameters, such as the physicochemical properties of the brush and the nano-microtopography and geometry of the surface, cross-talk to govern cellular behavior for both mammalian cells and bacteria. (2) A wider range of selective and reversible biocapture platforms for protein purification and biosensing need to be designed, in particular with fully protein resistant coatings and at high loading levels. (3) An improved understanding of protein–brush interactions and how they affect enzymatic

activity is essential for the development of brush coatings for biocatalysis or biosensing. (4) Controlling the aging of polymer brushes in complex media will improve long-term applications (e.g., for coating of implants and medical devices and longer term cell culture). (5) Considering recent developments in the field of tissue engineering and regenerative medicine, polymer brushes offer interesting features for the design of dynamically responsive biointerfaces able to guide cellular and bacterial response in space and time. (6) The potential of polymer brushes for controlling drug delivery systems (e.g., improving circulation time and targeting) should be exploited.

AUTHOR INFORMATION

Corresponding Authors

*E-mail: madeleine.ramstedt@chem.umu.se.

*E-mail: j.gautrot@qmul.ac.uk.

Notes

The authors declare no competing financial interest.

Biographies



Mahentha Krishnamoorthy was born in Tamil Eelam, North East Sri Lanka. She completed her secondary education at The Ellen Wilkinson School for Girls, London, and received her M.Eng. in medical engineering from Queen Mary University of London in 2010. She is currently a Ph.D. student in the School of Engineering & Materials Science at Queen Mary University of London under the supervision of Dr. Julien Gautrot.



Shoghik Hakobyan was born in Georgia in 1981. She graduated from the Armenian State Pedagogical University after Khachatur Abovyan, Faculty of Biology and Chemistry. In 2010 she received a Ph.D. in organic and bioorganic chemistry from the Institute of Fine Organic Chemistry, National Academy of Sciences of the Republic of Armenia (NAS RA), working with Prof. Noravyan. She worked as a researcher

at the Scientific Technological Centre of Organic and Pharmaceutical Chemistry, NAS RA. In 2011 she started a second Ph.D. study at Umeå University, Department of Chemistry, under the supervision of Prof. Ramstedt.



Madeleine Ramstedt was born in Sweden in 1975. She performed her undergraduate and graduate studies at Umeå University, Sweden. She received her Ph.D. in 2004 in inorganic chemistry from the Department of Chemistry, working with Prof. S. Sjöberg. She worked as a postdoctoral researcher in Materials Science, Ecole Polytechnique Fédérale de Lausanne (EPFL), in Switzerland with Prof. H. J. Mathieu and at the Melville Laboratory for Polymer Synthesis, University of Cambridge, United Kingdom, with Prof. W. T. S. Huck. In 2008 she was appointed Assistant Professor in the Department of Chemistry, Umeå University, and became Associate Professor in the same department in 2012.



Julien E. Gautrot was born in France in 1978. He studied at Lycée Saint-Louis in Paris and the Ecole Nationale Supérieure de Chimie de Montpellier. He received his Ph.D. from the University of Manchester, Department of Chemistry, in 2004, working with Prof. P. Hodge. He worked as a postdoctoral researcher with Prof. X. X. Zhu at the Université de Montréal and with Profs. W. Huck and F. Watt at the University of Cambridge, United Kingdom. In 2011, he was appointed Lecturer in Biomaterials at Queen Mary University of London, United Kingdom.

ACKNOWLEDGMENTS

Funding from the Royal Society and the Engineering and Physical Sciences Research Council (Grant EP/J501360/1) and the Swedish Research Council (Grant 621-2011-3504) is acknowledged.

REFERENCES

- (1) Ishii, H.; Sugiyama, K.; Ito, E.; Seki, K. *Adv. Mater.* **1999**, *11*, 605.
- (2) Braun, S.; Salaneck, W. R.; Fahlman, M. *Adv. Mater.* **2009**, *21*, 1450.
- (3) Bredas, J.-L.; Norton, J. E.; Cornil, J.; Coropceanu, V. *Acc. Chem. Res.* **2009**, *42*, 1691.
- (4) Gratzel, M. *Acc. Chem. Res.* **2009**, *42*, 1788.
- (5) Rolison, D. R.; Long, J. W.; Lytle, J. C.; Fischer, A.; Rhodes, C. P.; McEvoy, T. M.; Bourg, M. E.; Lubers, A. M. *Chem. Soc. Rev.* **2009**, *38*, 226.
- (6) Marx, K. A. *Biomacromolecules* **2003**, *4*, 1099.
- (7) Wink, T.; van Zuilen, S. J.; Bult, A.; van Bennekom, W. P. *Analyst* **1997**, *122*, 43R.
- (8) Homola, J.; Yee, S. S.; Gauglitz, G. *Sens. Actuators, B* **1999**, *54*, 3.
- (9) Anker, J. N.; Hall, W. P.; Lyandres, O.; Shah, N. C.; Zhao, J.; van Duyne, R. P. *Nat. Mater.* **2008**, *7*, 442.
- (10) Svec, F.; Frechet, J. M. J. *Science* **1996**, *273*, 205.
- (11) Blakley, C. R.; Vestal, M. L. *Anal. Chem.* **1983**, *55*, 750.
- (12) Guiochon, G. *J. Chromatogr., A* **2007**, *1168*, 101.
- (13) Hennion, M.-C. *J. Chromatogr., A* **1999**, *856*, 3.
- (14) Stevens, M. M.; George, J. H. *Science* **2005**, *310*, 1135.
- (15) Lutolf, M. P.; Hubbell, J. A. *Nat. Biotechnol.* **2005**, *23*, 47.
- (16) Wilson, C. J.; Clegg, R. E.; Leavesley, D. I.; Pearcey, M. J. *Tissue Eng.* **2005**, *11*, 1.
- (17) Cole, M. A.; Voelcker, N. H.; Thissen, H.; Griesser, H. J. *Biomaterials* **2009**, *30*, 1827.
- (18) van Loosdrecht, M. C. M.; Lyklema, J.; Norde, W.; Zehnder, A. J. B. *Microbiol. Rev.* **1990**, *54*, 75.
- (19) Lichten, J. A.; Van Vliet, K. J.; Rubner, M. F. *Macromolecules* **2009**, *42*, 8573.
- (20) Schierholz, J. M.; Beuth, J. *J. Hosp. Infect.* **2001**, *49*, 87.
- (21) Judeinstein, P.; Sanchez, C. *J. Mater. Chem.* **1996**, *6*, 511.
- (22) Fu, S.-Y.; Feng, X.-Q.; Lauke, B.; Mai, Y.-W. *Composites, Part B* **2008**, *39*, 933.
- (23) George, J.; Sreekala, M. S.; Thomas, S. *Polym. Eng. Sci.* **2001**, *41*, 1471.
- (24) Somorjai, G. A.; Contreras, A. M.; Montano, M.; Rioux, R. M. *Proc. Natl. Acad. Sci. U.S.A.* **2006**, *103*, 10577.
- (25) Woll, C. *Prog. Surf. Sci.* **2007**, *82*, 55.
- (26) Guzey, D.; McClements, D. J. *Adv. Colloid Interface Sci.* **2006**, *128–130*, 227.
- (27) Hickner, M. A. *Mater. Today* **2010**, *13*, 34.
- (28) Kasprzyk-Hordern, B. *Adv. Colloid Interface Sci.* **2004**, *110*, 19.
- (29) Zhou, F.; Huck, W. T. S. *Phys. Chem. Chem. Phys.* **2006**, *8*, 3815.
- (30) Tsujii, Y.; Ohno, K.; Yamamoto, S.; Goto, A.; Fukuda, T. *Adv. Polym. Sci.* **2006**, *197*, 1.
- (31) Edmondson, S.; Osborne, V. L.; Huck, W. T. S. *Chem. Soc. Rev.* **2004**, *33*, 14.
- (32) Advincula, R. C.; Brittain, W. J.; Caster, K. C.; Ruhe, J. *Polymer Brushes*; Wiley-VCH Verlag GmbH & Co. KGaA: Weinheim, Germany, 2004.
- (33) Liu, F.; Du, C.-H.; Zhu, B.-K.; Xu, Y.-Y. *Polymer* **2007**, *48*, 2910.
- (34) Yang, Y.-F.; Li, Y.; Li, Q.-L.; Wan, L.-S.; Xu, Z.-K. *J. Membr. Sci.* **2010**, *362*, 255.
- (35) Tan, K. Y.; Gautrot, J. E.; Huck, W. T. S. *Soft Matter* **2011**, *7*, 7013.
- (36) Azzaroni, O.; Moya, S.; Farhan, T.; Brown, A. A.; Huck, W. T. S. *Macromolecules* **2005**, *38*, 10192.
- (37) Lego, B.; Skene, W. G.; Giasson, S. *Macromolecules* **2010**, *43*, 4384.
- (38) Jung, D.-H.; Park, I. J.; Choi, Y. K.; Lee, S.-B.; Park, H. S.; Ruhe, J. *Langmuir* **2002**, *18*, 6133.
- (39) Goicochea, A. G.; Mayoral, E.; Klapp, J.; Pastorino, C. *Soft Matter* **2014**, *10*, 166.
- (40) Zhang, Z.; Morse, A. J.; Armes, S. P.; Lewis, A. L.; Geoghegan, M.; Leggett, G. J. *Langmuir* **2011**, *27*, 2514.
- (41) Rodrigues, D. C.; Gilbert, J. L.; Bader, R. A.; Hasenwinkel, J. M. *J. Mater. Sci.: Mater. Med.* **2014**, *25*, 79.
- (42) Xiong, D.; Deng, Y.; Wang, N.; Yang, Y. *Appl. Surf. Sci.* **2014**, *298*, 54.

- (43) Malmstrom, J.; Nieuwoudt, M. K.; Strover, L. T.; Hackett, A.; Laita, O.; Brimble, M. A.; Williams, D. E.; Travas-Sejdic, J. *Macromolecules* **2013**, *46*, 4955.
- (44) Choi, E.-Y.; Azzaroni, O.; Cheng, N.; Zhou, F.; Kelby, T. S.; Huck, W. T. S. *Langmuir* **2007**, *23*, 10389.
- (45) Whiting, G. L.; Snaith, H. J.; Khodabakhsh, S.; Andreasen, J. W.; Breiby, D. W.; Nielsen, M. M.; Greenham, N. C.; Friend, R. H.; Huck, W. T. S. *Nano Lett.* **2006**, *6*, 573.
- (46) Snaith, H. J.; Whiting, G. L.; Sun, B.; Greenham, N. C.; Huck, W. T. S.; Friend, R. H. *Nano Lett.* **2005**, *5*, 1653.
- (47) Murata, H.; Prucker, O.; Ruhe, J. *Macromolecules* **2007**, *40*, 5497.
- (48) Kitano, H.; Takahashi, Y.; Mizukami, K.; Matsuura, K. *Colloids Surf., B* **2009**, *70*, 91.
- (49) Anraku, Y.; Takahashi, Y.; Kitano, H.; Hakari, M. *Colloids Surf., B* **2007**, *57*, 61.
- (50) Lee, B. S.; Chi, Y. S.; Lee, K.-B.; Kim, Y.-G.; Choi, I. S. *Biomacromolecules* **2008**, *8*, 3922.
- (51) Gautrot, J. E.; Huck, W. T. S.; Welch, M.; Ramstedt, M. *ACS Appl. Mater. Interfaces* **2010**, *51*, 193.
- (52) Kawai, T.; Saito, K.; Lee, W. *J. Chromatogr., B* **2003**, *790*, 131.
- (53) Fernandes, A. E.; Dirani, A.; d'Haese, C.; Deumer, G.; Guo, W.; Hensenne, P.; Nahra, F.; Laloyaux, X.; Haufroid, V.; Nysten, B.; Riant, O.; Jonas, A. M. *Chem.—Eur. J.* **2012**, *18*, 16223.
- (54) Basavaraju, K. C.; Sharma, S.; Maurya, R. A.; Kim, D.-P. *Angew. Chem., Int. Ed.* **2013**, *52*, 6735.
- (55) Liu, J.; Ma, S.; Wei, Q.; Jia, L.; Yu, B.; Wang, D.; Zhou, F. *Nanoscale* **2013**, *5*, 11894.
- (56) Oren, R.; Liang, Z.; Barnard, J. S.; Warren, S. C.; Wiesner, U.; Huck, W. T. S. *J. Am. Chem. Soc.* **2009**, *131*, 1670.
- (57) Presa, M. J. R.; Gassa, L. M.; Azzaroni, O.; Gervasi, C. A. *Anal. Chem.* **2009**, *81*, 7936.
- (58) Lee, H.-S.; Penn, L. S. *Langmuir* **2009**, *25*, 7983.
- (59) Gupta, S.; Uhlmann, P.; Agrawal, M.; Chapuis, S.; Oertel, U.; Stamm, M. *Macromolecules* **2008**, *41*, 2874.
- (60) Raynor, J. E.; Capadona, J. R.; Collard, D. M.; Petrie, T. A.; Garcia, A. *Biointerphases* **2009**, *4*, 3.
- (61) Tugulu, S.; Silacci, P.; Stergiopoulos, N.; Klok, H.-A. *Biomaterials* **2007**, *28*, 2536.
- (62) de las Heras Alarcon, C.; Farhan, T.; Osborne, V. L.; Huck, W. T. S.; Alexander, C. *J. Mater. Chem.* **2005**, *15*, 2089.
- (63) Barbey, R.; Lavanant, L.; Paripovic, D.; Schuwer, N.; Sugnaux, C.; Tugulu, S.; Klok, H.-A. *Chem. Rev.* **2009**, *109*, 5437.
- (64) Matyjaszewski, K.; Xia, J. *Chem. Rev.* **2001**, *101*, 2921.
- (65) Matyjaszewski, K. *Macromolecules* **2012**, *45*, 4015.
- (66) Siegwart, D. J.; Oh, J. K.; Matyjaszewski, K. *Prog. Polym. Sci.* **2012**, *37*, 18.
- (67) Moad, G.; Rizzardo, E.; Thang, S. H. *Polymer* **2008**, *49*, 1079.
- (68) Lowe, A. B.; McCormick, C. L. *Prog. Polym. Sci.* **2007**, *32*, 283.
- (69) Perrier, S.; Takolpuckdee, P. *J. Polym. Sci., A: Polym. Chem.* **2005**, *43*, 5347.
- (70) Sciannamea, V.; Jerome, R.; Detrembleur, C. *Chem. Rev.* **2008**, *108*, 1104.
- (71) Grubbs, R. B. *Polym. Rev.* **2011**, *51*, 104.
- (72) Otsu, T. *J. Polym. Sci., A: Polym. Chem.* **2000**, *38*, 2121.
- (73) Otsu, T. *Adv. Polym. Sci.* **1998**, *136*, 75.
- (74) Estillore, N. C.; Park, J. Y.; Advincula, R. C. *Macromolecules* **2010**, *43*, 6588.
- (75) Feng, W.; Chen, R.; Brash, J. L.; Zhu, S. *Macromol. Rapid Commun.* **2005**, *26*, 1383.
- (76) Brown, A. A.; Khan, N. S.; Steinbock, L.; Huck, W. T. S. *Eur. Polym. J.* **2005**, *41*, 1757.
- (77) Wang, S.; Zhu, Y. *Langmuir* **2009**, *25*, 13448.
- (78) Husseman, M.; Malmstrom, E.; McNamara, M.; Mate, M.; Mecerreyres, D.; Benoit, D. G.; Hedrick, J. L.; Mansky, P.; Huang, E.; Russell, T. P.; Hawker, C. J. *Macromolecules* **1999**, *32*, 1424.
- (79) Perruchot, C.; Khan, M. A.; Kamitsi, A.; Armes, S. P. *Langmuir* **2001**, *17*, 4479.
- (80) Ohno, K.; Morinaga, T.; Koh, K.; Tsuji, Y.; Fukuda, T. *Macromolecules* **2005**, *38*, 2137.
- (81) Huang, C.; Tassone, T.; Woodberry, K.; Sunday, D.; Green, D. L. *Langmuir* **2009**, *25*, 13351.
- (82) Ma, H.; Li, D.; Sheng, X.; Zhao, B.; Chilkoti, A. *Langmuir* **2006**, *22*, 3751.
- (83) Wang, X.; Ye, Q.; Gao, T.; Liu, J.; Zhou, F. *Langmuir* **2012**, *28*, 2574.
- (84) White, M. A.; Johnson, J. A.; Koberstein, J. T.; Turro, N. J. *J. Am. Chem. Soc.* **2006**, *128*, 11356.
- (85) Jones, D. M.; Huck, W. T. S. *Adv. Mater.* **2001**, *13*, 1256.
- (86) Jones, D. M.; Brown, A. A.; Huck, W. T. S. *Langmuir* **2002**, *18*, 1265.
- (87) Bedair, T. M.; Cho, Y.; Kim, T. J.; Kim, Y. D.; Park, B. J.; Joung, Y. K.; Han, D. K. *Langmuir* **2014**, *30*, 8020.
- (88) Lego, B.; Francois, M.; Skene, W. G.; Giasson, S. *Langmuir* **2009**, *25*, 5313.
- (89) Lego, B.; Skene, W. G.; Giasson, S. *Langmuir* **2008**, *24*, 379.
- (90) Steenackers, M.; Gigler, A. M.; Zhang, N.; Deubel, F.; Seifert, M.; Hess, L. H.; Lim, C. H. Y. X.; Loh, K. P.; Garrido, J. A.; Jordan, R.; Stutzmann, M.; Sharp, I. D. *J. Am. Chem. Soc.* **2011**, *133*, 10490.
- (91) Badri, A.; Whittaker, M. R.; Zetterlund, P. B. *J. Polym. Sci., A: Polym. Chem.* **2012**, *50*, 2981.
- (92) Zeng, L.; Wang, H.; Fu, G.; Jiang, J.; Zhang, X. *J. Colloid Interface Sci.* **2010**, *352*, 36.
- (93) He, J.; Yang, X.; Mao, J.; Xu, F.; Cai, Q. *Appl. Surf. Sci.* **2012**, *258*, 6826.
- (94) Majoinen, J.; Walther, A.; McKee, J. R.; Kontturi, E.; Aseyev, V.; Malho, J. M.; Ruokolainen, J.; Ikkala, O. *Biomacromolecules* **2011**, *12*, 2997.
- (95) Ameringer, T.; Ercole, F.; Tsang, K. M.; Coad, B. R.; Hou, X.; Rodda, A.; Nisbet, D. R.; Thissen, H.; Evans, R. A.; Meagher, L.; Forsythe, J. S. *Biointerphases* **2013**, *8*, 16.
- (96) Coad, B. R.; Lu, Y.; Meagher, L. *Acta Biomater.* **2012**, *8*, 608.
- (97) Yameen, B.; Khan, H. U.; Knoll, W.; Forch, R.; Jonas, U. *Macromol. Rapid Commun.* **2011**, *32*, 1735.
- (98) Rodriguez-Emmenegger, C.; Kylian, O.; Houska, M.; Brynda, E.; Artemenko, A.; Lousal, J.; Bologna Alles, A.; Biederman, H. *Biomacromolecules* **2011**, *12*, 1058.
- (99) Telford, A. M.; Neto, C.; Meagher, L. *Polymer* **2013**, *54*, 5490.
- (100) Hucknall, A.; Simnick, A. J.; Hill, R. T.; Chilkoti, A.; Garcia, A.; Johannes, M. S.; Clark, R. L.; Zauscher, S.; Ratner, B. D. *Biointerphases* **2009**, *4*, FA50.
- (101) Patrucco, E.; Ouasti, S.; Vo, C. D.; De Leonardi, P.; Pollicino, A.; Armes, S. P.; Scandola, M.; Tirelli, N. *Biomacromolecules* **2009**, *10*, 3130.
- (102) Pranantyo, D.; Xu, L. Q.; Neoh, K.-G.; Kang, E.-T.; Yang, W.; Teo, S. L.-M. *J. Mater. Chem. B* **2014**, *2*, 398.
- (103) Farhan, T.; Huck, W. T. S. *Eur. Polym. J.* **2004**, *40*, 1599.
- (104) Xu, F. J.; Wang, Z. H.; Yang, W. T. *Biomaterials* **2010**, *31*, 3139.
- (105) Xu, F. J.; Zheng, Y. Q.; Zhen, W. J.; Yang, W. T. *Colloids Surf., B* **2011**, *85*, 40.
- (106) Yameen, B.; Alvarez, M.; Azzaroni, O.; Jonas, U.; Knoll, W. *Langmuir* **2009**, *25*, 6214.
- (107) Jain, P.; Dai, J.; Grajales, S.; Saha, S.; Baker, G. L.; Bruening, M. *Langmuir* **2007**, *23*, 11360.
- (108) Goncalves, S.; Leiros, A.; van Kooten, T.; Dourado, F.; Rodrigues, L. R. *Colloids Surf., B* **2013**, *109*, 228.
- (109) Bozukova, D.; Pagnoulle, C.; De Pauw-Gillet, M.-C.; Ruth, N.; Jérôme, R.; Jérôme, C. *Langmuir* **2008**, *24*, 6649.
- (110) Pei, Y.; Travas-Sejdic, J.; Williams, D. E. *Langmuir* **2012**, *28*, 8072.
- (111) Strover, L.; Roux, C.; Malmstrom, J.; Pei, Y.; Williams, D. E.; Travas-Sejdic, J. *Synth. Met.* **2012**, *162*, 381.
- (112) Zhao, H.; Zhu, B.; Luo, S.-C.; Lin, H.-A.; Nakao, A.; Yamashita, Y.; Yu, H.-h. *ACS Appl. Mater. Interfaces* **2013**, *5*, 4536.
- (113) Tria, M. C. R.; Grande, C. D. T.; Ponnappati, R. R.; Advincula, R. C. *Biomacromolecules* **2010**, *11*, 3422.

- (114) Ayres, N. *Polym. Chem.* **2010**, *1*, 769.
- (115) Lu, Y.; Wittemann, A.; Ballauff, M. *Macromol. Rapid Commun.* **2009**, *30*, 806.
- (116) Bunsow, J.; Kelby, T. S.; Huck, W. T. S. *Acc. Chem. Res.* **2010**, *43*, 466.
- (117) Radhakrishnan, B.; Ranjan, R.; Brittain, W. J. *Soft Matter* **2006**, *2*, 386.
- (118) Xu, F. J.; Neoh, K. G.; Kang, E. T. *Prog. Polym. Sci.* **2009**, *34*, 719.
- (119) Jiang, H.; Xu, F.-J. *Chem. Soc. Rev.* **2013**, *42*, 3394.
- (120) Becker, A. L.; Henzler, K.; Welsch, N.; Ballauff, M.; Borisov, O. *Curr. Opin. Colloid Interface Sci.* **2012**, *17*, 90.
- (121) Kuroki, H.; Tokarev, I.; Minko, S. *Annu. Rev. Mater. Res.* **2012**, *42*, 343.
- (122) Zhao, B.; Zhu, L. *Macromolecules* **2009**, *42*, 9369.
- (123) Fristrup, C. J.; Jankova, K.; Hvilsted, S. *Soft Matter* **2009**, *5*, 4623.
- (124) Hui, C. M.; Pietrasik, J.; Schmitt, M.; Mahoney, C.; Choi, J.; Bockstaller, M. R.; Matyjaszewski, K. *Chem. Mater.* **2014**, *26*, 745.
- (125) Olivier, A.; Meyer, F.; Raquez, J.-M.; Damman, P.; Dubois, P. *Prog. Polym. Sci.* **2012**, *37*, 157.
- (126) Ballauff, M. *Prog. Polym. Sci.* **2007**, *32*, 1135.
- (127) Ballauff, M.; Borisov, O. *Curr. Opin. Colloid Interface Sci.* **2006**, *11*, 316.
- (128) Minko, S. *J. Macromol. Sci., Part C: Polym. Rev.* **2006**, *46*, 397.
- (129) Chen, T.; Ferris, R.; Zhang, J.; Ducker, R.; Zauscher, S. *Prog. Polym. Sci.* **2010**, *35*, 94.
- (130) Welch, M. E.; Ober, C. K. *J. Polym. Sci., B: Polym. Phys.* **2013**, *51*, 1457.
- (131) Peng, S.; Bhushan, B. *RSC Adv.* **2012**, *2*, 8557.
- (132) de Gennes, P. G. *Macromolecules* **1980**, *13*, 1069.
- (133) Wu, T.; Efimenko, K.; Vlcek, P.; Subr, V.; Genzer, J. *Macromolecules* **2003**, *36*, 2448.
- (134) Alexander, S. *J. Phys. (Paris)* **1977**, *38*, 983.
- (135) Jonas, A. M.; Hu, Z.; Glinel, K.; Huck, W. T. S. *Nano Lett.* **2008**, *8*, 3819.
- (136) Spiliopoulos, N.; Koutsioubas, A. G.; Anastassopoulos, D. L.; Vradis, A. A.; Toprakcioglu, C.; Menelle, A.; Mountrichas, G.; Pispas, S. *Macromolecules* **2009**, *42*, 6209.
- (137) Milner, S. T.; Witten, T. A.; Cates, M. E. *Macromolecules* **1988**, *21*, 2610.
- (138) Milner, S. T.; Witten, T. A.; Cates, M. E. *Macromolecules* **1989**, *22*, 853.
- (139) Zhulina, E. B.; Borisov, O. V.; Pryamitsyn, V. A.; Birshtein, T. M. *Macromolecules* **1991**, *24*, 140.
- (140) Wijmans, C. M.; Zhulina, E. B. *Macromolecules* **1993**, *26*, 7214.
- (141) Elliott, I. G.; Kuhl, T. L.; Faller, R. *Macromolecules* **2010**, *43*, 9131.
- (142) de Vos, W. M.; Leermakers, F. A. M.; Lindhoud, S.; Prescott, S. W. *Macromolecules* **2011**, *44*, 2334.
- (143) Polotsky, A. A.; Gillich, T.; Borisov, O. V.; Leermakers, F. A. M.; Textor, M.; Birshtein, T. M. *Macromolecules* **2010**, *43*, 9555.
- (144) Aoki, H.; Kitamura, M.; Ito, S. *Macromolecules* **2008**, *41*, 285.
- (145) Lenz, S.; Ruhm, A.; Major, J.; Berger, R.; Gutmann, J. S. *Macromolecules* **2011**, *44*, 360.
- (146) Edmondson, S.; Nguyen, N. T.; Lewis, A. L.; Armes, S. P. *Langmuir* **2010**, *26*, 7216.
- (147) Sanjuan, S.; Perrin, P.; Pantoustier, N.; Tran, Y. *Langmuir* **2007**, *23*, 5769.
- (148) Tan, K. Y.; Gautrot, J. E.; Huck, W. T. S. *Langmuir* **2011**, *27*, 1251.
- (149) Bracha, D.; Bar-Ziv, R. H. *J. Am. Chem. Soc.* **2014**, *136*, 4945.
- (150) Chen, M.; Briscoe, W. H.; Armes, S. P.; Klein, J. *Science* **2009**, *323*, 1698.
- (151) Xue, C.; Yonet-Tanyeri, N.; Brouette, N.; Sferrazza, M.; Braun, P. V.; Leckband, D. E. *Langmuir* **2011**, *27*, 8810.
- (152) Paik, M. Y.; Xu, Y.; Rastogi, A.; Tanaka, M.; Yi, Y.; Ober, C. K. *Nano Lett.* **2010**, *10*, 3873.
- (153) Navarro, M.; Benetti, E. M.; Zapotoczny, S.; Planell, J. A.; Vancso, G. J. *Langmuir* **2008**, *24*, 10996.
- (154) Burkert, S.; Bittrich, E.; Kuntzsch, M.; Muller, M.; Eichhorn, K.-J.; Bellmann, C.; Uhlmann, P.; Stamm, M. *Langmuir* **2010**, *26*, 1786.
- (155) Jonas, A. M.; Glinel, K.; Oren, R.; Nysten, B.; Huck, W. T. S. *Macromolecules* **2007**, *40*, 4403.
- (156) Schuwer, N.; Klok, H.-A. *Langmuir* **2011**, *27*, 4789.
- (157) Fielding, L. A.; Edmondson, S.; Armes, S. P. *J. Mater. Chem.* **2011**, *21*, 11773.
- (158) Willott, J. D.; Murdoch, T. J.; Humphreys, B. A.; Edmondson, S.; Webber, G. B.; Wanless, E. J. *Langmuir* **2014**, *30*, 1827.
- (159) Li, D.; He, Q.; Cui, Y.; Li, J. *Chem. Mater.* **2007**, *19*, 412.
- (160) Ross, R. S.; Pincus, P. *Macromolecules* **1992**, *25*, 2177.
- (161) Israels, R.; Leermakers, F. A. M.; Fleer, G. J.; Zhulina, E. B. *Macromolecules* **1994**, *27*, 3249.
- (162) Abraham, S.; So, A.; Unsworth, L. D. *Biomacromolecules* **2011**, *12*, 3567.
- (163) Mi, L.; Bernards, M. T.; Cheng, G.; Yu, Q.; Jiang, S. *Biomaterials* **2010**, *31*, 2919.
- (164) Rauch, S.; Uhlmann, P.; Eichhorn, K.-J. *Anal. Bioanal. Chem.* **2013**, *405*, 9061.
- (165) Ishida, N.; Biggs, S. *Macromolecules* **2010**, *43*, 7269.
- (166) Cheng, N.; Brown, A. A.; Azzaroni, O.; Huck, W. T. S. *Macromolecules* **2008**, *41*, 6317.
- (167) Malham, I. B.; Bureau, L. *Langmuir* **2010**, *26*, 4762.
- (168) Nagase, K.; Kimura, A.; Shimizu, T.; Matsuura, K.; Yamato, M.; Takeda, N.; Okano, T. *J. Mater. Chem.* **2012**, *22*, 19514.
- (169) Bittrich, E.; Burkert, S.; Muller, M.; Eichhorn, K.-J.; Stamm, M.; Uhlmann, P. *Langmuir* **2012**, *28*, 3439.
- (170) Choi, B. C.; Choi, S.; Leckband, D. E. *Langmuir* **2013**, *29*, 5841.
- (171) Williams, D. R. M. *J. Phys. II* **1993**, *3*, 1313.
- (172) Lutz, J. F.; Akdemir, O.; Hoth, A. *J. Am. Chem. Soc.* **2006**, *128*, 13046.
- (173) Laloyaux, X.; Mathy, B.; Nysten, B.; Jonas, A. M. *Langmuir* **2010**, *26*, 838.
- (174) Azzaroni, O.; Brown, A. A.; Huck, W. T. S. *Angew. Chem., Int. Ed.* **2006**, *45*, 1770.
- (175) Polzer, F.; Heigl, J.; Schneider, C.; Ballauff, M.; Borisov, O. V. *Macromolecules* **2011**, *44*, 1654.
- (176) de Vos, W. M.; Leermakers, F. A. M.; de Keizer, A.; Kleijn, J. M.; Cohen Stuart, M. A. *Macromolecules* **2009**, *42*, 5881.
- (177) Halperin, A.; Kroger, M.; Zhulina, E. B. *Macromolecules* **2011**, *44*, 3622.
- (178) Yoshikawa, C.; Goto, A.; Tsujii, Y.; Ishizuka, N.; Nakanishi, K. *J. Polym. Sci., A: Polym. Chem.* **2007**, *45*, 4795.
- (179) Nagase, K.; Kobayashi, J.; Kikuchi, A.; Akiyama, Y.; Kanazawa, H.; Okano, T. *Langmuir* **2008**, *24*, 511.
- (180) Nagase, K.; Kobayashi, J.; Kikuchi, A.; Akiyama, Y.; Kanazawa, H.; Okano, T. *Biomacromolecules* **2008**, *9*, 1340.
- (181) Rodriguez Presa, M. J.; Gassa, L. M.; Azzaroni, O.; Gervasi, C. A. *Anal. Chem.* **2009**, *81*, 7936.
- (182) Schuh, C.; Ruhe, J. *Macromolecules* **2011**, *44*, 3502.
- (183) Lee, H.-S.; Penn, L. S. *Macromolecules* **2008**, *41*, 8124.
- (184) Milchev, A.; Egorov, S. A.; Binder, K. *Soft Matter* **2014**, *10*, 5974.
- (185) Singh, N.; Cui, X.; Boland, T.; Husson, S. M. *Biomaterials* **2007**, *28*, 763.
- (186) Claesson, P. M.; Blomber, E.; Froberg, J. C.; Nylander, T.; Arnebrant, T. *Adv. Colloid Interface Sci.* **1995**, *57*, 161.
- (187) Wang, Y.-X.; Robertson, J. L.; Spillman, W. B.; Claus, R. O. *Pharm. Res.* **2004**, *21*, 1362.
- (188) Sakata, S.; Inoue, Y.; Ishihara, K. *Langmuir* **2014**, *30*, 2745.
- (189) Halperin, A.; Fragneto, G.; Schollier, A.; Sferrazza, M. *Langmuir* **2007**, *23*, 10603.
- (190) de Vos, W. M.; Biesheuvel, P. M.; de Keizer, A.; Kleijn, J. M.; Cohen Stuart, M. A. *Langmuir* **2008**, *24*, 6575.

- (191) Wang, S.; Chen, K.; Kayitmazer, A. B.; Li, L.; Guo, X. *Colloids Surf. B* **2013**, *107*, 251.
- (192) Wang, S.; Kaimin, C.; Li, L.; Xuhong, G. *Biomacromolecules* **2013**, *14*, 818.
- (193) Delcroix, M. F.; Demoustier-Champagne, S.; Dupont-Gillain, C. C. *Langmuir* **2014**, *30*, 268.
- (194) Wittemann, A.; Ballauff, M. *Phys. Chem. Chem. Phys.* **2006**, *8*, 5269.
- (195) Leermakers, F. A. M.; Ballauff, M.; Borisov, O. V. *Langmuir* **2007**, *23*, 3937.
- (196) Biesheuvel, P. M.; Wittemann, A. *J. Phys. Chem. B* **2005**, *109*, 4209.
- (197) Becker, A. L.; Welsch, N.; Schneider, C.; Ballauff, M. *Biomacromolecules* **2011**, *12*, 3936.
- (198) Henzler, K.; Haupt, B.; Lauterbach, K.; Wittemann, A.; Borisov, O. V.; Ballauff, M. *J. Am. Chem. Soc.* **2010**, *132*, 3159.
- (199) Hollmann, O.; Gutberlet, T.; Czeslik, C. *Langmuir* **2007**, *23*, 1347.
- (200) Hollmann, O.; Steitz, R.; Czeslik, C. *Phys. Chem. Chem. Phys.* **2008**, *10*, 1448.
- (201) Henzler, K.; Haupt, B.; Rosenfeldt, S.; Harnau, L.; Narayanan, T.; Ballauff, M. *Phys. Chem. Chem. Phys.* **2011**, *13*, 17599.
- (202) Henzler, K.; Wittemann, A.; Breininger, E.; Ballauff, M.; Rosenfeldt, S. *Biomacromolecules* **2007**, *8*, 3674.
- (203) Henzler, K.; Rosenfeldt, S.; Wittemann, A.; Harnau, L.; Finet, S.; Narayanan, T.; Ballauff, M. *Phys. Rev. Lett.* **2008**, *100*, No. 158301.
- (204) Tan, K. Y.; Lin, H.; Ramstedt, M.; Watt, F. M.; Huck, W. T. S.; Gautrot, J. E. *Integr. Biol.* **2013**, *5*, 899.
- (205) Rzhepishevskaya, O.; Hakobyan, S.; Ruhal, R.; Gautrot, J.; Barbero, D.; Ramstedt, M. *Biomater. Sci.* **2013**, *1*, 589.
- (206) Ayres, N.; Holt, D. J.; Jones, C. F.; Corum, L. E.; Grainger, D. W. *J. Polym. Sci., A: Polym. Chem.* **2008**, *46*, 7713.
- (207) Kumar, S.; Tong, X.; Dory, Y. L.; Lepage, M.; Zhao, Y. H. *Chem. Commun.* **2013**, *49*, 90.
- (208) Lei, H.; Wang, M.; Tang, Z.; Luan, Y.; Liu, W.; Song, B.; Chen, H. *Langmuir* **2014**, *30*, 501.
- (209) Choi, S.; Choi, B.-C.; Xue, C.; Leckband, D. E. *Biomacromolecules* **2013**, *14*, 92.
- (210) Rastogi, A.; Nad, S.; Tanaka, M.; Da Mota, N.; Tague, M.; Baird, B. A.; Abruna, H. D.; Ober, C. K. *Biomacromolecules* **2009**, *10*, 2750.
- (211) Halperin, A.; Kroger, M. *Macromolecules* **2011**, *44*, 6986.
- (212) Yin, Z.; Zhang, J.; Jiang, L.-P.; Zhu, J.-J. *J. Phys. Chem. C* **2009**, *113*, 16104.
- (213) Hu, X.; Gorman, C. B. *Acta Biomater.* **2014**, *10*, 3497.
- (214) Hentschel, C.; Wagner, H.; Smiatek, J.; Heuer, A.; Fuchs, H.; Zhang, X.; Studer, A.; Chi, L. *Langmuir* **2013**, *29*, 1850.
- (215) Wang, X.; Gan, H.; Sun, T. *Adv. Funct. Mater.* **2011**, *21*, 3276.
- (216) Yu, K.; Kizhakkedathu, J. N. *Biomacromolecules* **2010**, *11*, 3073.
- (217) Yu, K.; Creagh, A. L.; Haynes, C. A.; Kizhakkedathu, J. N. *Anal. Chem.* **2013**, *85*, 7786.
- (218) Xu, Z.; Uddin, K. M. A.; Kamra, T.; Schnadt, J.; Ye, L. *ACS Appl. Mater. Interfaces* **2014**, *6*, 1406.
- (219) Ma, H.; Hyun, J.; Stiller, P.; Chilkoti, A. *Adv. Mater.* **2004**, *16*, 338.
- (220) Chang, Y.; Ko, C.-Y.; Shih, Y.-J.; Quemener, D.; Deratani, A.; Wei, T.-C.; Wang, D.-M.; Lai, J.-Y. *J. Membr. Sci.* **2009**, *345*, 160.
- (221) Kizhakkedathu, J. N.; Janzen, J.; Le, Y.; Kainthan, R. K.; Brooks, D. E. *Langmuir* **2009**, *25*, 3794.
- (222) Trmcic-Cvita, J.; Hasan, E.; Ramstedt, M.; Li, X.; Cooper, M.; Abel, C.; Huck, W. T. S.; Gautrot, J. E. *Biomacromolecules* **2009**, *10*, 2885.
- (223) Gautrot, J. E.; Trappmann, B.; Oceguera-Yanez, F.; Connelly, J.; He, X.; Watt, F. M.; Huck, W. T. S. *Biomaterials* **2010**, *31*, 5030.
- (224) Rodriguez-Emmenegger, C.; Brynda, E.; Riedel, T.; Houska, M.; Subr, V.; Alles, A. B.; Hasan, E.; Gautrot, J. E.; Huck, W. T. S. *Macromol. Rapid Commun.* **2011**, *32*, 952.
- (225) Tugulu, S.; Klok, H.-A. *Biomacromolecules* **2008**, *9*, 906.
- (226) Zhao, C.; Li, L.; Wang, Q.; Yu, Q.; Zheng, J. *Langmuir* **2011**, *27*, 4906.
- (227) Yandi, W.; Mieszkin, S.; Martin-Tanchereau, P.; Callow, M. E.; Callow, J. A.; Tyson, L.; Liedberg, B.; Ederth, T. *ACS Appl. Mater. Interfaces* **2014**, *6*, 11448.
- (228) Yoshikawa, C.; Hattori, S.; Honda, T.; Huang, C.-F.; Kobayashi, H. *Mater. Lett.* **2012**, *83*, 140.
- (229) Genzer, J.; Arifuzzaman, S.; Bhat, R. R.; Efimenko, K.; Ren, C.-I.; Szleifer, I. *Langmuir* **2012**, *28*, 2122.
- (230) Liu, Q.; Singh, A.; Lalani, R.; Liu, L. *Biomacromolecules* **2012**, *13*, 1086.
- (231) Zhang, N.; Pompe, T.; Amin, I.; Luxenhofer, R.; Werner, C.; Jordan, R. *Macromol. Biosci.* **2012**, *12*, 926.
- (232) Yang, Q.; Kaul, C.; Ulbricht, M. *Langmuir* **2010**, *26*, 5746.
- (233) Lau, K. H. A.; Ren, C.; Park, S. H.; Szleifer, I.; Messersmith, P. B. *Langmuir* **2012**, *28*, 2288.
- (234) Taylor, W.; Jones, R. A. L. *Langmuir* **2013**, *29*, 6116.
- (235) Inoue, Y.; Nakanishi, T.; Ishihara, K. *Langmuir* **2013**, *29*, 10752.
- (236) Gunkel, G.; Weinhart, M.; Becherer, T.; Haag, R.; Huck, W. T. S. *Biomacromolecules* **2012**, *12*, 4169.
- (237) Benhabbour, S. R.; Sheardown, H.; Adronov, A. *Macromolecules* **2008**, *41*, 4817.
- (238) Zhao, C.; Li, L.; Zheng, J. *Langmuir* **2010**, *26*, 17375.
- (239) de los Santos Pereira, A.; Rodriguez-Emmenegger, C.; Surman, F.; Riedel, T.; Alles, A. B.; Brynda, E. *RSC Adv.* **2014**, *4*, 2318.
- (240) Yang, J.; Zhang, M.; Chen, H.; Chang, Y.; Chen, Z.; Zheng, J. *Biomacromolecules* **2014**, *15*, 2982.
- (241) Ladd, J.; Zhang, Z.; Chen, S.; Hower, J. C.; Jiang, S. *Biomacromolecules* **2008**, *9*, 1357.
- (242) Wu, J.; Lin, W.; Wang, Z.; Chen, S. *Langmuir* **2012**, *28*, 7436.
- (243) Wu, J.; Zhao, C.; Hu, R.; Lin, W.; Wang, Q.; Zhao, J.; Bilibovich, S. M.; Leeper, T. C.; Li, L.; Cheung, H. M.; Chen, S.; Zheng, J. *Acta Biomater.* **2014**, *10*, 751.
- (244) Shao, Q.; He, Y.; White, A. D.; Jiang, S. *J. Phys. Chem. B* **2010**, *114*, 16625.
- (245) Leng, C.; Han, X.; Shao, Q.; Zhu, Y.; Li, Y.; Jiang, S. *J. Phys. Chem. C* **2014**, *118*, 15840.
- (246) Rodriguez-Emmenegger, C.; Brynda, E.; Riedel, T.; Sedlakova, Z.; Houska, M.; Bologna Alles, A. *Langmuir* **2009**, *25*, 6328.
- (247) Yang, W.; Xue, H.; Li, W.; Zhang, J.; Jiang, S. *Langmuir* **2009**, *25*, 11911.
- (248) Chang, Y.; Liao, S.-C.; Higuchi, A.; Ruaan, R.-C.; Chu, C.-W.; Chen, W.-Y. *Langmuir* **2008**, *24*, 5453.
- (249) Zhang, Z.; Finlay, J. A.; Wang, L.; Gao, Y.; Callow, J. A.; Callow, M. E.; Jiang, S. *Langmuir* **2009**, *25*, 13516.
- (250) Chang, Y.; Chang, Y.; Higuchi, A.; Shih, Y.-J.; Li, P.-T.; Chen, W.-Y.; Tsai, E.-M.; Hsieh, G.-H. *Langmuir* **2012**, *28*, 4309.
- (251) Chang, Y.; Shih, Y.-J.; Lai, C.-J.; Kung, H.-H.; Jiang, S. *Adv. Funct. Mater.* **2013**, *23*, 1100.
- (252) Schon, P.; Kutnyanszky, E.; Donkelaar, B. t.; Santonicola, M. G.; Tecim, T.; Aldred, N.; Clare, A. S.; Vancso, G. J. *Colloids Surf., B* **2013**, *102*, 923.
- (253) Wang, T.; Wang, X.; Long, Y.; Guangming, L.; Guangzhao, Z. *Langmuir* **2013**, *29*, 6588.
- (254) Inoue, Y.; Ishihara, K. *Colloids Surf., B* **2010**, *81*, 350.
- (255) Brault, N. D.; Sundaram, H. S.; Li, Y.; Huang, C.-J.; Yu, Q.; Jiang, S. *Biomacromolecules* **2012**, *13*, 589.
- (256) Huang, C.-J.; Li, Y.; Krause, J. B.; Brault, N. D.; Jiang, S. *Macromol. Rapid Commun.* **2012**, *33*, 1003.
- (257) Rodriguez Emmenegger, C.; Hasan, E.; Pop-Georgievski, O.; Houska, M.; Brynda, E.; Alles, A. B. *Macromol. Biosci.* **2012**, *12*, 525.
- (258) Quintana, R.; Janczewski, D.; Vasanthan, V. A.; Jana, S.; Lee, S. S. C.; Parra-Velandia, F. J.; Guo, S.; Parthiban, A.; Teo, S. L.-M.; Vancso, G. J. *Colloids Surf., B* **2014**, *120*, 118.
- (259) Riedel, T.; Riedelova-Reicheltova, Z.; Majek, P.; Rodriguez-Emmenegger, C.; Houska, M.; Dyr, J. E.; Brynda, E. *Langmuir* **2013**, *29*, 3388.
- (260) Gunkel, G.; Huck, W. T. S. *J. Am. Chem. Soc.* **2013**, *135*, 7047.

- (261) Iwata, R.; Suk-In, P.; Hoven, V. P.; Takahara, A.; Akiyoshi, K.; Iwasaki, Y. *Biomacromolecules* **2004**, *5*, 2308.
- (262) Liu, Q.; Singh, A.; Liu, L. *Biomacromolecules* **2013**, *14*, 226.
- (263) Liu, Q.; Li, W.; Singh, A.; Cheng, G.; Liu, L. *Acta Biomater.* **2014**, *10*, 2956.
- (264) Bernards, M. T.; Cheng, G.; Zhang, Z.; Chen, S.; Jiang, S. *Macromolecules* **2008**, *41*, 4216.
- (265) Herzberg, M.; Sweity, A.; Brami, M.; Kaufman, Y.; Freger, V.; Oron, G.; Belfer, S.; Kasher, R. *Biomacromolecules* **2011**, *12*, 1169.
- (266) Tu, Q.; Wang, J.-C.; Liu, R.; He, J.; Zhang, Y.; Shen, S.; Xu, J.; Liu, J.; Yuan, M.-S.; Wang, J. *Colloids Surf., B* **2013**, *102*, 361.
- (267) Yu, K.; Lai, B. F. L.; Kizhakkedathu, J. N. *Adv. Healthcare Mater.* **2012**, *1*, 199.
- (268) Wittemann, A.; Ballauff, M. *Anal. Chem.* **2004**, *76*, 2813.
- (269) Reichhart, C.; Czeslik, C. *Langmuir* **2009**, *25*, 1047.
- (270) Haupt, B.; Neumann, R.; Wittemann, A.; Ballauff, M. *Biomacromolecules* **2005**, *6*, 948.
- (271) Neumann, T.; Haupt, B.; Ballauff, M. *Macromol. Biosci.* **2004**, *4*, 13.
- (272) Henzler, K.; Haupt, B.; Ballauff, M. *Anal. Biochem.* **2008**, *378*, 184.
- (273) Kudina, O.; Zakharchenko, A.; Trotsenko, O.; Tokarev, A.; Ionov, L.; Stoychev, G.; Puretskiy, N.; Pryor, S. W.; Voronov, A.; Minko, S. *Angew. Chem., Int. Ed.* **2014**, *53*, 483.
- (274) Wittemann, A.; Ballauff, M. *Macromol. Biosci.* **2005**, *5*, 13.
- (275) Reichhart, C.; Czeslik, C. *Colloids Surf., B* **2010**, *75*, 612.
- (276) Hucknall, A.; Kim, D.-H.; Rangarajan, S.; Hill, R. T.; Reichert, W. M.; Chilkoti, A. *Adv. Mater.* **2009**, *21*, 1968.
- (277) Hu, W.; Liu, Y.; Lu, Z.; Li, C. M. *Adv. Funct. Mater.* **2010**, *20*, 3497.
- (278) Fang, Y.; Xu, W.; Meng, X.-L.; Ye, X.-Y.; Wu, J.; Xu, Z.-K. *Langmuir* **2012**, *28*, 13318.
- (279) Dai, J.; Bao, Z.; Sun, L.; Hong, S. U.; Baker, G. L.; Bruening, M. *Langmuir* **2006**, *22*, 4274.
- (280) Cullen, S. P.; Liu, X.; Mandel, I. C.; Himpel, F. J.; Gopalan, P. *Langmuir* **2008**, *24*, 913.
- (281) Jain, P.; Sun, L.; Dai, J.; Baker, G. L.; Bruening, M. *Biomacromolecules* **2007**, *8*, 3102.
- (282) Xu, F.; Geiger, J. H.; Baker, G. L.; Bruening, M. *Langmuir* **2011**, *27*, 3106.
- (283) Jain, P.; Vyas, M. K.; Geiger, J. H.; Baker, G. L.; Bruening, M. *Biomacromolecules* **2010**, *11*, 1019.
- (284) Jain, P.; Dai, J.; Baker, G. L.; Bruening, M. L. *Macromolecules* **2008**, *41*, 8413.
- (285) Diamanti, S.; Arifuzzaman, S.; Elsen, A.; Genzer, J.; Vaia, R. A. *Polymer* **2008**, *49*, 3770.
- (286) Raynor, J. E.; Petrie, T. A.; Garcia, A. J.; Collard, D. M. *Adv. Mater.* **2007**, *19*, 1724.
- (287) Zhao, L.; Qin, H.; Hu, Z.; Zhang, Y.; Wu, R.; Zou, H. *Chem. Sci.* **2012**, *3*, 2828.
- (288) Schuwer, N.; Geue, T.; Hinestrosa, J. P.; Klok, H.-A. *Macromolecules* **2011**, *44*, 6868.
- (289) Barbey, R.; Laporte, V.; Alnabulsi, S.; Klok, H.-A. *Macromolecules* **2013**, *46*, 6151.
- (290) Raynor, J. E.; Petrie, T. A.; Fears, K. P.; Latour, R. A.; Garcia, A. J.; Collard, D. M. *Biomacromolecules* **2009**, *10*, 748.
- (291) Glinel, K.; Jonas, A. M.; Jouenne, T.; Leprince, J.; Galas, L.; Huck, W. T. S. *Bioconjugate Chem.* **2009**, *20*, 71.
- (292) Gao, G.; Yu, K.; Kindrachuk, J.; Brooks, D. E.; Hancock, R. E.; Kizhakkedathu, J. N. *Biomacromolecules* **2011**, *12*, 3715.
- (293) Costa, P.; Gautrot, J. E.; Connelly, J. *Acta Biomater.* **2014**, *10*, 2415.
- (294) He, F.; Luo, B.; Yuan, S.; Liang, B.; Choong, C.; Pehkonen, S. O. *RSC Adv.* **2014**, *4*, 105.
- (295) Lee, B. S.; Lee, J. K.; Kim, W.-J.; Jung, Y. H.; Sim, S. J.; Lee, J.; Choi, I. S. *Biomacromolecules* **2007**, *8*, 744.
- (296) Takahashi, H.; Matsuzaka, N.; Nakayama, M.; Kikuchi, A.; Yamato, M.; Okano, T. *Biomacromolecules* **2012**, *13*, 253.
- (297) Tsarevsky, N. V.; Bencherif, S. A.; Matyjaszewski, K. *Macromolecules* **2007**, *40*, 4439.
- (298) Chandrasekhar, S.; Reddy, C. R.; Babu, B. N.; Chandrasekhar, G. *Tetrahedron Lett.* **2002**, *43*, 3801.
- (299) Terada, A.; Yuasa, A.; Kushimoto, T.; Tsuneda, S.; Katai, A.; Tamada, M. *Microbiology* **2006**, *152*, 3575.
- (300) Zhao, G.; Wang, J.; Li, Y.; Huang, H.; Chen, X. *Biochem. Eng. J.* **2012**, *68*, 159.
- (301) Barbey, R.; Klok, H.-A. *Langmuir* **2010**, *26*, 18219.
- (302) Hensarling, R. M.; Doughty, V. A.; Chan, J. W.; Patton, D. L. *J. Am. Chem. Soc.* **2009**, *131*, 14673.
- (303) Saha, S.; Bruening, M.; Baker, G. L. *Macromolecules* **2012**, *45*, 9063.
- (304) Lee, J.; Kim, J. M.; Kim, J.; Kim, J. *Bull. Korean Chem. Soc.* **2012**, *33*, 2043.
- (305) Dong, R.; Krishnan, S.; Baird, B. A.; Lindau, M.; Ober, C. K. *Biomacromolecules* **2007**, *8*, 3082.
- (306) Zhang, F.; Zhang, Z.; Zhu, X.; Kang, E.-T.; Neoh, K.-G. *Biomaterials* **2008**, *29*, 4751.
- (307) Yuan, S.; Xiong, G.; Wang, X.; Zhang, S.; Choong, C. J. *Mater. Chem.* **2012**, *22*, 13039.
- (308) Yang, W. J.; Cai, T.; Neoh, K.-G.; Kang, E.-T.; Dickinson, G. H.; Teo, S. L.-M.; Rittschof, D. *Langmuir* **2011**, *27*, 7065.
- (309) Wu, Y.; Coyer, S. R.; Ma, H.; Garcia, A. J. *Acta Biomater.* **2010**, *6*, 2898.
- (310) Ren, X.; Wu, Y.; Cheng, Y.; Ma, H.; Wei, S. *Langmuir* **2011**, *27*, 12069.
- (311) Yuan, S.; Wan, D.; Liang, B.; Pehkonen, S. O.; Ting, Y. P.; Neoh, K.-G.; Kang, E. T. *Langmuir* **2011**, *27*, 2761.
- (312) Petrie, T. A.; Raynor, J. E.; Reyes, C. D.; Burns, K. L.; Collard, D. M.; Garcia, A. J. *Biomaterials* **2008**, *29*, 2849.
- (313) Petrie, T. A.; Raynor, J. E.; Dumbauld, D. W.; Lee, T. T.; Jagtap, S.; Templeman, K. L.; Collard, D. M.; Garcia, A. *Sci. Transl. Med.* **2010**, *2*, 45ra60.
- (314) Xu, F. J.; Liu, L. Y.; Yang, W. T.; Kang, E. T.; Neoh, K.-G. *Biomacromolecules* **2009**, *10*, 1665.
- (315) Xu, F. J.; Li, Y. L.; Kang, E. T.; Neoh, K.-G. *Biomacromolecules* **2005**, *6*, 1759.
- (316) Zou, Y.; Yeh, P.-Y. J.; Rossi, N. A. A.; Brooks, D. E.; Kizhakkedathu, J. N. *Biomacromolecules* **2010**, *11*, 284.
- (317) Ahmad, S. A.; Hucknall, A.; Chilkoti, A.; Leggett, G. J. *Langmuir* **2010**, *26*, 9937.
- (318) Cullen, S. P.; Mandel, I. C.; Gopalan, P. *Langmuir* **2008**, *24*, 13701.
- (319) Barbey, R.; Kauffmann, E.; Ehrat, M.; Klok, H.-A. *Biomacromolecules* **2010**, *11*, 3467.
- (320) Li, C. Y.; Xu, F. J.; Yang, W. T. *Langmuir* **2013**, *29*, 1541.
- (321) Vaisocherova, H.; Yang, W.; Zhang, Z.; Cao, Z.; Cheng, G.; Piliarik, M.; Homola, J.; Jiang, S. *Anal. Chem.* **2008**, *80*, 7894.
- (322) Tah, T.; Bernard, M. T. *Colloids Surf., B* **2012**, *93*, 195.
- (323) Vaisocherova, H.; Zhang, Z.; Yang, W.; Cao, Z.; Cheng, G.; Taylor, A. D.; Piliarik, M.; Homola, J.; Jiang, S. *Biosens. Bioelectron.* **2009**, *24*, 1924.
- (324) Huang, C.-J.; Li, Y.; Jiang, S. *Anal. Chem.* **2012**, *84*, 3440.
- (325) Brault, N. D.; Sundaram, H. S.; Huang, C.-J.; Li, Y.; Yu, Q.; Jiang, S. *Biomacromolecules* **2012**, *13*, 4049.
- (326) de Groot, G. W.; Demarche, S.; Santonicola, M. G.; Tiefenauer, L.; Vancso, G. J. *Nanoscale* **2014**, *6*, 2228.
- (327) Tugulu, S.; Arnold, A.; Sielaff, I.; Johnsson, K.; Klok, H.-A. *Biomacromolecules* **2005**, *6*, 1602.
- (328) Sui, Y.; Gao, X.; Wang, Z.; Gao, C. J. *Membr. Sci.* **2012**, *394–395*, 107.
- (329) Meng, J.-Q.; Chen, C.-L.; Huang, L.-P.; Du, Q.-Y.; Zhang, Y.-F. *Appl. Surf. Sci.* **2011**, *257*, 6282.
- (330) Cai, T.; Wang, R.; Yang, W. J.; Lu, S.; Neoh, K.-G.; Kang, E.-T. *Soft Matter* **2011**, *7*, 11133.
- (331) Teixeira, F.; Popa, A. M.; Guimond, S.; Hegemann, D.; Rossi, R. M. J. *Appl. Polym. Sci.* **2013**, *636*.

- (332) Wandera, D.; Wickramasinghe, S. R.; Husson, S. M. *J. Membr. Sci.* **2011**, *373*, 178.
- (333) Tischer, T.; Rodriguez Emmenegger, C.; Trouillet, V.; Welle, A.; Schueler, V.; Mueller, J. A.; Goldmann, A. S.; Brynda, E.; Barner-Kowollik, C. *Adv. Mater.* **2014**, *26*, 4087.
- (334) Zhu, L.-P.; Dong, H.-B.; Wei, X.-Z.; Yi, Z.; Zhu, B.-K.; Xu, Y. *J. Membr. Sci.* **2008**, *320*, 407.
- (335) Anuraj, N.; Bhattacharjee, S.; Geiger, J. H.; Baker, G. L.; Bruening, M. *J. Membr. Sci.* **2012**, *389*, 117.
- (336) Chen, Y.; Deng, Q.; Xiao, J.; Nie, H.; Wu, L.; Zhou, W.; Huang, B. *Polymer* **2007**, *48*, 7604.
- (337) Zhou, S.; Xue, A.; Zhang, Y.; Li, M.; Wang, J.; Zhao, Y.; Xing, W. *J. Membr. Sci.* **2014**, *450*, 351.
- (338) Zhu, L.-J.; Zhu, L.-P.; Jiang, J.-H.; Yi, Z.; Zhao, Y.-F.; Zhu, B.-K.; Xu, Y.-Y. *J. Membr. Sci.* **2014**, *451*, 157.
- (339) Zhao, X.; Chen, W.; Su, Y.; Zhu, W.; Peng, J.; Jiang, Z.; Kong, L.; Li, Y.; Liu, J. *J. Membr. Sci.* **2013**, *441*, 93.
- (340) Chang, Y.; Shih, Y.-J.; Ko, C.-Y.; Jhong, J.-F.; Liu, Y.-L.; Wei, T.-C. *Langmuir* **2011**, *27*, 5445.
- (341) Singh, N.; Chen, Z.; Tomer, N.; Wickramasinghe, S. R.; Soice, N.; Husson, S. M. *J. Membr. Sci.* **2008**, *311*, 225.
- (342) Huang, X.; Doneski, L. J.; Wirth, M. *J. Anal. Chem.* **1998**, *70*, 4023.
- (343) Huang, R.; Ferhan, A. R.; Guo, L.; Qiu, B.; Lin, Z.; Kim, D.-W.; Chen, G. *RSC Adv.* **2014**, *4*, 4883.
- (344) Huang, G.; Xiong, Z.; Qin, H.; Zhu, J.; Sun, Z.; Zhang, Y.; Peng, X.; Ou, J.; Zou, H. *Anal. Chim. Acta* **2014**, *809*, 61.
- (345) Mitrovic, B.; Eastwood, S.; Wong, V.; Dyer, D.; Kinsel, G.; Scott, C. *Langmuir* **2013**, *29*, 696.
- (346) Huang, G.; Sun, Z.; Qin, H.; Zhao, L.; Xiong, Z.; Peng, X.; Ou, J.; Zou, H. *Analyst* **2014**, *139*, 2199.
- (347) Kurosawa, S.; Aizawa, H.; Talib, Z. A.; Atthoff, B.; Hilborn, J. *Biosens. Bioelectron.* **2004**, *20*, 1165.
- (348) Kitano, H.; Anraku, Y.; Shinohara, H. *Biomacromolecules* **2006**, *7*, 1065.
- (349) Luna-Vera, F.; Ferguson, J. D.; Alvarez, J. C. *Anal. Chem.* **2011**, *83*, 2012.
- (350) Welch, M. E.; Ritzert, N. L.; C, H.; Smith, N. L.; Tague, M. E.; Xu, Y.; Baird, B. A.; Abruna, H. D.; Ober, C. K. *J. Am. Chem. Soc.* **2014**, *136*, 1879.
- (351) Konradi, R.; Textor, M.; Reimhult, E. *Biosensors* **2012**, *2*, 341.
- (352) Brault, N. D.; White, A. D.; Taylor, A. D.; Yu, Q.; Jiang, S. *Anal. Chem.* **2013**, *85*, 1447.
- (353) Constantini, F.; Nascetti, A.; Scipinotti, R.; Domenici, F.; Sennato, S.; Gazza, L.; Bordi, F.; Pogna, N.; Manetti, C.; Caputo, D.; de Cesare, G. *RSC Adv.* **2014**, *4*, 2073.
- (354) Nguyen, A. T.; Baggerman, J.; Paulusse, J. M. J.; Zhuilhof, H.; van Rijn, C. J. M. *Langmuir* **2012**, *28*, 604.
- (355) Sebra, R. P.; Masters, K. S.; Bowmann, C. N.; Anseth, K. *Langmuir* **2005**, *21*, 20907.
- (356) Liu, Y.; Wang, W.; Hu, W.; Lu, Z.; Zhou, X.; Li, C. M. *Biomed. Microdevices* **2011**, *13*, 769.
- (357) Aied, A.; Zheng, Y.; Pandit, A.; Wang, W. *ACS Appl. Mater. Interfaces* **2012**, *4*, 826.
- (358) Laopa, P. S.; Vilaivan, T.; Hoven, V. P. *Analyst* **2013**, *138*, 269.
- (359) Sung, D.; Shin, D. H.; Jon, S. *Biosens. Bioelectron.* **2011**, *26*, 3967.
- (360) Sung, D.; Park, S.; Jon, S. *Langmuir* **2012**, *28*, 4507.
- (361) Hu, W.; Li, X.; He, G.; Zhang, Z.; Zheng, X.; Li, P.; Li, C. M. *Biosens. Bioelectron.* **2013**, *50*, 338.
- (362) Ma, H.; Wu, Y.; Yang, X.; Liu, X.; He, J.; Fu, L.; Wang, J.; Xu, H.; Shi, Y.; Zhong, R. *Anal. Chem.* **2010**, *82*, 6338.
- (363) Thomson, D. A. C.; Cooper, M. A. *Biosens. Bioelectron.* **2013**, *50*, 499.
- (364) Riedel, T.; Rodriguez-Emmenegger, C.; de los Santos Pereira, A.; Bedajankova, A.; Jinoch, P.; Boltovets, P. M.; Brynda, E. *Biosens. Bioelectron.* **2014**, *55*, 278.
- (365) Shiddiky, M. J. A.; Kithva, P. H.; Kozak, D.; Trau, M. *Biosens. Bioelectron.* **2012**, *38*, 132.
- (366) Vaisocherova, H.; Sevcu, V.; Adam, P.; Spackova, B.; Hegnerova, K.; de los Santos Pereira, A.; Rodriguez-Emmenegger, C.; Riedel, T.; Houska, M.; Brynda, E.; Homola, J. *Biosens. Bioelectron.* **2014**, *51*, 150.
- (367) Huang, C.-J.; Brault, N. D.; Li, Y.; Yu, Q.; Jiang, S. *Adv. Mater.* **2012**, *24*, 1834.
- (368) Akkahat, P.; Kiatkamjornwong, S.; Yusa, S.-I.; Hoven, V. P.; Iwasaki, Y. *Langmuir* **2012**, *28*, 5872.
- (369) Ma, J.; Luan, S.; Song, L.; Jin, J.; Yuan, S.; Yan, S.; Yang, H.; Shi, H.; Yin, J. *ACS Appl. Mater. Interfaces* **2014**, *6*, 1971.
- (370) Akkahat, P.; Hoven, V. P. *Colloids Surf., B* **2011**, *86*, 198.
- (371) Kitayama, Y.; Takeuchi, T. *Anal. Chem.* **2014**, *86*, 5587.
- (372) Hess, L. H.; Lyuleeva, A.; Blaschke, B. M.; Sachsenhauser, M.; Seifert, M.; Garrido, J. A. *ACS Appl. Mater. Interfaces* **2014**, *6*, 9705.
- (373) Liu, Y.; Zhang, Y.; Zhao, Y.; Yu, J. *Colloids Surf., B* **2014**, *121*, 21.
- (374) Qian, H.; He, L. *Anal. Chem.* **2009**, *81*, 4536.
- (375) Qian, H.; He, L. *Anal. Chem.* **2009**, *81*, 9824.
- (376) Kaastrup, K.; Chan, L.; Sikes, H. D. *Anal. Chem.* **2013**, *85*, 8055.
- (377) Barbee, K. D.; Chandragsu, M.; Huang, X. *Macromol. Biosci.* **2011**, *11*, 607.
- (378) Lane, S. M.; Kuang, Z.; Yom, J.; Arifuzzaman, S.; Genzer, J.; Farmer, B.; Naik, R.; Vaia, R. A. *Biomacromolecules* **2011**, *12*, 1822.
- (379) Xu, F. J.; Cai, Q. J.; Li, Y. L.; Kang, E. T.; Neoh, K.-G. *Biomacromolecules* **2005**, *6*, 1012.
- (380) Fan, X.; Lin, L.; Messersmith, P. B. *Biomacromolecules* **2006**, *7*, 2443.
- (381) Bhat, R. R.; Chaney, B. N.; Rowley, J.; Liebmann-Vinson, A.; Genzer, J. *Adv. Mater.* **2005**, *17*, 2802.
- (382) Mei, Y.; Wu, T.; Xu, C.; Langenbach, K. J.; Elliott, J. T.; Vogt, B. D.; Beers, K. L.; Amis, E. J.; Washburn, N. R. *Langmuir* **2005**, *21*, 12309.
- (383) Sofia, S. J.; Premnath, V.; Merrill, E. W. *Macromolecules* **1998**, *31*, 5059.
- (384) Du, H.; Chandaroy, P.; Hui, S. W. *Biochim. Biophys. Acta, Biomembr.* **1997**, *1326*, 236.
- (385) Jiang, H.; Wang, X. B.; Li, C. Y.; Li, J. S.; Xu, F. J.; Mao, C.; Yang, W. T.; Shen, J. *Langmuir* **2011**, *27*, 11575.
- (386) Wang, X.; Miao, J.; Zhao, H.; Mao, C.; Chen, X.; Shen, J. *J. Biomater. Appl.* **2014**, *29*, 14.
- (387) Ameringer, T.; Fransen, P.; Bean, P.; Johnson, G.; Pereira, S.; Evans, R. A.; Thissen, H.; Meagher, L. *J. Biomed. Mater. Res., Part A* **2012**, *100A*, 370.
- (388) Wei, Y.; Ji, Y.; Xiao, L. L.; Lin, Q. K.; Ji, J. A. *Colloids Surf., B* **2011**, *84*, 369.
- (389) Koegler, P.; Pasic, P.; Gardiner, J.; Glattauer, V.; Kingshott, P. *Biomacromolecules* **2014**, *15*, 2265.
- (390) Bhat, R. R.; Tomlinson, M. R.; Genzer, J. *J. Polym. Sci., B: Polym. Phys.* **2005**, *43*, 3384.
- (391) Bisson, I.; Kosinski, M.; Ruault, S.; Gupta, B.; Hilborn, J.; Wurm, F.; Frey, P. *Biomaterials* **2002**, *23*, 3149.
- (392) Ivanov, A. E.; Eccles, J.; Panahi, H. A.; Kumar, A.; Kuzimenko, M. V.; Nilsson, L.; Bergenstahl, B.; Long, N.; Phillips, G. J.; Mikhalovsky, S. V.; Galaev, I. Y.; Mattiason, B. *J. Biomed. Mater. Res., Part A* **2009**, *88*, 213.
- (393) Ivanov, A. E.; Kumar, A.; Nilsang, S.; Auilar, M. R.; Mikhalovsky, L. I.; Savina, I. N.; Nilsson, L.; Scheblykin, I. G.; Kuzimenko, M. V.; Galaev, I. Y. *Colloids Surf., B* **2010**, *75*, 510.
- (394) Shi, X. J.; Wang, Y. Y.; Li, D.; Yuan, L.; Zhou, F.; Wang, Y. W.; Song, B.; Wu, Z. Q.; Chen, H.; Brash, J. L. *Langmuir* **2012**, *28*, 17011.
- (395) Zhou, F.; Li, D.; Wu, Z. Q.; Song, B.; Yuan, L.; Chen, H. *Macromol. Biosci.* **2012**, *12*, 1391.
- (396) Lobbicke, R.; Chanana, M.; Schlaad, H.; Pilz-Allen, C.; Gunter, C.; Mohwald, H.; Tauber, A. *Biomacromolecules* **2011**, *12*, 3753.
- (397) Villa-Diaz, L. G.; Nandivada, H.; Ding, J.; Nogueira-de-Souza, N. C.; Krebsbach, P. H.; O'Shea, K. S.; Lahann, J.; Smith, G. D. *Nat. Biotechnol.* **2010**, *28*, 581.

- (398) Wang, X.; Gan, H.; Zhang, M.; Sun, T. *Langmuir* **2012**, *28*, 2791.
- (399) Yuan, S.; Xiong, G.; Roguin, A.; Choong, C. *Biointerphases* **2012**, *7*, 30.
- (400) Gunnewiek, M. K.; Benetti, E. M.; Di Luca, A.; van Blitterswijk, C. A.; Moroni, L.; Vancso, G. J. *Langmuir* **2013**, *29*, 13843.
- (401) Sin, M.-C.; Sun, Y.-M.; Chang, Y. *ACS Appl. Mater. Interfaces* **2014**, *6*, 861.
- (402) Ochsenhirt, S. E.; Kokkoli, E.; McCarthy, J. B.; Tirrell, M. *Biomaterials* **2006**, *27*, 3863.
- (403) Seo, J. H.; Kakinoki, S.; Inoue, Y.; Yamaoka, T.; Ishihara, K.; Yui, N. *J. Am. Chem. Soc.* **2013**, *135*, 5513.
- (404) Deng, Y.; Zhang, X.; Zhao, X.; Li, Q.; Ye, Z.; Li, Z.; Liu, Y.; Zhou, Y.; Ma, H.; Pan, G.; Pei, D.; Fang, J.; Wei, S. *Acta Biomater.* **2013**, *9*, 8840.
- (405) Paripovic, D.; Hall-Bozic, H.; Klok, H.-A. *J. Mater. Chem.* **2012**, *22*, 19570.
- (406) Petrie, T. A.; Capadona, J. R.; Reyes, C. D.; Garcia, A. *Biomaterials* **2006**, *27*, 5459.
- (407) Nakanishi, J.; Nakayama, H.; Yamaguchi, K.; Garcia, A.; Horiike, Y. *Sci. Technol. Adv. Mater.* **2011**, *12*, 044608.
- (408) Christman, K. L.; Vazquez-Dorbatt, V.; Schopf, E.; Kolodziej, C. M.; Li, R. C.; Broyer, R. M.; Chen, Y.; Maynard, H. D. *J. Am. Chem. Soc.* **2008**, *130*, 16585.
- (409) Bharali, D. J.; Klejbor, I.; Stachowiak, E. K.; Dutta, P.; Roy, I.; Kaur, N.; Bergey, E. J.; Prasad, P. N.; Stachowiak, M. K. *Proc. Natl. Acad. Sci. U.S.A.* **2005**, *102*, 11539.
- (410) Mintzer, M. A.; Simanek, E. E. *Chem. Rev.* **2009**, *109*, 259.
- (411) Pack, D. W.; Hoffman, A. S.; Pun, S.; Stayton, P. S. *Nat. Rev. Drug Discovery* **2005**, *4*, 581.
- (412) Sun, J. T.; Hong, C. Y.; Pan, C. Y. *J. Phys. Chem. C* **2010**, *114*, 12481.
- (413) Layman, J. M.; Ramirez, S. M.; Green, M. D.; Long, T. E. *Biomacromolecules* **2009**, *10*, 1244.
- (414) Jiang, X.; Lok, M. C.; Hennink, W. E. *Bioconjugate Chem.* **2007**, *18*, 2077.
- (415) Samsonova, O.; Pfeiffer, C.; Hellmund, M.; Merkel, O. M.; Kissel, T. *Polymer* **2011**, *3*, 693.
- (416) Zhang, P.; Yang, J. H.; Li, W. C.; Wang, W.; Liu, C. J.; Griffith, M.; Liu, W. G. *J. Mater. Chem.* **2011**, *21*, 7755.
- (417) Schallon, A.; Synatschke, C. V.; Jerome, V.; Muller, A. H. E.; Freitag, R. *Biomacromolecules* **2012**, *13*, 3463.
- (418) Majewski, A. P.; Stahlschmidt, U.; Jerome, V.; Freitag, R.; Muller, A. H. E.; Schmalz, H. *Biomacromolecules* **2013**, *14*, 3081.
- (419) Synatschke, C. V.; Schallon, A.; Jerome, V.; Freitag, R.; Muller, A. H. E. *Biomacromolecules* **2011**, *12*, 4247.
- (420) Ohno, K.; Mori, C.; Akashi, T.; Yoshida, S.; Tago, Y.; Tsujii, Y.; Tabata, Y. *Biomacromolecules* **2013**, *14*, 3453.
- (421) Yan, P.; Zhao, N.; Hu, H.; Lin, X.; Liu, F.; Xu, F.-J. *Acta Biomater.* **2014**, *10*, 3786.
- (422) Cheng, Y.; Samia, A. C.; Meyers, J. D.; Panagopoulos, I.; Fei, B. W.; Burda, C. *J. Am. Chem. Soc.* **2008**, *130*, 10643.
- (423) Freese, C.; Gibson, M. I.; Klok, H.-A.; Unger, R. E.; Kikpatrick, C. J. *Biomacromolecules* **2012**, *13*, 1533.
- (424) Liu, R.; Liao, P. H.; Liu, J. K.; Feng, P. Y. *Langmuir* **2011**, *27*, 3095.
- (425) Sahoo, B.; Devi, K. S. P.; Banerjee, R.; Maiti, T. K.; Pramanik, P.; Dhar, D. *ACS Appl. Mater. Interfaces* **2013**, *5*, 3884.
- (426) Liu, G.; Cai, M.; Zhou, F.; Liu, W. *J. Phys. Chem. B* **2014**, *118*, 4920.
- (427) Ohno, K.; Akashi, T.; Tsujii, Y.; Yamamoto, M.; Tabata, Y. *Biomacromolecules* **2012**, *13*, 927.
- (428) Zhang, W.; Peng, B.; Tian, F.; Qin, W.; Qian, X. *Anal. Chem.* **2014**, *86*, 482.
- (429) Zhang, G.; Jia, X.; Liu, Z.; Hu, J.; Ma, Z.; Zhou, F. *Macromol. Biosci.* **2013**, *13*, 1259.
- (430) Jia, X.; Zhang, G.; Li, W.; Sheng, W.; Li, C. *J. Polym. Sci., A: Polym. Chem.* **2014**, *52*, 1807.
- (431) Chen, L.; Peng, Z.; Zeng, Z.; She, Y.; Wei, J.; Chen, Y. *J. Polym. Sci., A: Polym. Chem.* **2014**, *52*, 2202.
- (432) Tang, Z.; Akiyama, Y.; Okano, T. *Polymers* **2012**, *4*, 1478.
- (433) Kumashiro, Y.; Yamato, M.; Okano, T. *Ann. Biomed. Eng.* **2010**, *38*, 1977.
- (434) Elloumi-Hannachi, I.; Yamato, M.; Okano, T. *J. Intern. Med.* **2010**, *267*, 54.
- (435) Nishida, K.; Yamato, M.; Hayashida, Y.; Watanabe, K.; Yamamoto, K.; Adachi, E.; Nagai, S.; Kikuchi, A.; Maeda, N.; Watanabe, O.; Tano, Y. *N. Engl. J. Med.* **2004**, *351*, 1187.
- (436) Umemoto, T.; Yamato, M.; Nishida, K.; Okano, T. *Chin. Sci. Bull.* **2013**, *58*, 4349.
- (437) Nagase, K.; Mukae, N.; Kikuchi, A.; Okano, T. *Macromol. Biosci.* **2013**, *12*, 333.
- (438) Iwata, T.; Yamato, M.; Tsuchioka, H.; Takagi, R.; Mukobata, S.; Washio, K.; Okano, T.; Ishikawa, I. *Biomaterials* **2009**, *30*, 2716.
- (439) Memon, I. A.; Sawa, Y.; Fukushima, N.; Matsumiya, G.; Miyagawa, S.; Taketani, S.; Sakakida, S. K.; Kondoh, H.; Aleshin, A. N.; Shimizu, T.; Okano, T.; Matsuda, H. *J. Thorac. Cardiovasc. Surg.* **2005**, *130*, 1333.
- (440) Ohki, T.; Yamato, M.; Murakami, D.; Takagi, R.; Yang, J.; Namiki, H.; Okano, T.; Takasaki, K. *Gut* **2006**, *55*, 1704.
- (441) Alexander, C.; Shakesheff, K. M. *Adv. Mater.* **2006**, *18*, 3321.
- (442) Mizutani, A.; Kikuchi, A.; Yamato, M.; Kanazawa, H.; Okano, T. *Biomaterials* **2008**, *29*, 2073.
- (443) Dworak, A.; Utrata-Wesolek, A.; Oleszko, N.; Walach, W.; Trzebicka, B.; Aniol, J.; Sieron, A. L.; Llama-Baryla, A.; Kawecki, M. *J. Mater. Sci.: Mater. Med.* **2014**, *25*, 1149.
- (444) Kong, B.; Choi, J. S.; Jeon, S.; Choi, I. S. *Biomaterials* **2009**, *30*, 5514.
- (445) Zhang, C. H.; Vernier, P. T.; Wu, Y. H.; Yang, W. R. *J. Biomed. Mater. Res., Part B* **2012**, *100B*, 217.
- (446) Xu, F. J.; Zhong, S. P.; Yung, L. Y. L.; Kang, E. T.; Neoh, K. G. *Biomacromolecules* **2004**, *5*, 2392.
- (447) Ernst, O.; Lieske, A.; Jager, M.; Lankenau, A.; Duschl, C. *Lab Chip* **2007**, *7*, 1322.
- (448) Wischerhoff, E.; Uhlig, K.; Lankenau, A.; Borner, H. G.; Laschewsky, A.; Duschl, C.; Lutz, J.-F. *Angew. Chem., Int. Ed.* **2008**, *47*, 5666.
- (449) Takahashi, H.; Nakayama, M.; Yamato, M.; Okano, T. *Biomacromolecules* **2010**, *11*, 1991.
- (450) Akiyama, Y.; Kikuchi, A.; Yamato, M.; Okano, T. *Langmuir* **2004**, *20*, 5506.
- (451) Canavan, H. E.; Cheng, X. H.; Graham, D. J.; Ratner, B. D.; Castner, D. G. *Langmuir* **2005**, *21*, 1949.
- (452) Canavan, H. E.; Cheng, X. H.; Graham, D. J.; Ratner, B. D.; Castner, D. G. *J. Biomed. Mater. Res., Part A* **2005**, *75*, 1.
- (453) Yu, Q.; Johnson, L. M.; Lopez, G. P. *Nanoscale* **2014**, *24*, 3751.
- (454) Fukumori, K.; Akiyama, Y.; Kumashiro, Y.; Kobayashi, J.; Yamato, M.; Sakai, K.; Okano, T. *Macromol. Biosci.* **2010**, *10*, 1117.
- (455) Li, L. H.; Zhu, Y.; Li, B.; Gao, C. Y. *Langmuir* **2008**, *24*, 13632.
- (456) Xue, C. Y.; Choi, B. C.; Choi, S.; Braun, P. V.; Leckband, D. E. *Adv. Funct. Mater.* **2012**, *22*, 2394.
- (457) Dworak, A.; Itrata-Wesolek, A.; Szweda, D.; Kowalcuk, A.; Trzebicka, B.; Aniol, J.; Sieron, A. L.; Klama-Baryla, A.; Kawecki, M. *ACS Appl. Mater. Interfaces* **2013**, *5*, 2197.
- (458) He, X.-L.; Nie, P.-P.; Sun, Y.-K.; Wang, Y.; Dong, Y.-Y.; Chen, L. *J. Colloid Interface Sci.* **2010**, *350*, 471.
- (459) Li, L. H.; Wu, J. D.; Gao, C. Y. *Colloids Surf., B* **2011**, *85*, 12.
- (460) Shimizu, T.; Yamato, M.; Kikuchi, A.; Okano, T. *Biomaterials* **2003**, *24*, 2309.
- (461) Okano, T.; Yamada, N.; Okuhara, M.; Sakai, H.; Sakurai, Y. *Biomaterials* **1995**, *16*, 297.
- (462) Wischerhoff, E.; Glatzel, S.; Uhlig, K.; Lankenau, A.; Lutz, J. F.; Laschewsky, A. *Langmuir* **2009**, *25*, 5949.
- (463) Takahashi, H.; Nakayama, M.; Itoga, K.; Yamato, M.; Okano, T. *Biomacromolecules* **2011**, *12*, 1414.
- (464) Tamura, A.; Kobayashi, J.; Yamato, M.; Okano, T. *Acta Biomater.* **2012**, *8*, 3904.

- (465) Tamura, A.; Nishi, M.; Kobayashi, J.; Nagase, K.; Yajima, H.; Yamato, M.; Okano, T. *Biomacromolecules* **2012**, *13*, 1765.
- (466) Yu, Q.; Zhang, Y. X.; Chen, H.; Zhou, F.; Wu, Z. Q.; Huang, H.; Brash, J. L. *Langmuir* **2010**, *26*, 8582.
- (467) da Silva, R. M. P.; Mano, J. F.; Reis, R. L. *Trends Biotechnol.* **2007**, *25*, 577.
- (468) Nagase, K.; Kobayashi, J.; Okano, T. *J. R. Soc., Interface* **2009**, *6*, S293.
- (469) Cooperstein, M. A.; Canavan, H. E. *Langmuir* **2009**, *26*, 7695.
- (470) Kikuchi, A.; Okano, T. *J. Controlled Release* **2005**, *101*, 69.
- (471) Halperin, A.; Kroger, M. *Biomaterials* **2012**, *33*, 4975.
- (472) Uhlig, K.; Boerner, H. G.; Wischerhoff, E.; Lutz, J. F.; Jaeger, M. S.; Laschewsky, A.; Duschl, C. *Polymers* **2014**, *6*, 1164.
- (473) Mandal, K.; Balland, M.; Bureau, L. *PLoS One* **2012**, *7*, e37548.
- (474) Kumashiro, Y.; Fukumori, K.; Takahashi, H.; Nakayama, M.; Akiyama, Y.; Yamato, M.; Okano, T. *Colloids Surf., B* **2013**, *106*, 198.
- (475) Virola, H.; Laukkonen, A.; Valtola, L.; Tenhu, H.; Hirvonen, J. *Biomaterials* **2005**, *26*, 3055.
- (476) Rzaev, Z. M. O.; Dincer, S.; Piskin, E. *Prog. Polym. Sci.* **2007**, *32*, 534.
- (477) Cunliffe, D.; de las Heras Alarcon, C.; Peters, V.; Smith, J. R.; Alexander, A. *Langmuir* **2003**, *19*, 2888.
- (478) Nagase, K.; Hatakeyama, Y.; Shimizu, T.; Matsuura, K.; Yamato, M.; Takeda, N.; Okano, T. *Biomacromolecules* **2013**, *14*, 3423.
- (479) Chernyy, S.; Jensen, B. E. B.; Shimizu, K.; Ceccato, M.; Pedersen, S. U.; Zelikin, A. N.; Daasbjerg, K.; Iruthayarat, J. *J. Colloid Interface Sci.* **2013**, *404*, 207.
- (480) Idota, N.; Ebara, M.; Kotsuchibashi, Y.; Narain, R.; Aoyagi, T. *Sci. Technol. Adv. Mater.* **2012**, *13*, 064206.
- (481) Lutz, J. F. *Adv. Mater.* **2011**, *23*, 2237.
- (482) Porsch, C.; Hansson, S.; Nordgren, N.; Malmstrom, E. *Polym. Chem.* **2011**, *2*, 1114.
- (483) Uhlig, K.; Boysen, B.; Lankenau, A.; Jaeger, M.; Wischerhoff, E.; Lutz, J. F.; Laschewsky, A.; Duschl, C. *Biomicrofluidics* **2012**, *6*, 024129.
- (484) Sefcik, L. S.; Kaminski, A.; Ling, K.; Laschewsky, A.; Lutz, J. F.; Wischerhoff, E. *Cell. Mol. Bioeng.* **2013**, *6*, 287.
- (485) Lin, J. B.; Isenberg, B. C.; Shen, Y.; Schorsch, K.; Sazonova, O. V.; Wong, J. Y. *Colloids Surf., B* **2012**, *99*, 108.
- (486) Gong, Z.-L.; Tang, D.-Y.; Guo, Y.-D. *J. Mater. Chem.* **2012**, *22*, 16872.
- (487) Matsuzaka, N.; Nakayama, M.; Takahashi, H.; Yamato, M.; Kikuchi, A.; Okano, T. *Biomacromolecules* **2013**, *14*, 3164.
- (488) Liu, H. Y.; Li, Y.; Sun, K.; Fan, J.; Zhang, P.; Meng, J.; Wang, S.; Jiang, L. *J. Am. Chem. Soc.* **2013**, *135*, 7603.
- (489) Thery, M. *J. Cell Sci.* **2010**, *123*, 4201.
- (490) Falconnat, D.; Csucs, G.; Grandin, H. M.; Textor, M. *Biomaterials* **2006**, *27*, 3044.
- (491) Cho, W. K.; Kong, B.; Park, H. J.; Kim, J. B.; Chegal, W.; Choi, J. S.; Choi, I. S. *Biomaterials* **2010**, *31*, 9565.
- (492) Steinbach, A.; Tautzenberger, A.; Ignatius, A.; Pluntke, M.; Marti, O.; Volkmer, D. *J. Mater. Sci.: Mater. Med.* **2012**, *23*, 573.
- (493) Li, C.; Glidle, A.; Yuan, X.; Hu, Z.; Pulleine, E.; Cooper, J.; Yang, W.; Yin, H. *Biomacromolecules* **2013**, *14*, 1278.
- (494) Telford, A. M.; Meagher, L.; Glattauer, V.; Gengenbach, T. R.; Easton, C. D.; Neto, C. *Biomacromolecules* **2012**, *13*, 2989.
- (495) Connelly, J.; Gautrot, J. E.; Trappmann, B.; Tan, D. W. M.; Donati, G.; Huck, W. T. S.; Watt, F. M. *Nat. Cell Biol.* **2010**, *12*, 711.
- (496) Connelly, J.; Mishra, A.; Gautrot, J. E.; Watt, F. M. *PLoS One* **2011**, *6*, e27259.
- (497) Gautrot, J. E.; Wang, C.; Liu, X.; Goldie, S. J.; Trappmann, B.; Huck, W. T. S.; Watt, F. M. *Biomaterials* **2012**, *33*, 5221.
- (498) Sha, J.; Lippmann, E. S.; McNulty, J.; Ma, Y.; Ashton, R. S. *Biomacromolecules* **2013**, *14*, 3294.
- (499) Li, Y.; Zhang, J.; Fang, L.; Jiang, L.; Liu, W.; Wang, T.; Cui, L.; Sun, H.; Yang, B. *J. Mater. Chem.* **2012**, *22*, 25116.
- (500) Harris, B. P.; Kutty, J. K.; Fritz, E. W.; Webb, C. K.; Burg, K. J.; Metters, A. T. *Langmuir* **2006**, *22*, 4467.
- (501) Chiang, E. N.; Dong, R.; Ober, C. K.; Baird, B. A. *Langmuir* **2011**, *27*, 7016.
- (502) Dong, R.; Molloy, R. P.; Lindau, M.; Ober, C. K. *Biomacromolecules* **2010**, *11*, 2027.
- (503) Zhou, Z.; Yu, P.; Geller, H.; Ober, C. K. *Biomacromolecules* **2013**, *14*, 529.
- (504) Letsche, S. A.; Steinbach, A. M.; Pluntke, M.; Marti, O.; Ignatius, A.; Volkmer, D. *Front. Mater. Sci. China* **2009**, *3*, 132.
- (505) Kane, R. S.; Takayama, S.; Ostuni, E.; Ingber, D. E.; Whitesides, G. M. *Biomaterials* **1999**, *20*, 2363.
- (506) Yanker, D. M.; Maurer, J. A. *Mol. Biosyst.* **2008**, *4*, 502.
- (507) Reuther, C.; Tucker, R.; Ionov, L.; Diez, S. *Nano Lett.* **2014**, *14*, 4050.
- (508) Li, Y.; Zhang, J.; Liu, W.; Li, D.; Fang, L.; Sun, H.; Yang, B. *ACS Appl. Mater. Interfaces* **2013**, *5*, 2126.
- (509) Hoshi, Y.; Xu, Y.; Ober, C. K. *Polymer* **2013**, *54*, 1762.
- (510) Fors, B. P.; Hawker, C. J. *Angew. Chem., Int. Ed.* **2012**, *51*, 8850.
- (511) Poelma, J. E.; Fors, B. P.; Meyers, G. F.; Kramer, J. W.; Hawker, C. J. *Angew. Chem., Int. Ed.* **2013**, *52*, 6844.
- (512) Ren, T.; Mao, Z.; Guo, J.; Gao, C. *Langmuir* **2013**, *29*, 6386.
- (513) Gautrot, J. E.; Malmstrom, J.; Sundh, M.; Margadant, C.; Sonnenberg, A.; Sutherland, D. S. *Nano Lett.* **2014**, *14*, 3945.
- (514) Rimondini, L.; Fini, M.; Giardino, R. *J. Appl. Biomater. Biomech.* **2005**, *3*, 1.
- (515) Cloete, T. *Mater. Corros.* **2003**, *54*, 520.
- (516) da Silva, E.; De Martinis, E. *Appl. Microbiol. Biotechnol.* **2013**, *97*, 957.
- (517) Yang, W.; Neoh, K. G.; Kang, E. T.; Lee, S. B.; Teo, S.; Rittschof, D. *Biofouling* **2012**, *28*, 895.
- (518) Yu, Q.; Cho, J.; Shivapooja, P.; Ista, L. K.; Lopez, G. P. *ACS Appl. Mater. Interfaces* **2013**, *5*, 9295.
- (519) Joyce, E.; Al-Hashimi, A.; Mason, T. *J. Appl. Microbiol.* **2011**, *110*, 862.
- (520) Tiller, J. C.; Liao, C. J.; Lewis, K.; Klibanov, A. M. *Proc. Natl. Acad. Sci. U.S.A.* **2001**, *98*, 5981.
- (521) Vester, F.; Ingvorsen, K. *Appl. Environ. Microbiol.* **1998**, *64*, 1700.
- (522) Boulos, L.; Prevost, M.; Barbeau, B.; Coallier, J.; Desjardins, R. *J. Microbiol. Methods* **1999**, *37*, 77.
- (523) *Performance Standards for Antimicrobial Disk Susceptibility Tests; Approved Standard*, 9th ed.; Clinical and Laboratory Standards Institute: Wayne, PA, 2006; Vol. 26, p M2.
- (524) *Methods for Dilution Antimicrobial Susceptibility Tests for Bacteria That Grow Aerobically; Approved Standard*, 9th ed.; Clinical and Laboratory Standards Institute: Wayne, PA; 2012; Vol. 32, p M07.
- (525) Ramstedt, M.; Ekstrand-Hammarstrom, B.; Shchukarev, A. V.; Bucht, A.; Osterlund, L.; Welch, M.; Huck, W. T. S. *Biomaterials* **2009**, *30*, 1524.
- (526) Ozcam, A. E.; Roskov, K. E.; Spontak, R. J.; Genzer, J. *J. Mater. Chem.* **2012**, *22*, 5855.
- (527) Liu, X.; Zhang, H.; Tian, Z. C.; Sen, A.; Allcock, H. R. *Polym. Chem.* **2012**, *3*, 2082.
- (528) Lin, J.; Qiu, S. Y.; Lewis, K.; Klibanov, A. M. *Biotechnol. Prog.* **2002**, *18*, 1082.
- (529) Vooturi, S. K.; Firestone, S. M. *Curr. Med. Chem.* **2010**, *17*, 2292.
- (530) Ding, L.; Chi, E. Y.; Chemburu, S.; Ji, E.; Schanze, K. S.; Lopez, G. P.; Whitten, D. G. *Langmuir* **2009**, *25*, 13742.
- (531) Klibanov, A. M. *J. Mater. Chem.* **2007**, *17*, 2479.
- (532) Helander, I. M.; Alakomi, H. L.; Latva-Kala, K.; Koski, P. *Microbiology* **1997**, *143* (Pt 10), 3193.
- (533) Lee, S. B.; Koepsel, R. R.; Morley, S. W.; Matyjaszewski, K.; Sun, Y.; Russell, A. J. *Biomacromolecules* **2004**, *5*, 877.
- (534) Murata, H.; Koepsel, R. R.; Matyjaszewski, K.; Russell, A. J. *Biomaterials* **2007**, *28*, 4870.
- (535) Huang, J. Y.; Murata, H.; Koepsel, R. R.; Russell, A. J.; Matyjaszewski, K. *Biomacromolecules* **2007**, *8*, 1396.

- (536) Huang, J.; Koepsel, R.; Murata, H.; Wu, W.; Lee, S.; Kowalewski, T.; Russell, A.; Matyjaszewski, K. *Langmuir* **2008**, *24*, 6785.
- (537) Dong, H.; Huang, J.; Koepsel, R. R.; Ye, P.; Russell, A. J.; Matyjaszewski, K. *Biomacromolecules* **2011**, *12*, 1305.
- (538) Terada, A.; Okuyama, K.; Nishikawa, M.; Tsuneda, S.; Hosomi, M. *Biotechnol. Bioeng.* **2012**, *109*, 1745.
- (539) Lee, H.-S.; Eckmann, D. M.; Lee, D.-Y.; Hickok, N. J.; Composto, R. J. *Langmuir* **2011**, *27*, 12458.
- (540) Lee, H. S.; Yee, M. Q.; Eckmann, Y. Y.; Hickok, N. J.; Eckmann, D. M.; Composto, R. J. *J. Mater. Chem.* **2012**, *22*, 19605.
- (541) Cheng, Z. P.; Zhu, X. L.; Shi, Z. L.; Neoh, K. G.; Kang, E. T. *Surf. Rev. Lett.* **2006**, *13*, 313.
- (542) Yuan, S. J.; Pehkonen, S. O.; Ting, Y. P.; Neoh, K. G.; Kang, E. T. *ACS Appl. Mater. Interfaces* **2009**, *1*, 640.
- (543) Li, L.; Ke, Z.; Yan, G.; Wu, J. *Polym. Int.* **2008**, *57*, 1275.
- (544) Ignatova, M.; Voccia, S.; Gabriel, S.; Gilbert, B.; Cossement, D.; Jerome, R.; Jerome, C. *Langmuir* **2009**, *25*, 891.
- (545) Cheng, G.; Xite, H.; Zhang, Z.; Chen, S. F.; Jiang, S. Y. *Angew. Chem., Int. Ed.* **2008**, *47*, 8831.
- (546) Zhao, J.; Song, L.; Shi, Q.; Luan, S.; Yin, J. *ACS Appl. Mater. Interfaces* **2013**, *5*, 5260.
- (547) Yao, F.; Fu, G.-D.; Zhao, J.; Kang, E.-T.; Neoh, K. G. *J. Membr. Sci.* **2008**, *319*, 149.
- (548) Yuan, S. J.; Xu, F. J.; Pehkonen, S. O.; Ting, Y. P.; Neoh, K. G.; Kang, E. T. *Biotechnol. Bioeng.* **2009**, *103*, 268.
- (549) Cai, T.; Yang, W. J.; Neoh, K.-G.; Kang, E.-T. *Ind. Eng. Chem. Res.* **2012**, *51*, 15962.
- (550) Peng, Q.; Lu, S.; Chen, D.; Wu, X.; Fan, P.; Zhong, R.; Xu, Y. *Macromol. Biosci.* **2007**, *7*, 1149.
- (551) Song, J.; Jung, Y.; Lee, I.; Jang, J. *J. Colloid Interface Sci.* **2013**, *407*, 205.
- (552) Terada, A.; Yuasa, A.; Tsuneda, S.; Hirata, A.; Katakai, A.; Tamada, M. *Colloids Surf., B* **2005**, *43*, 99.
- (553) Yang, W.; Cai, T.; Neoh, K.; Kang, E.; Teo, S.; Rittschof, D. *Biomacromolecules* **2013**, *14*, 2041.
- (554) Malaisamy, R.; Berry, D.; Holder, D.; Raskin, L.; Lepak, L.; Jones, K. L. *J. Membr. Sci.* **2010**, *350*, 361.
- (555) Ye, Q.; Gao, T.; Wan, F.; Yu, B.; Pei, X.; Zhou, F.; Xue, Q. *J. Mater. Chem.* **2012**, *22*, 13123.
- (556) Gao, G.; Lange, D.; Hilpert, K.; Kindrachuk, J.; Zou, Y.; Cheng, J.; Kazemzadeh-Narbat, M.; Yu, K.; Wang, R.; Straus, S.; Brooks, D.; Chew, B.; Hancock, R.; Kizhakkedathu, J. *Biomaterials* **2011**, *32*, 3899.
- (557) Asadinezhad, A.; Novak, I.; Lehocky, M.; Sedlarik, V.; Vesel, A.; Junkar, I.; Saha, P.; Chodak, I. *Plasma Processes Polym.* **2010**, *7*, 504.
- (558) Asadinezhad, A.; Novak, I.; Lehocky, M.; Sedlarik, V.; Vesel, A.; Junkar, I.; Saha, P.; Chodak, I. *Colloids Surf., B* **2010**, *77*, 246.
- (559) Tang, F.; Zhang, L.; Zhang, Z.; Cheng, Z.; Zhu, X. *J. Macromol. Sci., Part A: Pure Appl. Chem.* **2009**, *46*, 989.
- (560) Sileika, T. S.; Kim, H.-D.; Maniak, P.; Messersmith, P. B. *ACS Appl. Mater. Interfaces* **2011**, *3*, 4602.
- (561) Muszanska, A. K.; Busscher, H. J.; Herrmann, A.; van, d. M. H. C.; Norde, W. *Biomaterials* **2011**, *32*, 6333.
- (562) Tai, Y.; McGuire, J.; Neff, J. *J. Colloid Interface Sci.* **2008**, *322*, 104.
- (563) Li, X.; Li, P.; Saravanan, R.; Basu, A.; Mishra, B.; Lim, S. H.; Su, X.; Tambyah, P. A.; Leong, S. S. J. *Acta Biomater.* **2014**, *10*, 258.
- (564) Hu, R.; Li, G.; Jiang, Y.; Zhang, Y.; Zou, J. J.; Wang, L.; Zhang, X. *Langmuir* **2013**, *29*, 3773.
- (565) Pangilinan, K. D.; Santos, C. M.; Estillore, N. C.; Rodrigues, D. F.; Advincula, R. C. *Macromol. Chem. Phys.* **2013**, *214*, 464.
- (566) Yu, Q.; Ista, L. K.; Lopez, G. P. *Nanoscale* **2014**, *6*, 4750.
- (567) Laloyaux, X.; Fautre, E.; Blin, T.; Purohit, V.; Leprince, J.; Jouenne, T.; Jonas, A. M.; Glinel, K. *Adv. Mater.* **2010**, *22*, 5024.
- (568) Blin, T.; Purohit, V.; Leprince, J.; Jouenne, T.; Glinel, K. *Biomacromolecules* **2011**, *12*, 1259.
- (569) Wan, D.; Yuan, S. J.; Neoh, K. G.; Kang, E. T. *ACS Appl. Mater. Interfaces* **2010**, *2*, 1653.
- (570) Ramstedt, M.; Cheng, N.; Azzaroni, O.; Mossialos, D.; Mathieu, H. J.; Huck, W. T. S. *Langmuir* **2007**, *23*, 3314.
- (571) Powers, C. M.; Wrench, N.; Ryde, I. T.; Smith, A. M.; Seidler, F. J.; Slotkin, T. A. *Environ. Health Perspect.* **2010**, *118*, 73.
- (572) Powers, C. M.; Badireddy, A. R.; Ryde, I. T.; Seidler, F. J.; Slotkin, T. A. *Environ. Health Perspect.* **2011**, *119*, 37.
- (573) Locht, L. J.; Pedersen, M.; Markholt, S.; Bibby, B. M.; Larsen, A.; Penkowa, M.; Stoltzenberg, M.; Rungby, J. *Basic Clin. Pharmacol. Toxicol.* **2011**, *109*, 1.
- (574) Dill, J.; Auxier, J.; Schilke, K.; McGuire, J. *J. Colloid Interface Sci.* **2013**, *395*, 300.
- (575) Mi, L.; Giarmarco, M. M.; Shao, Q.; Jiang, S. Y. *Biomaterials* **2012**, *33*, 2001.
- (576) Gon, S.; Kumar, K. N.; Nusslein, K.; Santore, M. M. *Macromolecules* **2012**, *45*, 8373.
- (577) Wei, J.; Ravn, D.; Gram, L.; Kingshott, P. *Colloids Surf., B* **2003**, *32*, 275.
- (578) Kingshott, P.; Wei, J.; Bagge-Ravn, D.; Gadegaard, N.; Gram, L. *Langmuir* **2003**, *19*, 6912.
- (579) Friedlander, R. S.; Vlamaris, H.; Kim, P.; Khan, M.; Kolter, R.; Aizenberg, J. *Proc. Natl. Acad. Sci. U.S.A.* **2013**, *110*, 5624.
- (580) Zhao, K.; Tseng, B. S.; Beckerman, B.; Jin, F.; Gibiansky, M. L.; Harrison, J. J.; Luijten, E.; Parsek, M. R.; Wong, G. C. *Nature* **2013**, *497*, 388.
- (581) Roosjen, A.; van der Mei, H. C.; Busscher, H. J.; Norde, W. *Langmuir* **2004**, *20*, 10949.
- (582) Nejadnik, M. R.; van, d. M. H. C.; Norde, W.; Busscher, H. J. *Biomaterials* **2008**, *29*, 4117.
- (583) Roosjen, A.; Busscher, H. J.; Nordel, W.; van der Mei, H. C. *Microbiology* **2006**, *152*, 2673.
- (584) Nejadnik, M. R.; van der Mei, H. C.; Busscher, H. J.; Norde, W. *Appl. Environ. Microbiol.* **2008**, *74*, 916.
- (585) Roosjen, A.; de Vries, J.; van der Mei, H. C.; Norde, W.; Busscher, H. J. *J. Biomed. Mater. Res., Part B* **2005**, *73*, 347.
- (586) Nejadnik, M. R.; Engelsman, A. F.; Saldarriaga, F. I. C.; Busscher, H. J.; Norde, W.; van, d. M. H. C. *J. Antimicrob. Chemother.* **2008**, *62*, 1323.
- (587) Qu, W.; Hooymans, J.; Qiu, J.; de-Bont, N.; Gelling, O.; Van der Mei, H.; Busscher, H. *J. Biomed. Mater. Res., Part B* **2013**, *101B*, 640.
- (588) Zhao, Y.-H.; Zhu, X.-Y.; Wee, K.-H.; Bai, R. *J. Phys. Chem. B* **2010**, *114*, 2422.
- (589) Cringus-Fundeanu, I.; Luijten, J.; van der Mei, H. C.; Busscher, H. J.; Schouten, A. *J. Langmuir* **2007**, *23*, 5120.
- (590) Fundeanu, I.; van der Mei, H. C.; Schouten, A. J.; Busscher, H. *J. Colloids Surf., B* **2008**, *64*, 297.
- (591) Fundeanu, I.; van der Mei, H. C.; Schouten, A. J.; Busscher, H. *J. Biomed. Mater. Res., Part A* **2010**, *94*, 997.
- (592) Fundeanu, I.; Klee, D.; Schouten, A. J.; Busscher, H. J.; van der Mei, H. C. *Acta Biomater.* **2010**, *6*, 4271.
- (593) Huang, C. J.; Mi, L.; Jiang, S. Y. *Biomaterials* **2012**, *33*, 3626.
- (594) Cheng, G.; Li, G. Z.; Xue, H.; Chen, S. F.; Bryers, J. D.; Jiang, S. Y. *Biomaterials* **2009**, *30*, 5234.
- (595) Roosjen, A.; Kaper, H. J.; van der Mei, H. C.; Norde, W.; Busscher, H. *J. Microbiology* **2003**, *149*, 3239.
- (596) Holmes, P.; Currie, E.; Thies, J.; Van der Mei, H.; Busscher, H.; Norde, W. *J. Biomed. Mater. Res., Part A* **2009**, *91A*, 824.
- (597) Venault, A.; Chang, Y.; Wang, D.-M.; Lai, J.-Y. *J. Membr. Sci.* **2012**, *423–424*, 53.
- (598) Zhao, C.; Zheng, J. *Biomacromolecules* **2011**, *12*, 4071.
- (599) Li, G. Z.; Xue, H.; Cheng, G.; Chen, S. F.; Zhang, F. B.; Jiang, S. Y. *J. Phys. Chem. B* **2008**, *112*, 15269.
- (600) Li, G. Z.; Cheng, G.; Xue, H.; Chen, S. F.; Zhang, F. B.; Jiang, S. Y. *Biomaterials* **2008**, *29*, 4592.
- (601) Kuang, J.; Messersmith, P. B. *Langmuir* **2012**, *28*, 7258.
- (602) Cheng, G.; Zhang, Z.; Chen, S. F.; Bryers, J. D.; Jiang, S. Y. *Biomaterials* **2007**, *28*, 4192.
- (603) Takahashi, N.; Iwasa, F.; Inoue, Y.; Morisaki, H.; Ishihara, K.; Baba, K. *J. Prosthet. Dent.* **2014**, *112*, 194.

- (604) Lau, K. H. A.; Ren, C.; Sileika, T. S.; Park, S. H.; Szleifer, I.; Messersmith, P. B. *Langmuir* **2012**, *28*, 16099.
- (605) Pidhatika, B.; M?ller, J.; Benetti, E.; Konradi, R.; Rakhmatullina, E.; Muhlebach, A.; Zimmermann, R.; Werner, C.; Vogel, V.; Textor, M. *Biomaterials* **2010**, *31*, 9462.
- (606) Statz, A. R.; Barron, A. E.; Messersmith, P. B. *Soft Matter* **2008**, *4*, 131.
- (607) Zhao, W.; Ye, Q.; Hu, H.; Wang, X.; Zhou, F. *J. Mater. Chem. B* **2014**, *2*, 5352.
- (608) Ignatova, M.; Voccia, S.; Gilbert, B.; Markova, N.; Cossement, D.; Gouttebaron, R.; Jerome, R.; Jerome, C. *Langmuir* **2006**, *22*, 255.
- (609) Ishihara, K.; Nomura, H.; Mihara, T.; Kurita, K.; Iwasaki, Y.; Nakabayashi, N. *J. Biomed Mater. Res.* **1998**, *39*, 323.
- (610) Pidhatika, B.; Rodenstein, M.; Chen, Y.; Rakhmatullina, E.; Muhlebach, A.; Acikgoz, C.; Textor, M.; Konradi, R. *Biointerphases* **2012**, *7*, 1.
- (611) Vogler, E. *Adv. Colloid Interface Sci.* **1998**, *74*, 69.